The effect of circadian rhythm on organisational immunity of ant colonies

by

Linda Sartoris

February, 2025

A thesis submitted to the
Graduate School
of the
Institute of Science and Technology Austria
in partial fulfilment of the requirements
for the degree of
Doctor of Philosophy

Committee in charge:
Georgios Katsaros, Chair
Sylvia Cremer
Florian Schur
Yuko E. Ulrich

The thesis of Linda Sartoris, titled *The effect of circadian rhythm on organisational immunity of ant colonies*, is approved by:

Supervisor: Sylvia Cremer, ISTA, Klosterneuburg, Austria

Signature: _____

Committee Member: Florian Schur, ISTA, Klosterneuburg, Austria

Signature: _____

Committee Member: Yuko E. Ulrich, Max Planck Institute for Chemical Ecology, Jena, Germany

Signature: _____

Defense Chair: Georgios Katsaros, ISTA, Klosterneuburg, Austria

Signature: _____

Signed page is on file

ISTA Thesis, ISSN: 2663-337X

I hereby declare that this thesis is my own work and that it does not contain other people's work without this being so stated; this thesis does not contain my previous work without this being stated, and the bibliography contains all the literature that I used in writing the dissertation.

I accept full responsibility for the content and factual accuracy of this work, including the data and their analysis and presentation, and the text and citation of other work.

I declare that this is a true copy of my thesis, including any final revisions, as approved by my thesis committee, and that this thesis has not been submitted for a higher degree to any other university or institution.

I certify that any republication of materials presented in this thesis has been approved by the relevant publishers and co-authors.

Signature: _____

Linda Sartoris
February, 2025

Signed page is on file

Abstract

Social interaction networks of insect colonies facilitate efficient information exchange and demonstrate adaptive changes to mitigate disease transmission. While circadian rhythms influence individual behaviour, their role in shaping colony-level defences against pathogens remains unexplored. Here, we investigate whether social networks of the black garden ant, *Lasius niger*, exhibit circadian rhythms and how these rhythms influence disease vulnerability when colonies are exposed to a pathogen during the day or the night.

We first establish baseline daily variations in activity and network dynamics in pathogen-free colonies, revealing constitutive daily fluctuations in disease susceptibility. Subsequently, we examine pathogen-induced changes in sanitary care and network dynamics by exposing foragers to a natural pathogen (*Metarhizium brunneum*) during either the day or the night. Individual pathogen loads were measured after a nine-hour post-exposure period to evaluate transmission outcomes.

Our results demonstrate that diurnal ant colonies maintain robust circadian patterns in network properties while flexibly adapting to pathogen exposure. Ants upregulate sanitary care irrespective of exposure timing, prioritising the protection of the valuable colony centre consisting of nurses and the queen. These findings underscore the robustness and adaptability of ant colonies in balancing circadian rhythms with effective social immune responses.

Acknowledgments

Thank you to Sylvia Cremer for initiating this collaboration with Nathalie Stroeymeyt, allowing me to work independently, and providing me opportunities to present my research at international conferences. My years in her group have been a great learning experience.

Thank you to Nathalie Stroeymeyt for welcoming me at her Ant Epidemiology Lab (AEL) in Bristol and for her unwavering support throughout all stages of analysis. This project would not have been possible without her generous help, including the shared resources such as the tracking data processing pipeline. Working together was a truly rewarding experience.

Thank you to my committee members, Yuko Ulrich and Florian Schur, for their steadfast support, trust in the process, and excellent input at just the right moments.

Thank you to the Lab Support Facility at ISTA. And thank you to Roger Mundry for his statistical advice, from navigating three-way-interactions to generously sharing his expertise and functions during a formative course on linear models.

Thank you to the European Research Council (ERC) for their funding under the European Union's Horizon 2020 research and innovation program (ERC Consolidator Grant EPIDEMICSonCHIP, No. 771402, to Sylvia Cremer, and ERC Starting Grant DISEASE, No. 802628, to Nathalie Stroeymeyt).

Thank you to all the past and present members of the Social Immunity Lab at ISTA for the laughter, encouragement, and support in my scientific endeavours – I feel tremendously lucky to have been supported like this. Florian, thank you for letting me use your beautiful ant pictures. A special thanks to Casi, Sina, and Anna for their friendship throughout the years.

And finally, thank you to all the members of the AEL at Bristol for making me feel part of the group from the very start, sharing their wisdom (tracking-related and otherwise) and turning a tracking experiment into one of the most memorable experience of my PhD. Adriano, Beki, Daniel, Florent, Luke, and Rachael thank you for being such wonderfully weird and kind people. My time in Bristol with you was, without a doubt, my favourite.

About the Author

Linda Sartoris holds a BSc in Biology from Freie Universität Berlin, and an MSc in Molecular Biology and Evolution from Christian-Albrechts-Universität zu Kiel. Since joining ISTA in September 2018, her research has focused on understanding how colony organisation influences collective disease defences in ants. Her PhD project, "The effect of circadian rhythm on organisational immunity of ant colonies" was conducted in collaboration with the Stroeymeyt Ant Epidemiology Lab at the University of Bristol. During her doctoral studies, Linda presented her findings at international conferences, including the international IUSSI Congress in San Diego, USA (2022), and the European IUSSI Congress in Lausanne, Switzerland (2024).

List of Collaborators and Publications (if applicable)

My project is a collaboration of the Social Immunity Lab at ISTA, Austria, and the Ant Epidemiology Lab led by Nathalie Stroeymeyt at the University of Bristol, UK. All experimental support received for this project is detailed in the results part of the thesis.
This thesis is the basis for a manuscript with the current working title “Robustness of organisational immunity to circadian rhythmicity in ant colonies”.

Table of Contents

Abstract i
Acknowledgments ii
About the Author iii
List of Collaborators and Publications (if applicable) iv
Table of Contents v
List of Figures vi
List of Tables ix
List of Abbreviations xii
1 Introduction 1
2 Methods 5
2.1 Model organisms 5
2.2 Experimental set-up 7
2.3 Molecular analysis 12
2.4 Tracking data processing 14
2.5 Statistical analysis 18
3 Results 22
3.1 Constitutive circadian patterns in ant behaviour and colony networks 22
3.2 Effect of exposure on circadian patterns in ant behaviour and colony networks 26
4 Discussion 39
5 Supplementary Materials 47
5.1 Supplementary Figures 47
5.2 Supplementary Tables 51
References 76

List of Figures

Fig. 1: Host-pathogen system. (A) *Lasius niger* queen with larvae and workers, and (B) *Metarhizium brunneum* outgrowth on a sporulating queen cadaver (white hyphae and green spores). Photographs © Florian Strahodinsky 6
Fig. 2: Experimental arena and tracking system. (A) Layout of the experimental arena and (B) the arena placed in the tracking system. 10
Fig. 3: Two-dimensional interaction capsules. Representation of the two-dimensional capsules used for detecting interaction between ants based on proximity. Each ant is modeled with two parts: a larger shaded green shape representing the body and a smaller schaded blue shape at the front representing the head. An interaction is inferred when the blue head capsule of one ant overlaps with the capsule of another. Capsule of a queen (A) and of workers (B). 15
Fig. 4: Two-dimensional grooming capsules. Representation of the two-dimensional capsule used for inferring allogrooming interactions between workers. Each worker is modeled with two parts: a larger shaded blue shape representing the body and a smaller schaded green shape at the front representing the head. The shape of the capsules used for allogrooming slightly differ from those used to infer general interactions. 18
Fig. 5: Diurnal circadian activity patterns. Foragers and nurses exhibit diurnal activity patterns, being more active during the day: (A) the proportion of time individuals were active, (B) the speed at which they travelled while active, and (C) the average distance travelled during a three-hour interval (GLMM; Table S2a-b). Black bars represent the group medians, while boxes indicate the 95 % confidence intervals (CIs). Significant differences between day and night are denoted by *** (two-sided $p < 0.001$). Sample sizes: $N = 1360$ foragers, $N = 2706$ nurses, across 41 colonies. 23
Fig. 6: Circadian network patterns. During the pre-exposure period (pre1 & pre2), colonies exhibited daily rhythms in their network properties, leading to distinct circadian patterns. Despite substantial variation between colonies, the amplitude of day-night differences was consistent, as demonstrated here for network density. Similar patterns were observed for both (A) day-colonies, where tracking began at the beginning of the day, and (B) night-colonies, where tracking began at the beginning of the night. Each dot in (A) and (B) represents the aggregated network density of the colony for a three-hour interval, with three intervals during the day and three during the night. Grey lines connect dots from the same colony ($N_{day.colonies} = 19$, $N_{night.colonies} = 22$). Network properties significantly differed between day and night (GLMM, Table S4), with (C) density, (D) degree, (E) clustering, and (G) efficiency being higher during the day, while (F) modularity and (H) diameter were higher at night. In (C) - (H), black bars represent medians, and boxes show the 95 % CIs (pooled for day- and night-colonies, $N = 41$). Significant day-night differences are denoted by ** ($p < 0.01$) and *** ($p < 0.001$). 25
Fig. 7: Early induced changes in allogrooming. The plot shows exposure-induced changes during the first three hours of the post-exposure period. Allogrooming events received by the treated foragers were aggregated per colony over 15-minute time windows, separately for colonies treated during the day or night, exposed to either control or pathogen treatment ($N_{pathogen.day} = 10$, $N_{pathogen.night} = 11$, $N_{control.day} = 9$, $N_{control.night} = 11$). Across the three-hour interval, allogrooming occurred significantly more frequent post exposure with a greater increase in pathogen-treated colonies (GLMM, $p = 0.018$, Table S6b). Each point represents the Δ change in events per colony, bars represent the median, and boxes indicate 95 % CIs, based on 41 colonies (187 treated foragers in total). Δ changes were calculated by subtracting pre1-values from post-values within each colony, with the zero line indicating no induced changes. 27

Fig. 8: Induced changes in allogrooming. The plot shows exposure-induced changes during the first, second and third three-hour post-exposure windows, separately for colonies treated during the day or night, exposed to either control or pathogen treatment ($N_{pathogen.day}$ = 10, $N_{pathogen.night}$ = 11, $N_{control.day}$ = 9, $N_{control.night}$ = 11). Allogrooming events received by the treated foragers were aggregated per colony over three-hour time windows, with 60 % of all post-exposure allogrooming events occurring during the first three hours. Each point represents the Δ change in events per colony, bars represent the median, and boxes indicate 95 % CIs, based on 41 colonies (187 treated foragers in total). Δ changes were calculated by subtracting pre1-values from post-values within each colony, with the zero line indicating no induced changes. 28
Fig. 9: **Timeline of induced changes in network properties following pathogen exposure.** The plot shows pathogen-induced changes during the first, second and third three-hour post-exposure intervals, separately for day- and night-colonies, in (A) network density, (B) degree, (C) clustering, (D) modularity, (E) efficiency, and (F) diameter. Δ changes were calculated by subtracting pre1-values from post-values within each colony and interval, with the zero line indicating no induced changes. Bars represent the median, and boxes indicate 95 % CIs ($N_{pathogen.day}$ = 10 colonies, $N_{pathogen.night}$ = 11 colonies). 30
Fig. 10: Robust day-night differences after pathogen exposure. (A) and (B) show colony network density during the circadian phases directly before (pre2) and after (post) pathogen exposure. To visualise the robustness of day-night differences post-exposure, we calculated the "Δ day relative to night" (C - H): the night-values were subtracted from the day-values, such that the solid zero line indicates no day-night differences. This analysis was done separately for colonies experiencing daytime exposure and those experiencing night-time exposure, i.e., colonies treated at the start of the day, or the night, respectively. The daytime exposure Δ represents day(post) minus night(pre2), while the night-time delta represents day(pre2) minus night(post). The dashed line represents the median day-night differences observed in constitutive colonies (Δ day minus night; Fig. 6). In (C - H), black dots represent the median, and shaded boxes indicate 95 % CIs, based on $N_{daytime.exposure}$ = 10 colonies, and $N_{night\text{-}time.exposure}$ = 11 colonies. Significant day-night differences are denoted by * ($p < 0.05$), ** ($p < 0.01$), and *** ($p < 0.001$), while ns ($p > 0.05$) denotes a non-significant difference. 33
Fig. 11: Simulated and realised pathogen transmission. (A) Simulated transmission rate in pathogen-induced networks was similar during daytime and night-time (GLM; Table S12; N = 21 colonies). (B) Simulated pathogen loads for untreated foragers were comparable between day and night (GLMM; Table S13; N = 649 foragers, N = 1325 nurses. N = 21 queens). Nurses exhibited lower simulated loads than foragers, with no significant differences across day and night. Queens received intermediate simulated loads compared to foragers and nurses. In the realised pathogen transmission, (C) untreated foragers had a higher likelihood of contracting the pathogen than nurses (GLMM; Table S14; $N_{foragers.day}$ = 111 workers, $N_{foragers.night}$ = 140, $N_{nurses.day}$ = 550, $N_{nurses.night}$ = 309). (D) Among workers that acquired pathogen, foragers had higher pathogen loads than nurses (GLMM; Table S15; $N_{foragers.day}$ = 79 workers, $N_{foragers.night}$ = 104, $N_{nurses.day}$ = 220, $N_{nurses.night}$ = 97). Only two of the 13 analysed queens had detectable pathogen loads – one following daytime exposure ($1.1 * 10^{-4}$ ng/µL) and one following night-time exposure ($0.9 * 10^{-4}$ ng/µL) – and were thus not included in the statistical analysis. Bars in (A) represent the median, with boxes indicating 95 % CIs. In (B) and (D), each point represents one individual, with bars showing the median. Error bars in (C) represent the standard error of the mean. Letters denote significant differences ($p < 0.05$) between groups following post-hoc tests, and *** indicates $p < 0.001$. 36
Fig. 12: Interactions with pathogen-treated foragers. (A) Untreated foragers were more likely to have contact with treated foragers compared to nurses (GLMM; Table S16). (B) Untreated foragers also allogroomed treated foragers more frequently than nurses did

(aggregated per colony; GLMM; Table S17). Black bars represent the group medians, while boxes indicate the 95 % CIs. Letters denote significant differences ($p < 0.05$) between groups following post-hoc tests, and *** indicates $p < 0.001$. Sample sizes: $N = 649$ foragers, $N = 1322$ nurses, across 21 colonies. 38

Fig. S1: Constitutive transmission simulations. (A) Simulated transmission rate in constitutive networks (i.e., pre-exposure) was significantly higher during the day compared to the night (GLMM; Table S4). (B) Simulated pathogen loads were highest for foragers during the day, and significantly higher compared to the night. Nurses and queens exhibited lower simulated loads than foragers, with no significant differences between nurses and queens or across day and night (GLMM; Table S5). Bars in (A) represent the median, and boxes indicate 95 % CIs ($N = 41$ colonies). In (B), each point represents one individual, with bars showing the median ($N = 1360$ foragers, $N = 2706$ nurses. $N = 41$ queens). Significant day-night differences in (A) are denoted by *** ($p < 0.001$). In (B) letters denote significant differences ($p < 0.05$) between groups following post-hoc tests. 47

Fig. S2: Timeline of induced changes in network properties following control exposure. The plot shows control-induced changes during the first, second and third three-hour post-exposure intervals, separately for day- and night colonies, in (A) network density, (B) degree, (C) clustering, (D) modularity, (E) efficiency, and (F) diameter. Δ changes were calculated by subtracting pre1-values from post-values within each colony and interval, with the zero line indicating no induced changes. Bars represent the median, and boxes indicate 95 % CIs ($N_{control.day} = 9$ colonies, $N_{control.night} = 11$ colonies). For diameter, one extreme Δ-value (control.night, time post exposure 0, $\Delta = -48$) was removed from the plot after calculating the median and 95 % CIs to improve visibility. 48

Fig. S3: Robust day-night differences after control exposure. (A) and (B) show colony network density during the circadian phases directly before (pre2) and after (post) control exposure. To visualise the robustness of day-night differences post-exposure, we calculated the "Δ day relative to night" (C - H): the night-values were subtracted from the day-values, such that the solid zero line indicates no day-night differences. This analysis was done separately for colonies experiencing daytime exposure and those experiencing night-time exposure, i.e., colonies treated at the start of the day, or the night, respectively. The daytime exposure Δ represents day(post) minus night(pre2), while the night-time delta represents day(pre2) minus night(post). The dashed line represents the median day-night differences observed in constitutive colonies (Δ day minus night; Fig. 6). In (C - H), black dots represent the median, and shaded boxes indicate 95 % CIs, based on $N_{daytime.exposure} = 9$ colonies, and $N_{night\text{-}time.exposure} = 11$ colonies. Significant day-night differences are denoted by ** ($p < 0.01$) and *** ($p < 0.001$), while ns ($p > 0.05$) denotes non-significant differences. 49

Fig. S4: Control-induced transmission simulations. (A) Simulated transmission rate in control-induced networks was significantly higher during the day compared to the night (GLM; Table S10). (B) Simulated pathogen loads were equal for untreated foragers during the day and night. Nurses exhibited lower simulated loads than foragers, with no significant differences across day and night. Queens received simulated loads intermediate between foragers and nurses, with no differences between day and night (GLMM; Table S11). Bars in (A) represent the median, and boxes indicate 95 % CIs ($N = 20$ colonies). In (B), each point represents one individual, with bars showing the median ($N = 530$ foragers, $N = 1376$ nurses. $N = 20$ queens). Significant day-night differences in (A) are denoted by $p = 0.038$. In (B) letters denote significant differences ($p < 0.05$) between groups following post-hoc tests. 50

List of Tables

Table 1: Experimental time-line. Each experimental round included one day-colony and one night-colony. Two experimental rounds were conducted per week, with four rounds completed during weeks when R. Kennard assisted with the tagging. 8
Table 2: Abiotic conditions in the tracking systems. Temperature, visible light, and UV light intensity were reduced during the night, while humidity remained constant. Transitions started at 8 a.m. and 8 p.m. and lasted 30 minutes each. 11
Table 3: Treatment groups. The foragers were exposed to either the pathogen or control treatment 20 min before being returned to their colony, either at 9:30 a.m. for the day-colonies or 9:30 p.m. for the night-colonies. 12
Table 4: Circadian phases of day-colonies and night-colonies during exposure periods. Pre1 and pre2 represent two periods in the pre-exposure period. Post refers to the single period in the post-exposure period. Circadian phases correspond to the experimental conditions aligning with either daytime or night-time. 15

Table S1: Statistical results for the proportion of time spent outside the nest by foragers during daytime and night-time. We used a generalised linear mixed model (GLMM) with beta error distribution, including circadian phase (day/night) as main effect and controlling for colony size and colony ID. The proportion of time spent "outside" (i.e. in the foraging space) was aggregated for each colony to test differences between day and night (N = 1360 foragers; N = 41 colonies). Nurses were excluded from this analysis as they, by definition, don't spend more than 1 % of their time outside the nest. The table reports model details (response variable and main predictor in bold), test statistic (χ^2), degrees of freedom (df), p-value (exact unless < 0.001), and effect size (odds ratio day/night). All p-values are two-sided, bolded when significant (< 0.05). 51
Table S2: Statistical results for the activity of foragers and nurses during daytime and night-time. GLMM results, including circadian phase (day/night) as main effect and controlling for colony size and colony ID. The behaviours (time active, speed while active, and distance travelled) were aggregated for each colony to test differences between day and night, separately for (a) foragers (N = 1360) and (b) nurses (N = 2706; N = 41 colonies). The tables report model details (response variable and main predictor in bold), test statistics (χ^2), degrees of freedom (df), p-values (exact unless < 0.001), and effect sizes (partial η^2). All p-values are two-sided, bolded when significant (< 0.05). 52
Table S3: Statistical results for constitutive colony network properties during daytime and night-time. GLMM results, including circadian phase (day/night) as main effect. In addition to colony size and colony ID, we controlled for starting phase (day-/night-colonies), i.e. whether the colonies started the experimental tracking during daytime (N= 19) or night-time (N = 22). The network properties were aggregated for each colony. The table reports model details (response variable and main predictor in bold), test statistics (χ^2), degrees of freedom (df), p-values (exact unless < 0.001), and effect sizes (partial η^2). All p-values are two-sided and bolded when significant (< 0.05). 53
Table S4: Simulated transmission rate in constitutive colony networks during daytime and night-time. GLMM results, including circadian phase (day/night) as main effect and controlling for starting phase (day-/night-colonies), colony size and colony ID. The simulation was run on the constitutive networks for both the nine hours of daytime and nine hours of night-time (N = 41 colonies), originating from the same workers, that were later exposed. The table reports model details (response variable and main predictor in bold), test statistic (χ^2), degrees

of freedom (df), p-value (exact unless < 0.001), and effect size (partial η^2). All p-values are two-sided and bolded when significant (< 0.05).....53
Table S5: Simulated pathogen load in constitutive networks. GLMM results, including task group (forager/nurse) and circadian phase (day/night) as main effects, including their interaction. We controlled for colony size and colony ID. Based on N = 1360 foragers, N = 2706 nurses. N = 41 queens across 41 colonies. The table reports model details (response variable and main predictor in bold), test statistics (χ^2), degrees of freedom (df), p-values (exact unless < 0.001), and effect size (partial η^2). All p-values are two-sided and bolded when significant (< 0.05).....54
Table S6: Exposure-induced changes in allogrooming received by treated foragers. We used a negative binomial GLMM with a logit link function to test for changes in allogrooming events. The main effects were exposure (control/pathogen), circadian phase (day/night) and experimental period (pre1/post), including all their interactions. The experimental periods covered (a) the first 30 minutes of the tracking (pre1) compared to the first 30 minutes after exposure (post), or (b) the first three hours of the tracking (pre1) compared to the first three hours after exposure (post). We controlled for time of day (beginning of the 15-minute intervals) and colony ID for tests with multiple values per colony. Based on 187 treated foragers across 41 colonies. The tables report model details (response variable and main predictor in bold), test statistics (χ^2), degrees of freedom (df), p-values (exact unless < 0.001), and effect sizes (odds ratio). All p-values are two-sided, bolded when significant (< 0.05), and corrected for multiple testing using BH method for the tests reported in (a) and (b). Whenever the interactions were non-significant, the effects of the main predictors were estimated from the reduced model.....56
Table S7: Exposure-induced changes in network properties during the first and third three-hour windows. GLMM results, including exposure (control/pathogen), experimental period (pre1/post) and circadian phase (day/night) as main effects, including all their interactions. The experimental periods covered (a) the first three-hour window of the tracking (pre1) and the first three-hour window post exposure (post), or (b) the third three-hour window of the tracking (pre1) and the third three-hour window of the tracking (post). We controlled for colony size and colony ID. Based on 10 “pathogen day”-colonies, 11 “pathogen night”-colonies, 9 “control day”-colonies, and 11 “control night”-colonies. The tables report model details (response variable and main predictor in bold), test statistics (χ^2), degrees of freedom (df), p-values (exact unless < 0.001), and effect sizes (partial η^2). All p-values are two-sided, bolded when significant (< 0.05), and corrected for multiple testing, i.e., testing the first and third three-hour window, using BH method for each network property. Because the interactions were non-significant, the effects of the main predictors were estimated based on the reduced model.....58
Table S8: Slope analysis of the exposure-induced changes in network properties across all three three-hour windows. GLMM results, including exposure (control/pathogen), circadian phase (day/night), and time hours post (0/3/6; start time of the three-hour window post exposure) as main effects, including all their interactions. The experimental periods covered the first nine hours of the tracking (pre1) and the last nine hours (post). We controlled for colony size and colony ID. The analysis was done on the delta values (post minus pre1) of each colony per time window in post. Based on 10 “pathogen day”-colonies, 11 “pathogen night”-colonies, 9 “control day”-colonies, and 11 “control night”-colonies. The table reports model details (response variable and main predictor in bold), test statistics (χ^2), degrees of freedom (df), p-values (exact unless < 0.001), and effect sizes (partial η^2). All p-values are two-sided and bolded when significant (< 0.05). Because the interactions were non-significant, the effects of the main predictors were estimated based on the reduced model.....62

Table S9: Day-night differences within colonies transitioning from the pre-exposure period into the post-exposure period. GLMM results, including circadian phase (day/night) as main effect, and controlling for colony size and colony ID. The experimental periods covered the second nine-hour interval of the tracking (pre2) and the last nine hours (post). The analysis was done separately for the four treatment groups, (a) 10 "pathogen day"-colonies transitioning from pre(night) to post(day), (b) 11 "pathogen night"-colonies transitioning from pre(day) to post(night), (c) 9 "control day"-colonies transitioning from pre(night) to post(day), and (d) 11 "control night"-colonies transitioning from pre(day) to post(night). The tables report model details (response variable and main predictor in bold), test statistics (χ^2), degrees of freedom (df), p-values (exact unless < 0.001), and effect sizes (partial η^2). All p-values are two-sided and bolded when significant (< 0.05). 65
Table S10: Simulated transmission rate in control-induced colony networks during daytime and night-time. GLM results, including circadian phase (day/night) as main effect and controlling for colony size. The simulation was run on the control-induced networks for both the nine hours of daytime ($N = 9$), and nine hours of night-time ($N = 11$), originating from the treated foragers. The table reports model details (response variable and main predictor in bold), test statistic (χ^2), degrees of freedom (df), exact p-value, and effect size (partial η^2). All p-values are two-sided and bolded when significant (< 0.05). 66
Table S11: Simulated pathogen load in control-induced networks. GLMM results, including task group (forager/nurse) and circadian phase (day/night) as main effects, including their interaction. We controlled for colony size and colony ID. Based only on the control-treated colonies (daytime exposure $N = 9$, and night-time exposure $N = 11$). The table reports model details (response variable and main predictor in bold), test statistics (χ^2), degrees of freedom (df), p-values (exact unless < 0.001), and effect size (partial η^2). All p-values are two-sided and bolded when significant (< 0.05). 67
Table S12: Simulated transmission rate in pathogen-induced colony networks during daytime and night-time. GLM results, including circadian phase (day/night) as main effect and controlling for colony size. The simulation was run on the pathogen-induced networks for both the nine hours of daytime ($N = 10$), and nine hours of night-time ($N = 11$), originating from treated foragers. The table reports model details (response variable and main predictor in bold), test statistic (χ^2), degrees of freedom (df) and exact, two-sided p-value. 69
Table S13: Simulated pathogen load in pathogen-induced networks. GLMM results, with task group (forager/nurse) and circadian phase (day/night) as main effects, including their interaction. We controlled for colony size and colony ID. Based only on the pathogen-treated colonies (daytime exposure $N = 10$, and night-time exposure $N = 11$). The table reports model details (response variable and main predictor in bold), test statistics (χ^2), degrees of freedom (df), p-values (exact unless < 0.001), and effect size (partial η^2). All p-values are two-sided and bolded when significant (< 0.05). 70
Table S14: Proportion of workers with detectable pathogen loads. Results for GLMM with binomial error distribution, including circadian phase (day/night) and task group (forager/nurse) as main effects, as well as their interaction. We controlled for colony ID. Based only on a subset of the pathogen-treated colonies (daytime exposure $N = 660$ workers across 7 colonies, and night-time exposure $N = 449$ across 6 colonies). The table reports model details (response variable and main predictor in bold), test statistics (χ^2), degrees of freedom (df), p-values (exact unless < 0.001), and effect size (odds ratio). All p-values are two-sided and bolded when significant (< 0.05). Because the interaction was non-significant, the effects of the main predictors were estimated from the reduced model. 71
Table S15: Measured qPCR pathogen loads. GLMM results, with circadian phase (day/night) and task group (forager/nurse) as main effects, including their interaction. We controlled for colony ID. Based only on those workers that had detectable pathogen loads

(daytime exposure N = 299 workers across 7 colonies, and night-time exposure N = 201 workers across 6 colonies). The table reports model details (response variable and main predictor in bold), test statistics (χ^2), degrees of freedom (df), p-values (exact unless < 0.001), and effect size (partial η^2). All p-values are two-sided and bolded when significant (< 0.05). Because the interaction was non-significant, the effects of the main predictors were estimated from the reduced model. 72
Table S16: Duration of contact with treated foragers. GLMM results, with task group (forager/nurse) and circadian phase (day/night) as main effects, including their interaction. We controlled for colony ID. Based only on the pathogen-treated colonies (daytime exposure N = 10, and night-time exposure N = 11). The table reports model details (response variable and main predictor in bold), test statistics (χ^2), degrees of freedom (df), p-values (exact unless < 0.001), and effect size (partial η^2). All p-values are two-sided and bolded when significant (< 0.05). 73
Table S17: Allogrooming rate direct toward treated foragers. GLMM results, with circadian phase (day/night) and task group (forager/nurse) as main effects, including their interaction. We controlled for colony ID. Based only on the pathogen-treated colonies (daytime exposure N = 10, and night-time exposure N = 11). The table reports model details (response variable and main predictor in bold), test statistics (χ^2), degrees of freedom (df), p-values (exact unless < 0.001), and effect size (partial η^2). All p-values are two-sided and bolded when significant (< 0.05). Because the interaction was non-significant, the effects of the main predictors were estimated from the reduced model. 74
Table S18: Proportion of allogrooming received by treated foragers outside the nest. Results for GLM with beta error distribution, including circadian phase (day/night) and exposure (control/pathogen) as main effects, as well as their interaction. Based only on the pathogen-treated colonies (daytime exposure N = 10, and night-time exposure N = 11). The table reports model details (response variable and main predictor in bold), test statistics (χ^2), degrees of freedom (df), and exact, two-sided p-value. 75
Table S19: List of consumables. 75

List of Abbreviations

AEL	Ant Epidemiology Lab
FORT	Formicidae Tracker
GL(M)M	Generalised linear (mixed) model
LED	Light-emitting diode
qPCR	Quantitative real-time PCR

1 Introduction

In social insects, various ecological and behavioural factors – such as high relatedness, dense populations, microbe-rich environments, and frequent physical contact – increase the risk of colony-wide infections (Cremer et al., 2007; Schmid-Hempel, 2017; Shykoff & Schmid-Hempel, 1991). To counter this risk, social insects have evolved effective strategies to prevent epidemics, including a colony-level immune defence known as social immunity (Cremer et al., 2007).

Social immunity is often likened to the immune system of multicellular organisms, with both providing similar layers of defence: border defence, soma defence and germline defence (Cremer & Sixt, 2009). In social insect colonies, these defences prevent pathogen entry, protect sterile workers, and safeguard the brood and reproductive queen, thereby ensuring colony fitness (Cremer et al., 2018). Social immunity includes organisational, behavioural, and physiological measures that mitigate the risks from their social and ecological environment (Cremer et al., 2007; Cremer et al., 2018; Evans & Spivak, 2010; Liu, Zhao, et al., 2019; Simone-Finstrom, 2017).

Organisational immune defences

Social interaction networks in insect colonies are not random but highly structured, with interactions following simple rules that give rise to sophisticated group-level properties (Charbonneau et al., 2013; Mersch et al., 2013). This social organisation plays a critical role in influencing disease propagation within the colony (Cremer et al., 2007; Naug & Camazine, 2002; Naug & Smith, 2007; Stroeymeyt et al., 2014; Stroeymeyt et al., 2018).

Organisational immunity operates on both structural and dynamic levels. Structurally, spatial fidelity in the nest and division of labour create distinct task groups, such as less mature nurses, and more mature foragers (Mersch, 2016; Richardson et al., 2021). Nurses typically remain in the nest to tend the brood, while foragers venture outside to gather resources for the colony (Kay et al., 2024). As a form of architectural immunity, ants may also alter the structure of their nest in response to pathogens introduced by exposed workers to reduce disease spread (Leckie et al., 2024). Dynamically, individual activity levels and contact rates further influence transmission pathways, either inhibiting or enhancing disease spread (Barthélemy et al., 2005; Blonder & Dornhaus, 2011; Lehue & Detrain, 2019; Pinter-Wollman et al., 2011; Quevillon et al., 2015; Stroeymeyt et al., 2014).

Importantly, social network dynamics are also plastic, adjusting in response to pathogen exposure. For example, when exposed to pathogenic fungi, colonies of the black garden ant *Lasius niger* altered their network properties to further inhibit transmission compared to pathogen-free conditions (Stroeymeyt et al., 2018). Specifically, originating from pathogen-foragers, the spread is largely contained within the forager task group. In contrast, nurses and the queen show a lower pathogen burden, highlighting the colony's ability to limit transmission to vulnerable individuals (Stroeymeyt et al., 2018). This demonstrates that organisational immunity can function both prophylactically and reactively, with structural and dynamic adjustments reinforcing disease resistance.

Behavioural immune defences

A key element of behavioural immune defences is allogrooming, a sanitary care behaviour in which nest mates remove particles from each other's cuticles (Rosengaus et al., 1998). In addition to allogrooming, some ants also engage in chemical disinfection, such as spraying antimicrobial poison (Pull, Metzler, et al., 2018; Tragust et al., 2013). These behaviours can be performed prophylactically to prevent contamination or in direct response to a pathogen to eliminate the threat or remove infections from within the colony. When a colony member becomes contaminated, naïve nest mates intensify their sanitary care behaviours to prevent the disease from establishing (Bos et al., 2012; Okuno et al., 2012; Qiu et al., 2014; Walker & Hughes, 2009). The contaminated individual increases self-grooming but reduces allogrooming (Casillas-Pérez et al., 2023; Theis et al., 2015). If prevention fails, ants take drastic measures, such as workers destroying infected pupae (Pull, Ugelvig, et al., 2018) or queens cannibalising infected larvae (Bizzell & Pull, 2024), to stop the infection from spreading.

Physiological immune defences

Sanitary care behaviours, while beneficial, can inadvertently lead to pathogen transmission among previously naïve nest mates (Theis et al., 2015), which may result in low-level infections. These infections often do not cause disease but can trigger protective physiological immune defences, such as immunisation against future exposure to the same pathogen (Konrad et al., 2012; Ugelvig & Cremer, 2007). However, it can also increase susceptibility to superinfections by other pathogens (Konrad et al., 2018).

Activity rhythms

The activity rates of social insects are not constant but follow rhythms that operate at both individual and colony levels. These rhythms are influenced by various factors and can vary between task groups.

Circadian rhythms, which oscillate over a 24-hour period, are regulated by endogenous (internal) and exogenous (external) components. Endogenous circadian rhythms persist in the absence of external synchronising cues, or *zeitgebers*, such as light or temperature (Aschoff, 1960; Dunlap et al., 2004). In social insects, these endogenous rhythms can differ between individuals within a colony, particularly between different task groups (e.g. nurses or foragers). For instance, nurses exhibit fewer genes with daily oscillating patterns compared to foragers, who show endogenous daily rhythms in gene expression (Das & Bekker, 2022; Ingram et al., 2009; Tomioka & Matsumoto, 2015). Similar clock genes are found across ants and bees, suggesting a shared circadian clock that may contribute to task-group differences (Ingram et al., 2012).

In *Camponotus compressus* ants, foragers exhibit endogenous circadian rhythms under constant darkness, while other workers are arrhythmic (Sharma et al., 2004). The same study also demonstrated the importance of exogenous zeitgebers: under light-dark cycles, previously arrhythmic workers adopt nocturnal (active during the night) or diurnal (active during the day)

patterns or stay arrhythmic. This highlights how rhythms result from both internal and external inputs, varying across individuals within a colony.

While light is a dominant zeitgeber for fruit flies (Schlichting & Helfrich-Förster, 2015), temperature and social context are equally important for social insects living in dark nests (Bloch et al., 2013; Cros et al., 1997; Fujioka et al., 2019, 2021; Lone & Sharma, 2011; Siehler et al., 2021). For example, some nurses that display endogenous circadian rhythms in isolation, become arrhythmic in a social context or when caring for brood that require constant attention, such as larvae reliant on around-the-clock feeding and sanitary care (Fujioka et al., 2017; Mildner & Roces, 2017).

Within the colony, nurses exhibit less pronounced daily rhythms, whereas foragers often display more distinct activity patterns. Both task groups, however, are highly flexible and adapt to various environmental and social cues.

Foraging preferences in ants can change in response to factors such as rain or predation risk (Dolai et al., 2024), food availability (Mildner & Roces, 2017), light conditions (Lei et al., 2019), and climate (Villalta et al., 2020). *L. niger* foragers – the species in this study – exhibit considerable variability in their activity. They prefer humid and cool weather, with peak activity at night and dawn in some cases (Depa, 2024), while in others, they adopt diurnal foraging patterns in spring and showing no clear preference during summer (Yamauchi & Hayashida, 1970).

This variability in foraging activity may have important implications for pathogen transmission. Foraging increases the likelihood of encountering pathogens, which can subsequently be passed on to others (Kurze et al., 2020). As a result, foragers' activity rhythms potentially create periods of heightened contamination risk for the colony during their preferred foraging times.

Colony rhythms

Driven by workers' activity, the colony also exhibits rhythms that can alter colony network properties, potentially affecting pathogen transmission. While the effect of activity cycles on transmission has often been studied without pathogens, simulations highlight the relevance of interaction networks structured in space and time for disease spread (Quevillon et al., 2015; Richardson & Gorochowski, 2015).

For instance, simulations across short-term activity cycles (~ 20 minutes) in diurnal *Leptothorax* ants suggest that periodic reductions in interaction rates inhibit transmission by allowing outdated information to be "forgotten" (Cole, 1991; Richardson et al., 2017). However, this inhibitory effect diminishes for agents with decay rates exceeding the duration of the cycles, such as many pathogens. Therefore, short-term burst of activity are unlikely to function as a form of organisational immunity.

While social network structures with two main communities are highly conserved across ant species (Kay et al., 2024), it remains unclear how organisational immunity – or sanitary care responses – may be influenced by daily rhythms.

Notably, Stroeymeyt et al. (2018) observed pathogen-induced organisational immunity in *L. niger* colonies over a full 24-hour day-night cycle, comparing post-treatment periods to their respective pre-treatment baselines. By including time of day as a random factor, they accounted for daily activity rhythms and detected pathogen-induced changes. However, this raises an intriguing question that underpins the current study: how do daily activity rhythms influence a colony's social defences and susceptibility to disease?

Study aim

For this reason, we studied whether circadian rhythms influence disease susceptibility in ant colonies and how social defences respond to pathogen contamination at different times of day. Using automated marker-based tracking of *L. niger* colonies, we employed a new "Behavioural Inference Tool" to automatically identify allogrooming interactions directly from the tracking data (Wanderlingh, 2024). To characterise the colony's network properties, we analysed aggregated, weighted contact networks and performed transmission simulations using time-ordered networks, given the critical role of interaction sequences in disease spread (Petter Holme & Saramäki, 2012; Mersch, 2016; Stroeymeyt et al., 2018).

Our study first characterises daily rhythms in worker activity and network dynamics in pathogen-free colonies to establish constitutive baseline variations in disease susceptibility throughout the day. Next, we explore pathogen-induced changes in sanitary care and network dynamics by exposing foragers to a natural pathogen (*Metarhizium brunneum*) either during the day or at night, while keeping pathogen dose consistent across exposure times. Finally, we assess the impact of these induced changes on pathogen transmission by measuring individual pathogen loads after a nine-hour post-exposure period. Colonies were maintained under 12-hour light-dark cycles with higher daytime temperatures to mimic natural activity rhythms driven by external zeitgebers.

During the more active phase, faster detection of pathogens and increased allogrooming may strengthen social defences, while during the less active phase, pathogens may be more easily overlooked. Nevertheless, ants likely possess mechanisms to intensify activity in response to disturbances, even during resting periods.

Pathogen transmission during less active phases could *increase* due to higher worker numbers inside the nest (Naug, 2009; Pie et al., 2004) and reduced separation of task groups, with fewer interactions to reinforce the community structure (Mersch et al., 2013; Richardson et al., 2021). Conversely, transmission could *decrease* due to fewer active individuals, slowing down interaction rates (Richardson et al., 2017), and reducing foraging activity, which limits food exchange between foragers and nurses (Charbonneau et al., 2013; Quevillon et al., 2015).

This duality underscores the complex relationship between activity rhythms, network dynamics, and disease transmission. If activity levels vary between day and night, network properties may shift accordingly. Yet, immunity must remain effective throughout the day, prompting us to investigate how colonies balance these demands.

2 Methods

2.1 Model organisms

Ant host Lasius niger

The black garden ant, *Lasius niger*, belonging to the Formicinae subfamily, is distributed across the Holarctic realm, encompassing biogeographic regions with varying climates, vegetation and altitudes (Arnan et al., 2017). *L. niger* is one of the most prevalent native ant species in Europe and is highly territorial, aggressively defending its monodomic (single) nests against neighbouring colonies (Arnan et al., 2017; Czechowski, 1984; Sommer & Hölldobler, 1995). Nuptial flights take place annually when the alates (winged virgin queens and males) emerge synchronously from their parental nests. After mating, typically with a single mate (Boomsma & van der Have, 1998), the males die, while the queens shed their wings, burrow into the ground, and begin founding a new colony independently, without worker assistance. During this initial phase, the queen will not forage but rather metabolise her wing muscles, fat body and even parts of her brain (Janet, 1907; Julian & Gronenberg, 2002). Although co-founding by multiple foundresses can occur, the queens will eventually fight until only one remains (monogyny), which usually happens after the first workers emerge (Fig. 1A) (Aron et al., 2009; Sommer & Hölldobler, 1995). At that stage, the workers – who are sterile – take over the brood care, nest maintenance, and foraging, allowing the colony to grow to an average size of 10,000 workers (Arnan et al., 2017). Colonies thrive on the sugar-rich honeydew produced by aphids, which *L. niger* foragers protect from predators in a mutualistic relationship (Depa, 2024). The workers can live for a few years, while the queen may reach an age of 20 years or more (Kramer et al., 2016). However, once the queen dies, the colony will eventually perish, as its fitness ultimately depends on her reproductive capabilities.

Newly mated queens can be easily collected in large numbers just after their nuptial flight and reared in the laboratory, making *L. niger* a suitable study organism for studying individual and colony-wide behaviours related to social immunity (Bizzell & Pull, 2024; Brütsch et al., 2017; Casillas-Pérez et al., 2022; Pull & Cremer, 2017; Stroeymeyt et al., 2018). The colonies used in this study were initiated from newly mated queens collected in Bristol, England, in July 2021. The Ant Epidemiology Lab (AEL) at the University of Bristol led by Dr. Nathalie Stroeymeyt kindly provided them for this experiment.

Fungal pathogen Metarhizium brunneum

The generalist entomopathogenic fungus *Metarhizium brunneum*, formerly known as *M. anisopliae* but since classified as a sister species (Bischoff et al., 2009), is ubiquitous in the soil and a natural pathogen of *L. niger* (Cremer et al., 2018; Keller et al., 2003; Pull et al., 2013). It is known to kill a wide range of insects on all continents except Antarctica and has been utilised in the biocontrol of insect pests (Roberts & St Leger, 2004). As a pathogen, *Metarhizium* is an obligate killer, relying on killing its host to complete its reproductive cycle. Its conidiospores (hereafter "spores") can easily be picked up by insects from the environment (Kurze et al., 2020). Once the spores adhere to the host's cuticle, they swell and germinate. At this stage, the individual is considered contaminated but behavioural interventions such as self- or allogrooming can still influence the course of the infection. These behaviours aid in removing

infectious spores, reducing the number of infective particles capable of penetrating the host. This is crucial, as the likelihood of developing disease increases with the infection dose (Hughes et al., 2002). After approximately 12 to 48 hours, a specialised structure called an "appressorium" forms, ensuring that the spores attach firmly to the insect cuticle and preventing their removal by grooming (Hänel, 1982; Vestergaard et al., 1995). This allows the fungus to penetrate the host's body surface. From this point onward, the infection establishes itself, and the host transitions from being contaminated to being infected. If the host's immune defences become overwhelmed, blastospores (sexual spores) are released into the haemolymph, where they metabolise sugars and produce toxins in the still living insect. Additionally, hyphae and hyphal bodies develop, releasing more toxins that can induce death as soon as 48 hours after contamination (Hänel, 1982). These toxins contain destruxins, which suppress the immune response and have a cytotoxic effect (Pedras et al., 2002; Roberts & St Leger, 2004). Notably, *M. brunneum* blastospores do not trigger a detectable individual immune response in *L. niger* (Masson et al., 2024). The mycelium continues to grow, with hyphae invading the fat body and other tissues until they eventually burst through the cuticle from the inside, producing conidiochains all over the cadaver (Fig. 1B) that are packed with infectious spores (Hänel, 1982). Host death typically occurs between two to eight days; however mortality depends on factors such as exposure dose, humidity and the composition of the insect's cuticle (Grizanova et al., 2019; Hänel, 1982; Hughes et al., 2002).

While group-living enhances the survival chances of the fungus-contaminated individuals, close social interactions and shared environments help the transfer of spores to naïve nest mates (Hughes et al., 2002; Kurze et al., 2020). When low numbers of spores are transferred, they can immunise nest mates against future encounters with *Metarhizium*. However, the transfer of high spores numbers increases the risk of mortality (Konrad et al., 2012; Kurze et al., 2020; Liu, Wang, et al., 2019).

Fig. 1: Host-pathogen system. (A) *Lasius niger* queen with larvae and workers, and (B) *Metarhizium brunneum* outgrowth on a sporulating queen cadaver (white hyphae and green spores). Photographs © Florian Strahodinsky

2.2 Experimental set-up

General experimental design

To assess the effect of a circadian rhythm on organisational immunity in ant colonies, we employed individual behavioural tracking of *L. niger* colonies both before ("pre-exposure") and after ("post-exposure") introducing foragers treated either with infectious *M. brunneum* spores, or with a non-infectious control solution (Triton X-100). To compare the transmission of pathogenic spores between day and night networks, we introduced the treated foragers either at the start of the day or the start of the night. The experiment concluded after a nine-hour post-exposure period, ensuring observations remained in the same circadian phase (see "Time line"; Table 1).

All colonies were size-standardised to approximately 100 workers (see "Set-up of experimental colonies"), and each ant was tagged with a unique barcode marker (see "Individual tagging"). The colonies were then transferred to the experimental arena, which consisted of a covered nest area and an open foraging space with access to water and 20 % sugar solution (see "Experimental arena"). The arena was placed inside the insulated tracking system (as outlined in Wanderlingh 2024), where temperature and light intensity were controlled in a 12-hour day/night cycle (see "Tracking system"; Table 2). Using the images from the tracking system, the position and orientation of the barcode markers were recorded in real time at eight frames per second, allowing for construction of proximity networks (see "Tracking data processing").

First, we aimed to establish whether the organisation of the colony network follows a circadian rhythm, and second, how this may influence pathogen transmission within the colony.

To address the first question, colonies experienced one undisturbed day/night cycle during the pre-exposure period, with half of the colonies starting at the beginning of the day ("day-colonies") and the other half at the beginning of the night ("night-colonies"). This setup allowed us to identify constitutive individual and colony-wide network characteristics for both daytime and night-time periods.

To address the second question, we collected approximately 5 % of the workers from the foraging space at the end of the pre-exposure period. These foragers were treated with either a suspension of *M. brunneum* spores or the control solution, with half of the colonies assigned to the "pathogen" group and the other half to the "control" group (see "Pathogen exposure"; Table 3). The post-exposure period began when the inoculated foragers were returned to their colonies ($N_{\text{pathogen.day}} = 12$ colonies; $N_{\text{control.day}} = 12$; $N_{\text{pathogen.night}} = 12$; $N_{\text{control.night}} = 11$; initial sample size but see "Colony exclusion"). Nine hours later, the state of pathogen transmission was conserved by gently placing the experimental arena in a polystyrene foam box filled with dry ice (-78.6 °C) to snap-freeze all the ants in place. Each ant in the pathogen group was then individually sampled to determine their pathogen load using quantitative real-time PCR (see "Molecular analysis"). The samples were stored at -70 °C.

The experiment was conducted during a research stay at the Ant Epidemiology Lab (AEL) of our collaboration partner, Dr. Nathalie Stroeymeyt, at the University of Bristol, England, from October to December 2022. During a subsequent visit in June and July 2023, I performed the pre-processing of the tracking data and started the post-processing. Molecular analysis was performed in the Social Immunity Lab at ISTA, Klosterneuburg, Austria.

Time line

The experiment spanned eight weeks, during four of which Rebecca Kennard, MSc student in the AEL in Bristol, assisted in applying barcode markers to 16 colonies (four colonies per week). The experiments lasted six or seven days, depending on whether tracking and forager exposure began during the day ("day-colony") or the night ("night-colony") (Table1).

For each round of experiments, one day-colony and one night-colony were tagged on the same day (Day1). If an ant had lost its tag, it was reapplied the following day before the entire colony was transferred into the experimental arena and placed into the tracking system (Day 2). The colonies were then left undisturbed for the next two days to acclimate to the new conditions (Days 3 & 4). On the following day (Day 5), the pre-exposure period began at 9:30 a.m. GMT for the day-colonies and at 9:30 p.m. GMT for the night-colonies, lasting nine hours until 6:30 a.m. or 6:30 p.m. GMT on Day 6, respectively. During the three-hour interval between the pre- and post-periods, foragers were collected from the foraging space, treated with the fungal suspension or control solution, and returned to their colonies five minutes before the post-exposure tracking started (Day 6). Nine hours later – at 6:30 p.m. for the day-colonies and 6:30 a.m. GMT the next day (Day 7) for the night-colonies – the post-exposure period ended, and the colonies were snap-frozen on dry ice. This procedure was repeated with another two colonies (one day-, one night-) on two consecutive days, resulting in a total of four colonies processed each week. In the weeks R. Kennard assisted with the tagging, eight colonies could be processed.

Table 1: Experimental time-line. Each experimental round included one day-colony and one night-colony. Two experimental rounds were conducted per week, with four rounds completed during weeks when R. Kennard assisted with the tagging.

Day	day-colony	night-colony
1	Tagging (morning)	Tagging (afternoon)
2	Re-tagging & move into tracking systems (evening)	Re-tagging & move into tracking systems (evening)
3	Acclimation	Acclimation
4	Acclimation	Acclimation
5	9:30 a.m. Start "pre-exposure" period	9:30 p.m. Start "pre-exposure" period
6	6:30 – 9:25 a.m. Forager collection & exposure 9:30 a.m. Beginning "post-exposure" period 6:30 p.m. End "post-exposure" period	6:30 – 9:25 p.m. Forager collection & exposure 9:30 p.m. Beginning "post-exposure" period
7		6:30 a.m. End "post-exposure" period

Set-up of experimental colonies

Four and a half weeks before each replicate's Day 1, the colonies were standardised to a size of 105 workers. The queen and larvae remained in the colony. At that time, the colonies were 15 months old, and the average worker size was 2.95 mm. Colonies were reared on a 20 % sugar solution provided *ad libitum* and fed weekly with *Drosophila hydei* fruit flies in a climate-controlled room, maintained at 25 °C with 65 % relative humidity and a 12-hour day/night light cycle.

Individual tagging

On Day 1 of the experiment, ants were tagged with unique fiducial markers that allowed us to track the position of each individual within the colony. These markers are two-dimensional barcodes printed on polycarbonate-sheet squares, designed to encode small data payloads of 4 to 12 bits (Tag library: "AprilTag 41H12 Standard Family") (Olson, 2011; Wang & Olson, 2016). The tag squares measured 0.76 mm per side for the workers and 1.52 mm for queens. Previous studies have shown that the tags' weight does not impair the ant movement or behaviour (Mersch et al., 2013; Stroeymeyt et al., 2018). Under CO_2 anaesthesia, the tags were affixed to the ants' mesoma (thorax) using a tiny droplet of glue (Pattex Power Easy Gel). After a 10-minute recovery period in isolation, the ants were placed in a simple temporary nest overnight with water provided *ad libitum*. The next day, any tags that had fallen off were reapplied, though the incident rate was very low.

Experimental arena

On Day 2 of the experiment, colonies were transferred to experimental arenas, which were designed by Adriano Wanderlingh, PhD student in the AEL in Bristol, for his own previous tracking experiments (Wanderlingh, 2024). The arenas, laser-cut from transparent acrylic, had two compartments: the nest and the foraging space, connected by a 6 x 3 x 3 mm (L x W x H) tunnel (Fig. 2A). The square nest area (59.76 x 59.76 x 6 mm) had a plastered floor, which was watered once with 530 µL at the start of the acclimation phase. The nest was covered with an infrared transmitting glass filter (Schott RG715), blocking light with wavelengths shorter than 715 nm. This created a relatively dark environment compared to the uncovered foraging space, while still allowing for the tracking of the barcode markers.

The foraging space, measuring 90 x 60 x 40 mm (L x W x H), had an open top and an acrylic floor, providing access to water and 20 % sugar solution *ad libitum* via two cotton-stoppered containers placed underneath. A thin layer of Fluon® (AGC Chemicals) was applied to prevent ants from climbing the arena walls. After transferring the colonies to the nest area at 4 °C, the experimental arenas were placed into the tracking system for the acclimation phase (Fig. 2B).

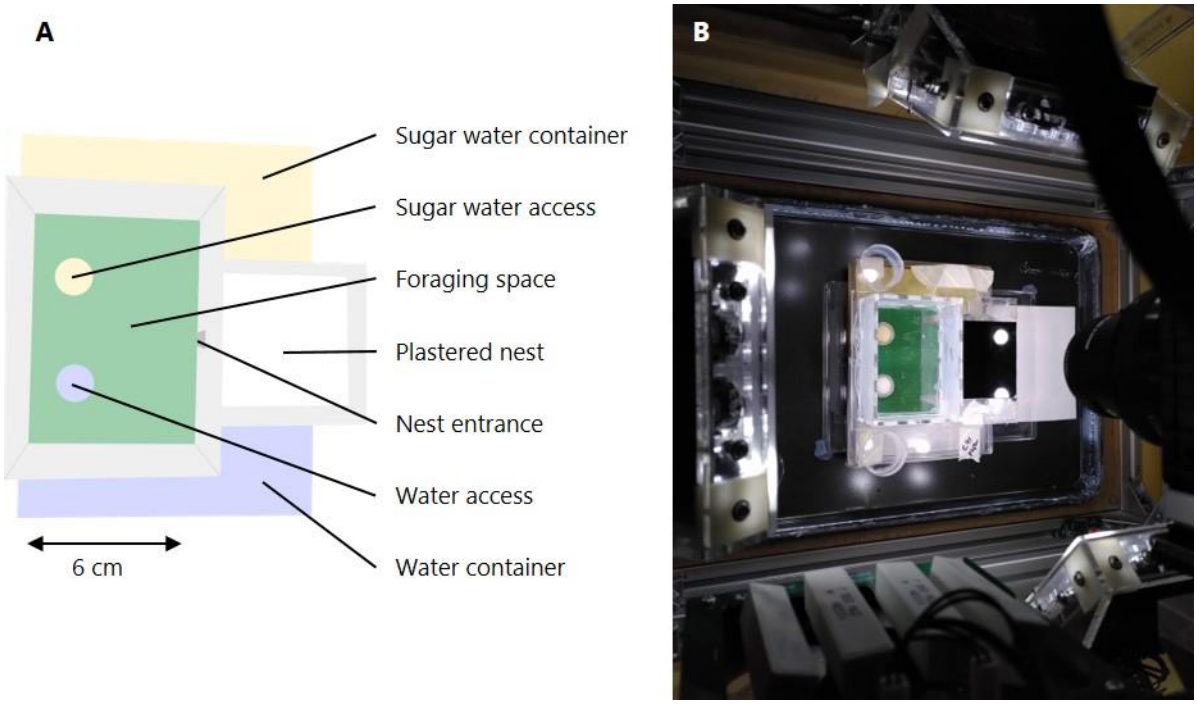

Fig. 2: Experimental arena and tracking system. (A) Layout of the experimental arena and (B) the arena placed in the tracking system.

Tracking system

On Days 3 & 4 of the experiment, the colonies acclimated to the conditions of the Formicidae Tracker (FORT) system, developed at the University of Lausanne, Switzerland (CERN Open Hardware Licence, Version 1.2). Each system was equipped with four panels of 16 warm white light-emitting diodes (LEDs), four panels of four UV light LEDs, a heating element, a mist maker, and a fan, all enclosed in a polystyrene box (Fig. 2B). This setup allowed us to control the climatic conditions and to simulate day-night cycles. Since the foraging behaviour of *L. niger* seems to be highly influenced by temperature and light intensity (Yamauchi & Hayashida, 1970), we reduced both during the night, with a 30-minute transition period starting at 8 a.m. and 8 p.m. GMT (Table 2). Humidity levels remained constant throughout the experiment.

On Day 5, the tracking of the pre-exposure period began, recording the colonies' constitutive network properties under the shifting day and night conditions.

To track the ants by their individual barcode marker, each tracking system featured a high-resolution monochrome camera (Flare 48M30-MCX) equipped with an enlarging lens (Apo-Rodagon-N 2.8/50) and a near-infrared longpass filter (MidOpt LP800/40.5). Additional infrared LEDs emitted light flashes synchronised with the camera trigger, which captured images at eight frames per second with a 7920 x 6004 pixel resolution. A feature detection algorithm analysed the images in real time, recording the position and orientation of the barcode markers. This information, along with a time stamp, constituted the tracking data for each individual. An MPEG-4 video of the captured images (8 fps) was saved with a 1424 x 1088 pixel resolution.

Table 2: Abiotic conditions in the tracking systems. Temperature, visible light, and UV light intensity were reduced during the night, while humidity remained constant. Transitions started at 8 a.m. and 8 p.m. and lasted 30 minutes each.

Conditions	Day (8 a.m. - 8 p.m.)	Night (8 p.m. – 8 a.m.)
Temperature [°C]	26	22
Visible light [%]	10	1
UV light [%]	10	0
Relative humidity [%]	60	60

Pathogen exposure

On Day 6 of the experiment, we aimed to collect five workers per colony from the foraging space. This number varied slightly between colonies (range: 3-5, mean: 4.7) due to occasional instances where fewer foragers appeared in the foraging space during the collection window. Foragers were gently collected using a brush and treated with either the fungal suspension or the control solution before being returned to the colony for the post-exposure period. The fungus treatment consisted of a *M. brunneum* suspension (strain MA275, KVL 03-143, which had been kindly provided by Joergen Eilenberg and Nicolai V. Meyling, University of Copenhagen, Denmark) in 0.05 % autoclaved Triton™ X-100 (Sigma) at a concentration of 10^9 spores per mL (Table 3). As a sham control, workers from half of the colonies were exposed to 0.05 % Triton X-100 alone.

The fungus was retrieved from long-term storage at -80 °C and cultured on Sabouraud dextrose agar (SDA) plates at 23 °C until sporulation. Spores were harvested and suspended in 0.05 % Triton X-100. The spore germination rate was verified to exceed 90 %, and fresh cultures were prepared every four weeks. Aliquots were stored at 4 °C until further use.

After collecting the workers, their individual IDs (from the barcode marker) were recorded in the FORT system. The workers were briefly cooled on ice for 40 to 60 seconds. A 0.3 µL droplet of the treatment (fungus or control) was then pipetted onto their gaster (abdomen). For the fungal treatment, this equated to an application dose of approximately 300,000 spores, of which 30,000 to 45,000 would typically adhere to the ants' cuticle (Stroeymeyt et al., 2018). The ants were allowed 20 minutes to recover in isolation in a 30 mm Ø petri dish on filter paper before being returned to their respective foraging spaces. Fungus-exposed ants were infectious to the rest of the colony. The nine-hour post-exposure period allowed pathogen to spread and nest mates to respond with behavioural interventions such as self- or allogrooming. However, within the period of the experiment, there would not be enough time for the spores to germinate and infect their hosts. At the end of the post-exposure period, the colonies were snap-frozen on dry ice.

Colonies tagged on the same day received the same treatment, either both the fungal suspension or both the control solution (Table 3). The assignment of colonies to the fungus or control group alternated weekly, but was otherwise random.

Table 3: Treatment groups. The foragers were exposed to either the pathogen or control treatment 20 min before being returned to their colony, either at 9:30 a.m. for the day-colonies or 9:30 p.m. for the night-colonies.

Exposure group	Return of treated workers	Treatment group	Exposure treatment	Applied volume [µL]
Control	Day (9:30 a.m.) Night (9:30 p.m.)	Control Day Control Night	0.05 % Triton X-100	0.3
Pathogen	Day (9:30 a.m.) Night (9:30 p.m.)	Pathogen Day Pathogen Night	1 x 10^9 spores/mL in 0.05 % Triton X-100	0.3

Colony exclusion

Due to some colonies rejecting the nest area and moving the queen ($N = 3$ colonies), or part of the brood ($N = 3$ colonies) into the foraging space, we excluded these replicates from the data analysis. This resulted in a finial samples size of 9 "control day" colonies, 11 "control night" colonies, 10 "pathogen day" colonies, and 11 "pathogen night" colonies.

2.3 Molecular analysis

To quantify each colony member's pathogen contamination, we determined the fungal spore load of each individual from a subset of pathogen-treated colonies ($N_{\text{pathogen.day}} = 7$; $N_{\text{pathogen.night}} = 6$).

DNA extraction

The ants' ID was recorded using the "Manual Tag Scanner for the FORmicidae Tracker" (https://github.com/formicidae-tracker/tag-scanner) before they were individually sampled into 1.2 mL collection microtubes (Qiagen, 96-well plate). Ants were homogenised using a TissueLyser II (Qiagen; 2 * 2 min at 30 Hz) with a mixture of one 2.8 mm ceramic bead (Qiagen), five 1 mm zirconia beads (BioSpec Products), 100 mg of 425 - 600 µm acid washed glass beads (Sigma-Aldrich) and 50 µL distilled water. The DNA extraction was performed using the Qiagen DNeasy 96 Blood & Tissue Kit following the manufacturer's instructions, with a final elution volume of 50 µL. To determine the baseline detection threshold of the fungus and to rule out cross contaminations during the experiment, we also extracted the DNA of eight workers from each control treated colony ($N_{\text{control.day}} = 9$; $N_{\text{control.night}} = 11$). This resulted in 1340 samples.

Quantitative real-time PCR (qPCR) protocol

Quantitative real-time PCR (qPCR) targeting the ITS2 rRNA gene region of *M. brunneum* was performed using the primers Met-ITS2-F (5'-CCCTGTGGACTTGGTGTTG-3') and Met-ITS2-R (5'-GCTCCTGTTGCGAGTGTTTT-3') (Giehr et al., 2017) to quantify fungal DNA. The reactions were set up in 10 µL volumes in a 384-well PCR microplate (Axygen). Each well contained 8 µL master mix and 2 µL of extracted DNA. The mastermix was prepared manually, while aliquoting the mix into the 384-well plate and adding DNA were done using a Beckman Coulter Biomek i5 liquid handling workstation (the program was written by Volodymyr Shubchynsky, Vienna BioCenter Core Facilities GmbH, Austria).

Master mix composition (per reaction):

- 5 µL KAPA SYBR® FAST qPCR Master Mix (Kapa Biosystems)
- 0.15 µL of each primer (10 µM; final concentration 3 pmol; Sigma-Aldrich)
- 2.7 µL ddH_2O

The qPCR was performed using a LightCycler® 480 (Roche). Amplification specificity was verified by melting curve analysis at the end of each run.

Thermal cycling conditions:

- Initial denaturation: 95 °C for 3 minutes
- 40 cycles: 95 °C for 3 seconds, 64 °C for 30 seconds
- 95 °C for 10 seconds
- Melt curve: 65 °C to 95 °C in 0.5 °C increments for 5 seconds

Each plate included a negative control (water instead of DNA) and a standard curve consisting of five standards (1×10^{-1}, 1×10^{-2}, 1×10^{-3}, 1×10^{-4}, and 5×10^{-5} ng/µL) of fungal DNA, quantified using a NanoDrop spectrophotometer (Thermo Scientific). Samples and standards were run in triplicates. The detection threshold was determined to be 5×10^{-5} ng/µL, below that a reliable quantification was not possible.

We set the following quality criteria:

1. The negative control must lie below the detection threshold, corresponding to the lowest standard.
2. PCR efficiency must be between 90 and 110 %.
3. The difference between the three replicates must not exceed 0.5 – if only one replicate did not match, it was excluded. If all three did not match, the sample was rerun.
4. The concentration of the samples must lie within the range of the standard curve.

2.4 Tracking data processing

The processing of the marker-based tracking data followed the methods outlined in Mersch et. al. (2013), Stroeymeyt et al. (2018), and the doctoral thesis of Wanderlingh (2024). Data analysis scripts, originally created by N. Stroeymeyt, T. O. Richardson and A. A. Wanderlingh, were adapted for this experiment with their guidance. Detailed analysis pipeline and scripts are available on the following GitHub repositories:

https://github.com/lindasartoris/circadian_rhythm

https://github.com/AdrianoWanderlingh/Ant_Tracking

Data processing

First, we created metadata files combining manual and automated steps. These files included details such as marker orientation, mortality, the identity of treated foragers, and queen identification. Because network analysis requires constant colony sizes over time, ants that could not be consistently tracked throughout the entire experiment – primarily due to mortality – had to be excluded from the analysis. This affected 3.3 % of the ants. Ants' bodies were modelled using two-dimensional capsules, centred based on the position and orientation of the barcode markers (Fig. 3) (Wanderlingh, 2024).

Using these capsules, we extracted ant-ant interactions (based on proximity), ant trajectories, and colony metadata from the marker-based tracking data. Based on the circadian phases (daytime and night-time), interactions were grouped by three exposure periods: pre1, pre2 and post (Table 4). Worker task groups were defined as follows: ants spending at least 1 % of their time in the foraging space were defined as foragers, while all others were defined as nurses (Stroeymeyt et al. 2018).

Finally, the proximity interaction network was analysed in three-hour intervals across day (9:30 a.m. – 6:30 p.m.), and night (9:30 p.m. – 6:30 a.m.). We calculated the network properties and summarised individual-level interactions.

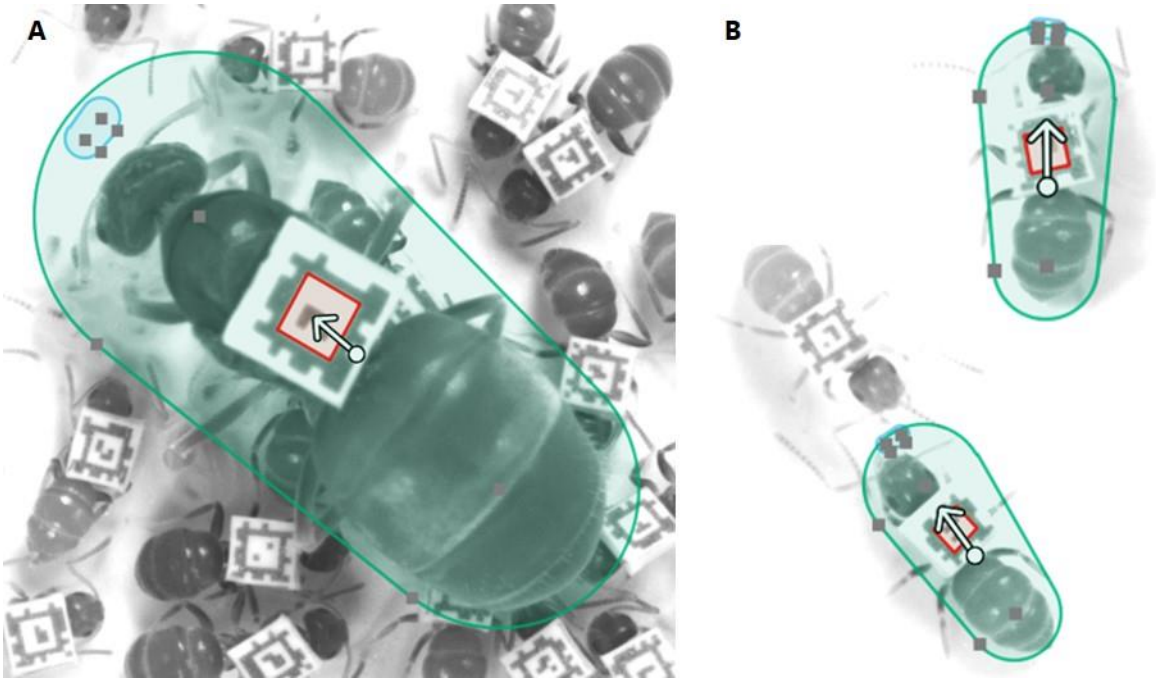

Fig. 3: Two-dimensional interaction capsules. Representation of the two-dimensional capsules used for detecting interaction between ants based on proximity. Each ant is modeled with two parts: a larger shaded green shape representing the body and a smaller schaded blue shape at the front representing the head. An interaction is inferred when the blue head capsule of one ant overlaps with the capsule of another. Capsule of a queen (A) and of workers (B).

Table 4: Circadian phases of day-colonies and night-colonies during exposure periods. Pre1 and pre2 represent two periods in the pre-exposure period. Post refers to the single period in the post-exposure period. Circadian phases correspond to the experimental conditions aligning with either daytime or night-time.

Exposure period	Circadian phase of day-colonies	Circadian phase of night-colonies
pre1	day	night
pre2	night	day
post	day	night

Network properties

Time-aggregated, weighted contact networks were constructed in three-hour intervals across day and night periods. Nodes represent individuals, edges denote interactions, and edge weights reflect the total interaction duration (Stroeymeyt et al., 2018; Wanderlingh, 2024). Network analyses were performed using the R package *igraph*, focussing on the following properties for their potential roles in transmission dynamics: density (Barthélemy et al., 2005), mean degree centrality (hereafter "degree") (Lloyd-Smith et al., 2005; Volz et al., 2011), efficiency (Latora & Marchiori, 2001), diameter (Richardson & Gorochowski, 2015), modularity (Sah et al., 2017; Volz et al., 2011), clustering (Danon et al., 2012; Volz et al., 2011), and task assortativity (Stroeymeyt et al., 2018) (Box 1 provides descriptions). Modularity, a measure of community

structure, was calculated using Louvain's method (Blondel et al., 2008), while task assortativity was based on Newman's method (Newman, 2002, 2003).

Simulated transmission

Using the observed time-ordered contact sequences from our tracking data, we simulated pathogen transmission with treated foragers as the infection seeds during the nine-hour daytime and night-time period. The simulations captured both the pathogen-free (constitutive) transmission dynamics during the pre-exposure period (pre1 and pre2) and exposure-induced transmission dynamics during the post-exposure period (post), for both the control and pathogen treated colonies (control-induced and pathogen-induced, respectively). Transmission dynamics were modelled on a temporal Susceptible-Infectious epidemiological framework adapted for fungal spore transmission by Stroeymeyt et al. (2018): the total pathogen load in the colony was kept constant (no replication), and pathogen transmission from one ant to another was determined by the current load of the infectious individual. The infectious individuals were assigned an initial load of 1, while susceptible individuals started with a load of 0. The contact sequences were then processed in chronological order. The transmission rate (r) followed an r-K logistic equation, where r represents the growth rate per second. Transmission was averaged over 500 simulations for each contact sequence to ensure robust results (Stroeymeyt et al., 2018).

Box 1. Colony network properties and their potential effects on disease transmission, with (+) typically enhancing, and (-) typically inhibiting transmission.

Density (+)
Proportion of realised connections of all possible connections in the network (Barthélemy & Barrat 2005)

Degree centrality (+)
Number of connections per individual. On the colony level, we evaluate mean degree centrality of all colony members (Loyd-Smith 2005; Volz et al. 2011)

Efficiency (+)
Inverse of the average pathway length between all pairs of individuals, i.e., if the pathway is short, efficiency is high (Latora & Marchiori 2001)

Diameter (-)
Maximum length of the shortest path between any two individuals (Richardson and Gorochowski 2015)

Modularity (-)
Compartmentalisation of the network into distinct sets of well-connected individuals (Sah et al. 2017; Volz et al. 2011)

Clustering coefficient (-) *depends on transmission rate*
Tendency of an individual and its neighbours to form a fully connected clique, i.e. a connection "triangle" (Danon et al. 2012; Volz et al. 2011)

Task assortativity (-) *node dependent*
Tendency of individuals of the same task group (e.g. foragers or nurses) to associate with each other (Stroeymeyt et al. 2018)

Adapted from Stroeymeyt et al. 2014

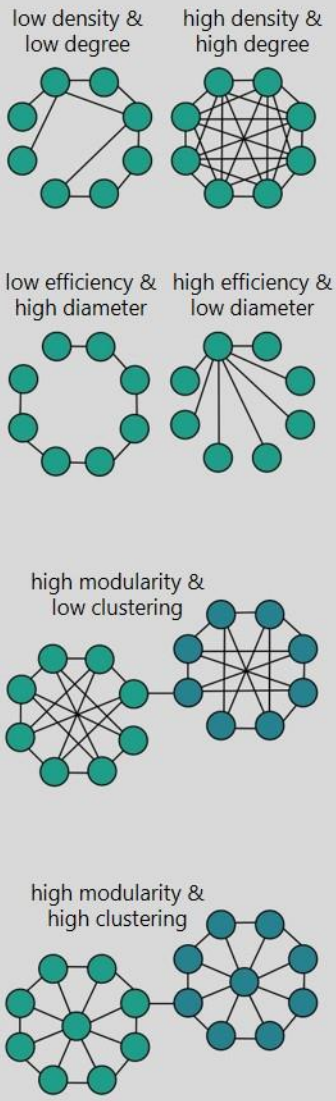

Allogrooming detection

The *Behavioural Inference Tool*, a machine-learning approach developed by Wanderlingh (2024), enabled the automated detection of allogrooming events. This tool infers grooming interactions by analysing the proximity and movement characteristics of two-dimensional capsules that model the ant's body and head (Fig. 4). While similar to the method used for detecting ant-ant interactions in proximity networks, it incorporates slightly different shaped capsules and adjusted interaction definition parameters, such as a minimum duration threshold of six seconds (Wanderlingh, 2024). In Wanderlingh (2024), the tool was trained on manually annotated behavioural data and detected allogrooming between workers with a precision of

71.6 % and sensitivity of 74.6 %. Grooming interactions with the queen are not considered by the tool.

Because the tool was developed on a slightly different experimental set-up – featuring the same host-pathogen system, nest design, and tracking systems, but different colony sizes – we are currently evaluating its generalisability to our data set. To this end, student intern Luisa Fiebig manually annotated 200 allogrooming events (occurring in the first 10 minutes post-exposure), focusing on one treated and one untreated forager per colony (N =37 colonies). All performed and received allogrooming events were documented. These annotations will later be evaluated by N. Stroeymeyt to assess the tool's precision and sensitivity within our experimental conditions.

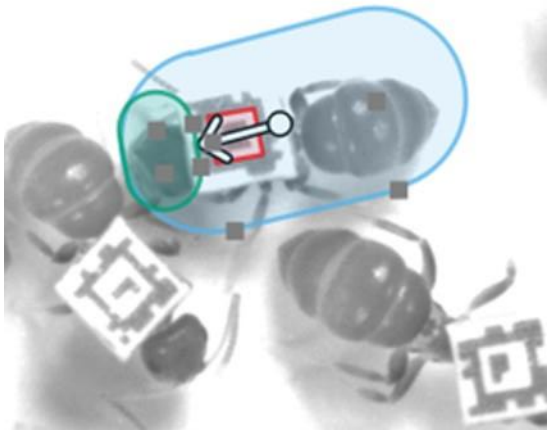

Fig. 4: Two-dimensional grooming capsules. Representation of the two-dimensional capsule used for inferring allogrooming interactions between workers. Each worker is modeled with two parts: a larger shaded blue shape representing the body and a smaller schaded green shape at the front representing the head. The shape of the capsules used for allogrooming slightly differ from those used to infer general interactions.

2.5 Statistical analysis

General

To examine the overall effects of day-night cycles, task groups, and exposure treatments, we performed full-null model comparisons using likelihood ratio tests (B. M. Bolker et al., 2009). For models including one interaction term, we compared full models to reduced models without the interaction. If the interaction was non-significant, the effect of the main predictors was estimated from the reduced models. If a model included multiple interaction terms, non-significant interactions were removed, starting with the three-way interaction, followed by all two-way interactions. When response variables contained multiple measurements per colony, colony ID was included as a random effect to account for dependent data. Colony size ranged from 90 to 114 workers per colony (mean: 103.6).

All analyses were conducted in R version 4.2.3 (R Core Team, 2023). The following packages were utilised: car (Fox & Weisberg, 2019), dplyr (Wickham et al., 2023), effectsize (Ben-

Shachar et al., 2020), emmeans (Lenth, 2023), glmmTMB (B. Bolker, 2019), influence.ME (Nieuwenhuis et al., 2012), lme4 (Bates et al., 2015), multcomp (Hothorn et al., 2008) and r2glmm (Jaeger, 2017). Response variables were transformed where necessary (log, square root, or BoxCox transformations) to meet model assumptions. In case a transformation or model was not able to handle zero-values, we added the smallest non-zero value from the data set divided by the square root of two before applying transformations.

For Gaussian models, the normality and homogeneity of residuals were assessed visually. For non-Gaussian models, overdispersion was checked. The absence of collinearity among predictors was verified using Variance Inflation Factor (VIF) values, and model stability was assessed using DFbetas to detect influential cases.

All reported p-values are both-sided. Post-hoc comparisons were performed using Tukey's method, with p-values adjusted using the Benjamini-Hochberg (BH) corrections (Benjamini & Hochberg, 1995) to control the false discovery rate at 5 %. Effect sizes are reported as partial eta-squared (η^2) for Gaussian models and odds ratio for non-Gaussian models.

The reported p-values from the full-null model comparison are uncorrected unless stated otherwise. When applying the BH corrections for multiple comparisons within the same dataset, the results remained unchanged.

Individual behaviours

Individual behaviours were aggregated per task group within each colony (N = 1360 foragers, N = 2706 nurses, N = 41 colonies). The effect of circadian phase (day/night) during the pre-exposure period was analysed separately for foragers and nurses, with colony size included as a fixed effect to control for its potential effect.

To estimate the effect of circadian phase on the time foragers spend outside the nest, a generalised linear mixed model (GLMM) with beta error distribution and logit link function was used. Differences in time active, speed while active, and distance travelled were estimated using Gaussian GLMMs.

For the nine-hour post exposure-period, we tested which individuals had more contact with pathogen-treated foragers. A Gaussian GLMM was fitted, with task group (untreated foragers and nurses) and circadian phase (day/night) as main effects, including their interaction (N = 649 untreated foragers, N = 1322 nurses, N = 10 day-colonies, N = 11 night-colonies).

Colony networks

For the per-exposure period, colony network properties were aggregated across the three three-hour intervals during daytime and night-time, respectively. The main predictor was circadian phase (day/night), and colony size was included as a control predictor. Since colonies began the experiment either at the start of the day (N = 19 day-colonies) or the night (N = 22 night-colonies), we also controlled for period (pre1/pre2), i.e. during which period the colonies experienced daytime and night-time.

For the post-exposure period, we first assessed the effect of exposure treatment (control/pathogen) on network properties by comparing the same circadian phase (day/night) across pre- and post-exposure periods (pre1/post). We examined the first three-hour interval to assess the immediate effect of exposure and the third three-hour period to evaluate longer-term effects. The model was fitted with the interactions between exposure treatment, exposure period, and circadian phase, while controlling for colony size. Additionally, we calculated the delta changes for each colony during the first, second and third three-hour intervals and analysed the slope to capture temporal changes in the network. This model included the interactions between exposure treatment, circadian phase, and time hours post, while controlling for colony size. "Time hours post" referred to the starting times of the three-hour intervals in the network analysis (0, 3 and 6 hours post-exposure). Colonies were exposed either at the start of the day ($N_{control}$ = 9; $N_{pathogen}$ = 10) or the night ($N_{control}$ = 11; $N_{pathogen}$ = 11). For the slope analysis, one replicate had to be excluded due to model assumption violations and instability (final $N_{control.night}$ = 10).

Finally, we estimated the effect of exposure treatment on day-night differences within each colony (pre2/post). Analyses were conducted separately for control and pathogen exposed colonies. Colonies exposed during the day were compared to their pre-exposure night phase, while colonies exposed during the night were compared to their pre-exposure day phase. This approach allowed us to determine whether pre-existing day-night differences persisted post-exposure.

Transmission simulations

To examine the effect of circadian phase and exposure treatment on simulated transmission rates, we fitted Gaussian GL(M)Ms. Simulated transmission in the constitutive pre-exposure period also originated from the same foragers later exposed during the experiment.

For the pre-exposure period, circadian phase was the main predictor, while starting period and colony size were included as control predictors (N = 41 colonies). For the post-exposure period, the effect of circadian phase was analysed separately for control- and pathogen exposed colonies ($N_{control}$ = 20, $N_{pathogen}$ = 21), with colony size as the sole control predictor.

To evaluate simulated pathogen loads, we added task group (foragers, nurses and queens) as a main predictor and included the interaction between task group and circadian phase (N = 1360 foragers, N = 2706 nurses, N = 41 queens, N = 41 colonies). Similar to transmission rate, pathogen loads during post-exposure were analysed separately for control- and pathogen exposed colonies.

Allogrooming

To estimate the changes in allogrooming induced by the exposure treatments, a negative binomial GLMM with Poisson error distribution was fitted. The response variable was the number of allogrooming events received by treated foragers per colony (N = 187 treated foragers, N = 41 colonies). Allogrooming events were aggregated into 15-minute time windows across the first three hours post-exposure. Post-exposure allogrooming levels (post) were

compared to pre-exposure levels of the same circadian phase (pre1), with time of day (starting times of the 15-minute time windows) included as a random effect.

In pathogen-exposed colonies, the rate of allogrooming performed by untreated foragers and nurses towards the treated foragers during the nine-hour post-exposure period was analysed. The response variable was the aggregated allogrooming events performed by each task group per colony, with circadian phase, task group, and their interaction included as main predictors.

The effect on proportion of allogrooming occurring in the foraging space during the nine-hour post-exposure period was tested using a GLM with beta error distribution and logit link function. This rate was aggregated at the colony level, with circadian phase, exposure treatment, and their interaction included as main predictors.

qPCR pathogen loads

To evaluate pathogen spread at the end of the nine-hour post-exposure period, we measured individual fungal loads in a subset of colonies (final samples size: $N = 7$ day-colonies with a total of 699 ants, $N = 6$ night-colonies with a total of 476 ants). Ants that could not be match to the tracking data file, e.g. because they had lost their tag or had already been excluded from the tracking data for other reasons, were not considered in the pathogen load analysis ($N = 47$ ants).

For the statistical analysis, we set the threshold for considering the ants to carry a detectable load, at a fungal DNA concentration higher than that of control individuals (6.5×10^{-5} ng/µL, which was just above the technical detection threshold of 5×10^{-5} ng/µL).

The probability of exposure (presence/absence of a detectable fungal load) across task groups ($N = 251$ foragers, $N = 809$ nurses), was assessed using a GLMM with binomial error distribution. Main effects included circadian phase, task group, and their interaction.

Pathogen loads of contaminated individuals were analysed using a GLMM. Circadian phase and task group were included as main predictors along with their interaction to evaluate differences in fungal loads.

Data visualisation

Data visualisation was conducted in R using the packages cowplot (Wilke, 2020), DescTools (Signorelli, 2024), and ggplot2 (Wickham, 2016). In most cases, replicate medians and the 95 % confidence intervals (CIs) of the median were plotted, along with the underlying data points. To represent changes induced by exposure, pre-exposure values were subtracted from post-exposure values within each colony, where values greater than zero indicated an increase post-exposure. Similarly, day-night differences after exposure were visualised by subtracting night values from the day values within a colony, where values greater than zero indicated higher values during the day.

3 Results

Contributions to the experimental work, molecular analysis, and data analysis

Experimental work

Experimental setup: 100 % own

Applying barcode-markers with R. Kennard: 75 % own

Worker exposure & sampling: 100 % own

Molecular analysis

DNA extractions: 100 % own

qPCR method establishment with A. V. Grasse: 50 % own

qPCR quantification of fungal loads with A. V. Grasse: 80 % own

Fungal load analysis: 10 % A. V. Grasse & F. B. Abbasi, 90 % own

Data analysis

Tracking data processing, with the support of N. Stroeymeyt, T. O. Richardson, and A. A. Wanderlingh who developed and shared the analysis pipeline: 100 % own

Data curation: 100 % own

Statistical data analysis: 100 % own

3.1 Constitutive circadian patterns in ant behaviour and colony networks

First, we examined the undisturbed, constitutive circadian patterns of individual behaviour and colony network properties across all 41 colonies.

Foragers and nurses show a diurnal circadian activity pattern

To understand how our experimental day (26° C, lights on) and night (22° C, lights off) conditions influenced the activity of foragers and nurses, we analysed their behaviour during both circadian phases (N = 1360 foragers, N = 2706 nurses, N = 41 colonies). Foragers spent more time in the foraging space during the day (GLMM, day-night differences $p < 0.001$; Table S1), although they did not fully retreat to the nest at night. Notably, both foragers and nurses showed a diurnal circadian pattern in their proportion of time being active, speed while active, and average distance travelled (Fig. 5A-C; GLMM, day-night differences: foragers all p-values < 0.001; Table S2a; nurses all p-values < 0.001; Table S2b), i.e. both task groups were overall more active during the day.

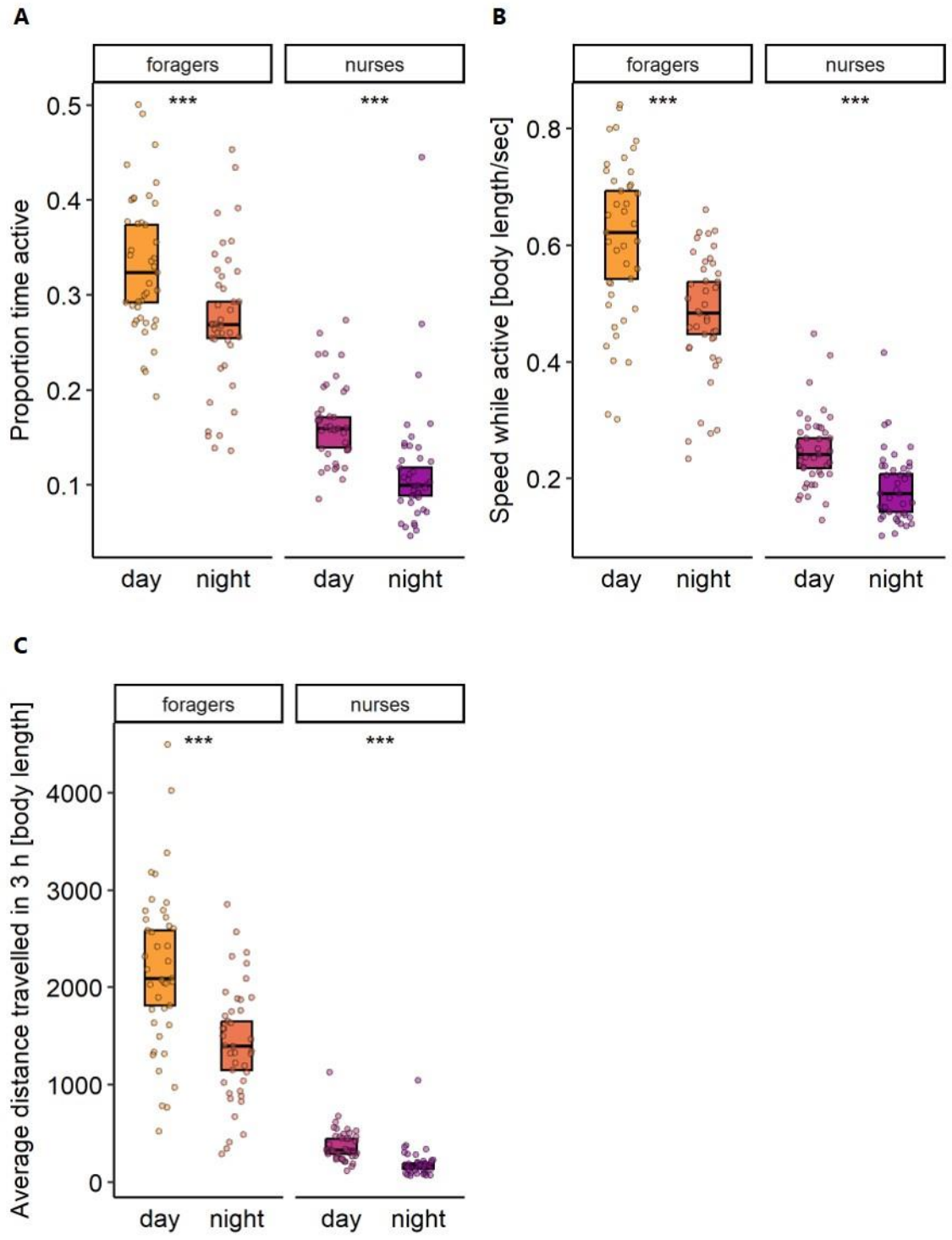

Fig. 5: Diurnal circadian activity patterns. Foragers and nurses exhibit diurnal activity patterns, being more active during the day: (A) the proportion of time individuals were active, (B) the speed at which they travelled while active, and (C) the average distance travelled during a three-hour interval (GLMM; Table S2a-b). Black bars represent the group medians, while boxes indicate the 95 % confidence intervals (CIs). Significant differences between day and night are denoted by *** (two-sided $p < 0.001$). Sample sizes: $N = 1360$ foragers, $N = 2706$ nurses, across 41 colonies.

Colony interaction networks show a circadian pattern

We assessed how these behavioural patterns affected colony network dynamics (N = 41 colonies), revealing consistent day-night differences across six network properties (Fig. 6; GLMM, see Table S3 for detailed statistics); exemplified by network density for each colony (Fig.2A-B). During daytime, colonies had a higher network density (Fig. 6C; day-night differences $p < 0.001$) and degree (Fig. 6D; $p < 0.001$), meaning a greater proportion of potential connections were realised, and each individual connected with more partners on average. Similarly, clustering, or the tendency to form fully-connected cliques, was higher during daytime (Fig. 6E; $p < 0.001$), while modularity, reflecting the network's compartmentalisation, decreased (Fig. 6F; $p < 0.001$). Connection efficiency between two individuals was higher during the day (Fig. 6G; $p = 0.010$), accompanied by a lower network diameter – the longest direct pathway between two individuals – during daytime (Fig. 6H; $p = 0.009$). Task assortativity – tendency to associate within own task group – showed no circadian pattern ($p = 0.806$). Interestingly, transmission-enhancing network properties were all elevated during daytime (density, degree & efficiency), whereas transmission-inhibiting properties were elevated during the night (diameter & modularity). This pattern was confirmed by a higher simulated transmission rate through the network (Fig. S1A; GLMM, day-night differences $p < 0.001$; Table S4), and a higher simulated pathogen load for the foragers during the day (Fig. S1B; GLMM, task group × circadian phase, $p = 0.017$; Table S5). Notably, the predicted loads for nurses and queens did not differ between day and night, and were significantly lower than those of foragers.

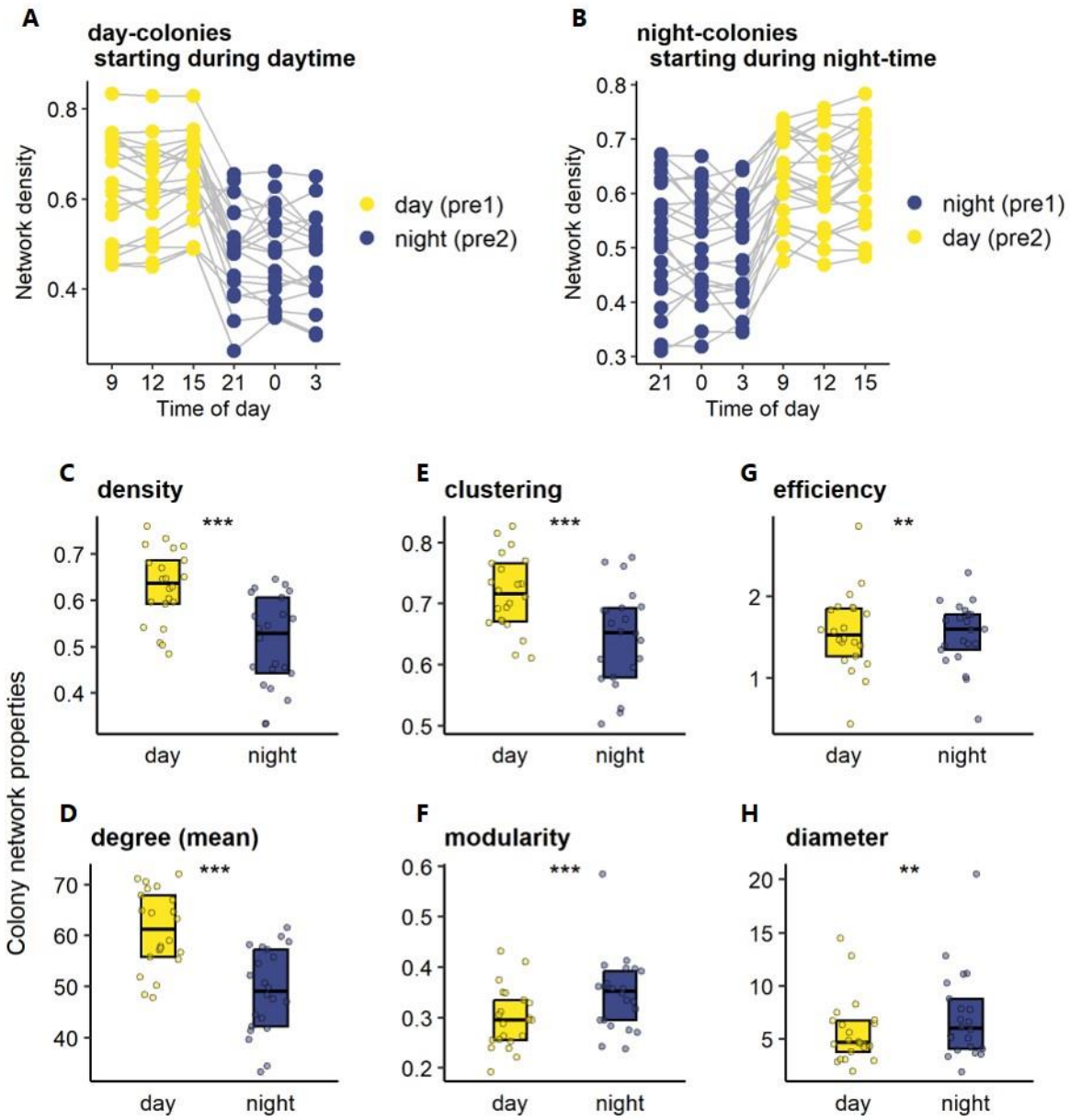

Fig. 6: Circadian network patterns. During the pre-exposure period (pre1 & pre2), colonies exhibited daily rhythms in their network properties, leading to distinct circadian patterns. Despite substantial variation between colonies, the amplitude of day-night differences was consistent, as demonstrated here for network density. Similar patterns were observed for both (A) day-colonies, where tracking began at the beginning of the day, and (B) night-colonies, where tracking began at the beginning of the night. Each dot in (A) and (B) represents the aggregated network density of the colony for a three-hour interval, with three intervals during the day and three during the night. Grey lines connect dots from the same colony ($N_{day.colonies}$ = 19, $N_{night.colonies}$ = 22). Network properties significantly differed between day and night (GLMM, Table S4), with (C) density, (D) degree, (E) clustering, and (G) efficiency being higher during the day, while (F) modularity and (H) diameter were higher at night. In (C) - (H), black bars represent medians, and boxes show the 95 % CIs (pooled for day- and night-colonies, N = 41). Significant day-night differences are denoted by ** ($p < 0.01$) and *** ($p < 0.001$).

3.2 Effect of exposure on circadian patterns in ant behaviour and colony networks

Next, we investigated how exposing a subset of foragers to infectious fungal spores affected individual ant behaviour and colony-level circadian patterns. Our aim was to understand how these rhythms may influence or interact with the colony's response to an incoming disease threat and the subsequent spread of infectious spores throughout the colony. Twenty-four hours after the start of their constitutive day-night cycle, we exposed approximately five foragers per colony to either the pathogen treatment ($N = 21$ colonies, 10 of which exposed during the day and 11 during the night) or the control treatment ($N = 20$ colonies, 9 of which exposed during the day and 11 during the night). Colonies were observed for an additional nine hours during the post-exposure period.

Exposure to *Metarhizium* is known to trigger an immediate increase in allogrooming by colony members (Bos et al., 2012; Okuno et al., 2012; Qiu et al., 2014; Walker & Hughes, 2009). In small groups of *Lasius neglectus*, a close relative of *L. niger*, where this has been studied in detail, allogrooming activity typically peaks in the first 10 – 20 minutes post exposure before it returns to baseline within one and a half hours (Casillas-Pérez et al., 2023). Consequently, collapsing the full nine-hour post-exposure period into a single analysis may obscure potential dynamic timelines driven by early effects that are prominent immediately after exposure but diminish over time. To address this, we analysed the first three-hour window of the pre- and post-exposure periods to capture the immediate dynamics of the sanitary care response following treatment. All allogrooming events received by treated foragers were aggregated into 15-minute intervals, resulting in 12 time windows per colony over three hours (Fig. 7).

Forager treatment increases sanitary care

Exposure of foragers to either pathogen (N = 95 foragers) or control (N = 92 foragers) treatments led to an increase in the allogrooming they received compared to the pre-exposure period. Allogrooming events were particularly concentrated in the first 30 minutes following exposure, with a significant increase compared to the same period before exposure. This effect was more pronounced following daytime exposure (Fig. 7; GLMM, change from pre to post × circadian phase, $p = 0.023$; Table S6a). The allogrooming response during this initial 30-minute period was independent of exposure type ($p = 0.178$; Table S6a).

To align with the time windows used in the network property analysis, we also looked at allogrooming dynamics during the first three hours of the post-exposure period. Over this longer time frame, the increase in allogrooming events remained significantly higher than in the pre-exposure period. Interestingly, while the initial effect of exposure timing (daytime or night-time) diminished, a stronger response emerged in pathogen-treated colonies (Fig. 7; GLMM, change from pre to post × exposure type, $p = 0.018$; Table S6b).

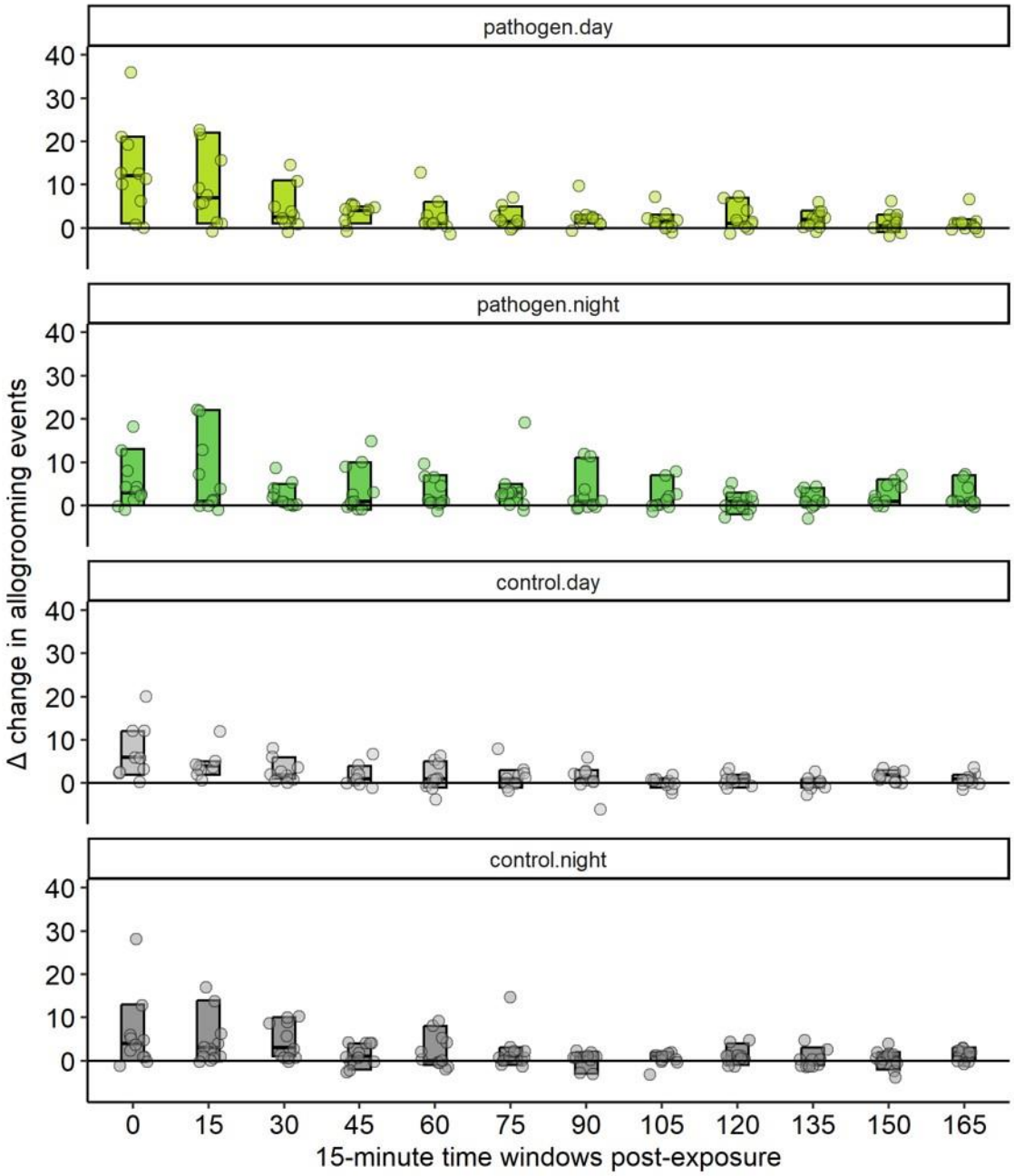

Fig. 7: Early induced changes in allogrooming. The plot shows exposure-induced changes during the first three hours of the post-exposure period. Allogrooming events received by the treated foragers were aggregated per colony over 15-minute time windows, separately for colonies treated during the day or night, exposed to either control or pathogen treatment ($N_{\text{pathogen.day}} = 10$, $N_{\text{pathogen.night}} = 11$, $N_{\text{control.day}} = 9$, $N_{\text{control.night}} = 11$). Across the three-hour interval, allogrooming occurred significantly more frequent post exposure with a greater increase in pathogen-treated colonies (GLMM, p = 0.018, Table S6b). Each point represents the Δ change in events per colony, bars represent the median, and boxes indicate 95 % CIs, based on 41 colonies (187 treated foragers in total). Δ changes were calculated by subtracting pre1-values from post-values within each colony, with the zero line indicating no induced changes.

Since 60 % of all post-exposure allogrooming events towards treated foragers occurred within the first three hours (Fig. 8), we next assessed whether these dynamic changes in sanitary care were reflected in the colony's network properties. Given that grooming interactions were defined as interactions lasting at least six seconds, and our network property analysis was weighted by interaction duration, these early effects may influence network structure. Additionally, we tested how the network properties changed over time, and how robust constitutive circadian patterns were after exposure.

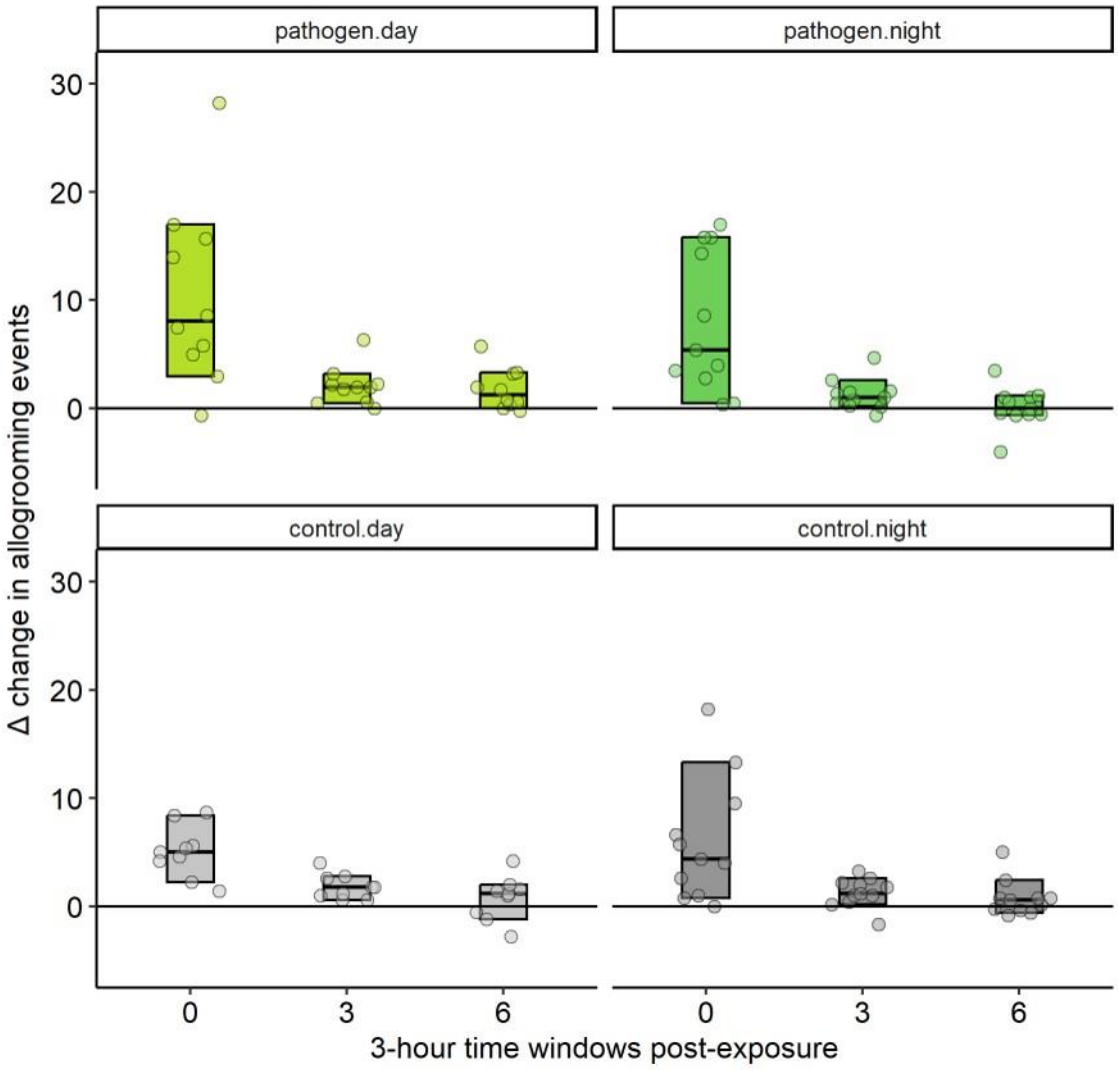

Fig. 8: Induced changes in allogrooming. The plot shows exposure-induced changes during the first, second and third three-hour post-exposure windows, separately for colonies treated during the day or night, exposed to either control or pathogen treatment ($N_{\text{pathogen.day}} = 10$, $N_{\text{pathogen.night}} = 11$, $N_{\text{control.day}} = 9$, $N_{\text{control.night}} = 11$). Allogrooming events received by the treated foragers were aggregated per colony over three-hour time windows, with 60 % of all post-exposure allogrooming events occurring during the first three hours. Each point represents the Δ change in events per colony, bars represent the median, and boxes indicate 95 % CIs, based on 41 colonies (187 treated foragers in total). Δ changes were calculated by subtracting pre1-values from post-values within each colony, with the zero line indicating no induced changes.

Colony networks respond dynamically to sanitary care but show a robust circadian pattern

To examine how forager exposure and the transient increase in allogrooming affected network properties, we analysed these properties across the first, second, and third three-hour intervals of the post-exposure period (Fig. 9A-F pathogen exposed; Fig. S2A-F control-exposed).

During the first three hours post exposure, network density and degree significantly increased from pre to post exposure (Fig. 9A-B and Fig. S2A-B; GLMM, changes pre to post: density $p = 0.003$, degree $p = 0.003$; Table S7a), independent of treatment type or timing (all model interactions were non-significant; Table S7a). Network clustering, modularity, efficiency, and diameter did not show significant changes during this period (Fig. 9C-G and Fig. S2C-G; GLMM; Table S7a). This suggests that when allogrooming was high, the ants established more connections within the network and, on average, interacted with a greater number of different partners.

To assess whether the network properties changed over time, we calculated the slope of delta-changes across the three three-hour intervals. Over the nine-hour post-exposure period, network density, degree, clustering, and efficiency significantly decreased with time (Fig. 9A-C, E and Fig. S2A-C, E; GLMM, delta slope: density $p < 0.001$, degree $p < 0.001$, clustering $p < 0.001$, efficiency $p = 0.001$; Table S8). In contrast, network modularity significantly increased with time (Fig. 9D and Fig. S2D; GLMM, delta slope: modularity $p < 0.001$; Table S8). These changes were independent of exposure timing or type (all interactions were non-significant; Table S8).

Next, we tested whether these temporal changes resulted in significant differences in exposure-induced network properties by the end of the experiment, i.e., during the third three-hour post-exposure interval. Among the network properties that had decreased over time, density, degree, and clustering were significantly lower in the third post-exposure interval compared to the same time in the pre-exposure period (Fig. 9A-C and Fig. S2A-C; GLMM, changes pre to post: density $p = 0.36$, degree $p = 0.043$, clustering $p = 0.002$; Table S7b). These effects were independent of exposure timing or type (all interactions were non-significant; Table S7b). However, the temporal changes in modularity and efficiency did not lead to significant differences by the end of the experiment when compared to the corresponding pre-exposure period.

These dynamic timelines highlight the impact of allogrooming on colony network properties: while the first three hours were characterised by increased sanitary care, the later transmission phase (starting from the second interval) showed a shift in the opposite direction.

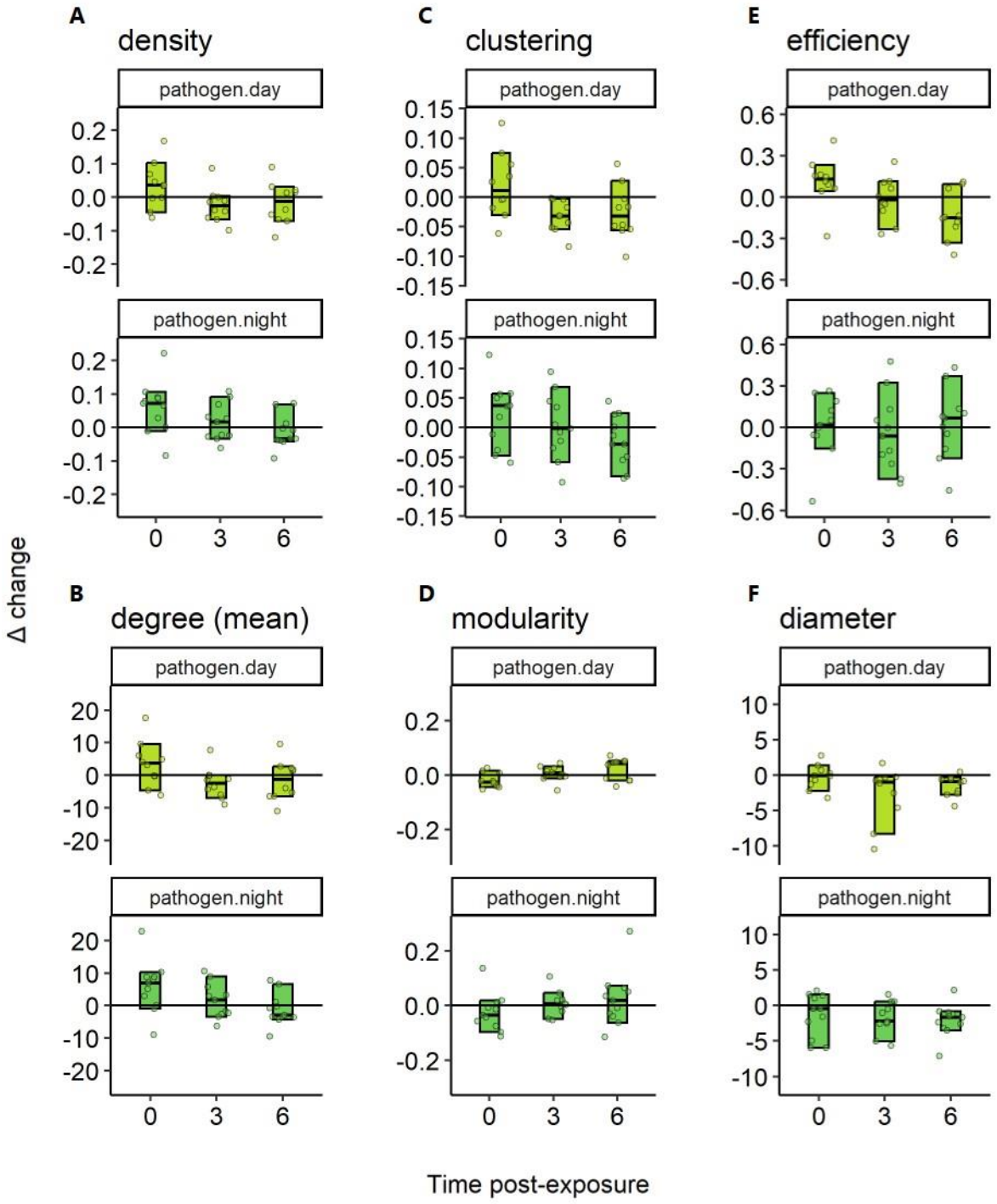

Fig. 9: **Timeline of induced changes in network properties following pathogen exposure.** The plot shows pathogen-induced changes during the first, second and third three-hour post-exposure intervals, separately for day- and night-colonies, in (A) network density, (B) degree, (C) clustering, (D) modularity, (E) efficiency, and (F) diameter. Δ changes were calculated by subtracting pre1-values from post-values within each colony and interval, with the zero line indicating no induced changes. Bars represent the median, and boxes indicate 95 % CIs ($N_{\text{pathogen.day}}$ = 10 colonies, $N_{\text{pathogen.night}}$ = 11 colonies).

Next, we assessed the robustness of the circadian network pattern observed in its undisturbed, constitutive state (Fig. 6) by analysing its response to the exposure of approximately five foragers to either the control or pathogen treatment. Half of the colonies were exposed at the start of the day ($N_{control}$ = 9, $N_{pathogen}$ = 10), while the other half were exposed at the start of the night ($N_{control}$ = 11, $N_{pathogen}$ = 11). To evaluate the impact of exposure timing on day-night differences in network properties within each colony, we compared colonies exposed during daytime to their pre-exposure night phase and colonies exposed during night-time to their pre-exposure day phase (day minus night; Fig. 10A-B). This approach enabled us to determine whether pre-existing day-night differences in network properties were maintained post-exposure.

We examined the effect of exposure timing of pathogen (Fig. 10) and control treatments (Fig. S3) on day-night differences in network properties separately. For the pathogen-exposed colonies, we additionally assessed how post-exposure day and night networks influenced both predicted and realised pathogen transmission. For the control-exposed colonies, only simulated pathogen transmission could be evaluated.

We found the same circadian patterns in colony networks following pathogen exposure as we did in the constitutive networks (Fig. 6) for network density, degree and clustering (higher during the day, Fig. 10C-E) as well as modularity (lower during the day, Fig. 10F). This was independent of whether pathogen-exposed foragers were introduced during the day or night (GLMM, daytime exposure, day-night differences: density $p < 0.001$, degree $p < 0.001$, clustering $p < 0.001$, modularity $p < 0.001$, $N_{pathogen.day}$ = 10 colonies; Table S9a; night-time exposure, day-night differences: density $p < 0.001$, degree $p < 0.001$, clustering $p < 0.001$, modularity $p < 0.001$, $N_{pathogen.night}$ = 11 colonies; Table S9b). The same circadian patterns were also present in control-exposed colonies (Fig. S3C-F; GLMM, daytime exposure, day-night differences: density $p < 0.001$, degree $p < 0.001$, clustering $p < 0.001$, modularity $p < 0.001$, $N_{control.day}$ = 9 colonies; Table S9c; night-time exposure, day-night differences: density $p < 0.001$, degree $p < 0.001$, clustering $p < 0.001$, modularity $p = 0.002$, $N_{control.night}$ = 11 colonies; Table S9d).

Though we did not directly test for it, an interesting pattern emerged for network density, degree, clustering and diameter following pathogen exposure (Fig. 10C-H): daytime exposure tended to amplify existing day-night differences, whereas night-time exposure appeared to diminish them. This pattern was not consistently observed after control exposure (Fig. S3C-H).

Day-night differences in network efficiency were no longer present when forager exposure occurred at night. Pre-exposure, efficiency was higher during daytime (Fig. 6G). However, previous day-night differences disappeared following night-time exposure (Fig. 10G; daytime exposure, day-night difference $p = 0.011$; Table S9a; night-time exposure, day-night difference $p = 0.611$; Table S9b).

For network diameter which was constitutively lower during the day (Fig. 6H), day-night differences became more pronounced following daytime exposure, while they disappeared following night-time exposure. This pattern held for both pathogen (Fig. 10H; daytime

exposure, day-night differences p = 0.003; Table S9a; night-time exposure, day-night differences p = 0.052; Table S9b) and control exposure (Fig. S3H; daytime exposure, day-night differences p = 0.009; Table S9c; night-time exposure, day-night differences p = 0.125; Table S9d).

Overall, even if only being a slight effect, pathogen exposure amplified "day-like" characteristics in colony networks, resulting in slightly larger day-night differences following daytime exposure and reduced differences following night-time exposure (i.e. night-time network properties became more "day-like"). This effect was most pronounced for density, degree, clustering, and diameter.

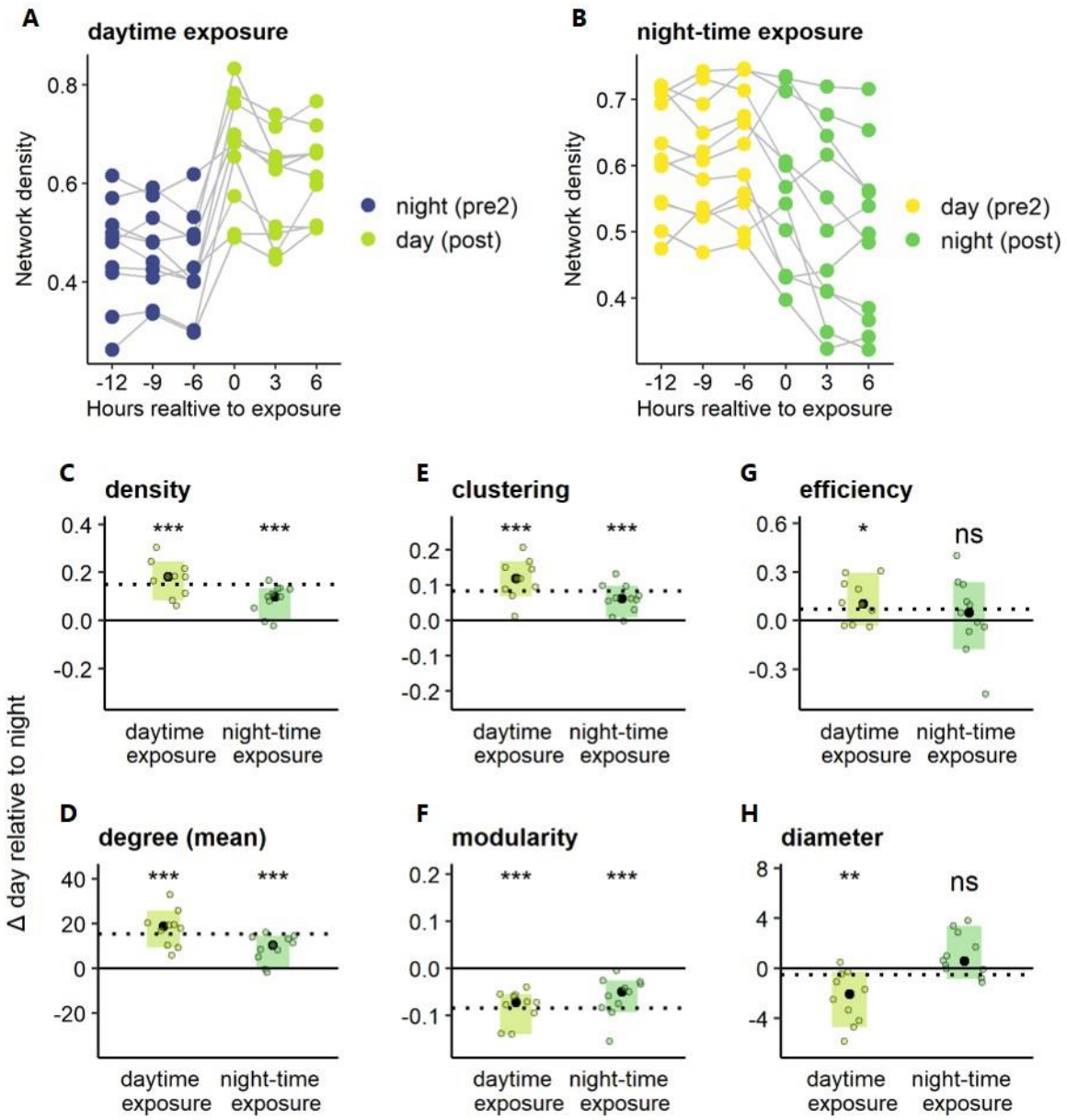

Fig. 10: Robust day-night differences after pathogen exposure. (A) and (B) show colony network density during the circadian phases directly before (pre2) and after (post) pathogen exposure. To visualise the robustness of day-night differences post-exposure, we calculated the "Δ day relative to night" (C - H): the night-values were subtracted from the day-values, such that the solid zero line indicates no day-night differences. This analysis was done separately for colonies experiencing daytime exposure and those experiencing night-time exposure, i.e., colonies treated at the start of the day, or the night, respectively. The daytime exposure Δ represents day(post) minus night(pre2), while the night-time delta represents day(pre2) minus night(post). The dashed line represents the median day-night differences observed in constitutive colonies (Δ day minus night; Fig. 6). In (C - H), black dots represent the median, and shaded boxes indicate 95 % CIs, based on $N_{daytime.exposure}$ = 10 colonies, and $N_{night-time.exposure}$ = 11 colonies. Significant day-night differences are denoted by * ($p < 0.05$), ** ($p < 0.01$), and *** ($p < 0.001$), while ns ($p > 0.05$) denotes a non-significant difference.

Next, we assessed how these network dynamics during the post-exposure period influenced pathogen transmission compared to the simulated transmissions in the constitutive networks (Fig. S1). In addition to simulated transmissions in the post-exposure period, we measured the realised pathogen transmission for the pathogen-exposed colonies.

Pathogen exposure resulted in similar transmission dynamics between day and night

Simulating transmission in colonies post-exposure, with the experimentally treated foragers as initial carriers (seeds), we found that the transmission rate in the control-exposed colonies remained higher during the day (Fig. S4A; GLM, $p = 0.038$; Table S10), consistent with the pattern observed in the constitutive networks (Fig. S1). However, for pathogen-exposed colonies, the previously higher daytime transmission rate was no longer observed (Fig. 11A; GLM, $p = 0.099$; Table S12).

For both control- and pathogen-exposed colonies, simulations of individual pathogen loads at the end of the nine-hour post-exposure period revealed a significant interaction between circadian phase and task group (GLMM, task group × circadian phase, pathogen-exposed $p = 0.002$; Table S13; control-exposed $p = 0.034$; Table S11). Post-hoc comparisons showed no differences in simulated loads based on daytime or night-time exposure for either task group (Fig. 11B pathogen-exposed; FigS5B control-exposed). Untreated foragers were predicted to carry higher loads than nurses, while queens had intermediate simulated loads.

These results indicate that, while transmission rates in control-exposed colonies remained slightly higher after daytime exposure compared to night-time exposure, differences in simulated pathogen loads among untreated foragers were no longer evident. Instead, simulated pathogen loads in control-exposed colonies had the same pattern as those in pathogen-exposed colonies.

Next, we tested whether the measured pathogen load reflected the simulations, which was only possible for the pathogen-exposed colonies.

Indeed, the individual pathogen loads quantified after daytime exposure ($N = 7$ colonies, $N = 699$ ants) and night-time exposure ($N = 6$ colonies, $N = 476$ ants) confirmed the pattern seen in the simulated loads of the exposed networks. Among untreated foragers, 73 % acquired a detectable pathogen load, whereas only 37 % of nurses did, representing a significant difference in exposure risk for the task groups (Fig. 11C; GLMM, forager vs nurse probability of spores being present in detectable amounts: $p < 0.001$; Table S14), independent of exposure timing (day- vs night-time exposure: $p = 0.452$; Table S14). Of the 13 analysed queens, only two had detectable pathogen loads – one following daytime exposure ($1.1 * 10^{-4}$ ng/µL) and one following night-time exposure ($0.9 * 10^{-4}$ ng/µL). This highlights the effectiveness of their protection, though it prevented further statistical analysis. Among workers who contracted pathogen, untreated foragers (median load $3.3 * 10^{-4}$ ng/µL) had, on average, 2.4 times higher pathogen loads than nurses (median load $1.4 * 10^{-4}$ ng/µL; Fig. 11D; GLMM, forager vs nurse pathogen load $p < 0.001$; Table S15). Consistent with the simulations, there was no difference in pathogen loads between daytime and night-time exposure in measured pathogen loads for each task group (Fig. 11D, day- vs night-time exposure: $p = 0.315$; Table S15).

Thus, despite robust differences in colony network properties, the risk of pathogen contraction among untreated workers did not differ between daytime and night-time exposures after the nine-hour post-exposure period. However, untreated foragers had both a higher likelihood of contracting the pathogen compared to the nurses and carried higher pathogen loads when contaminated.

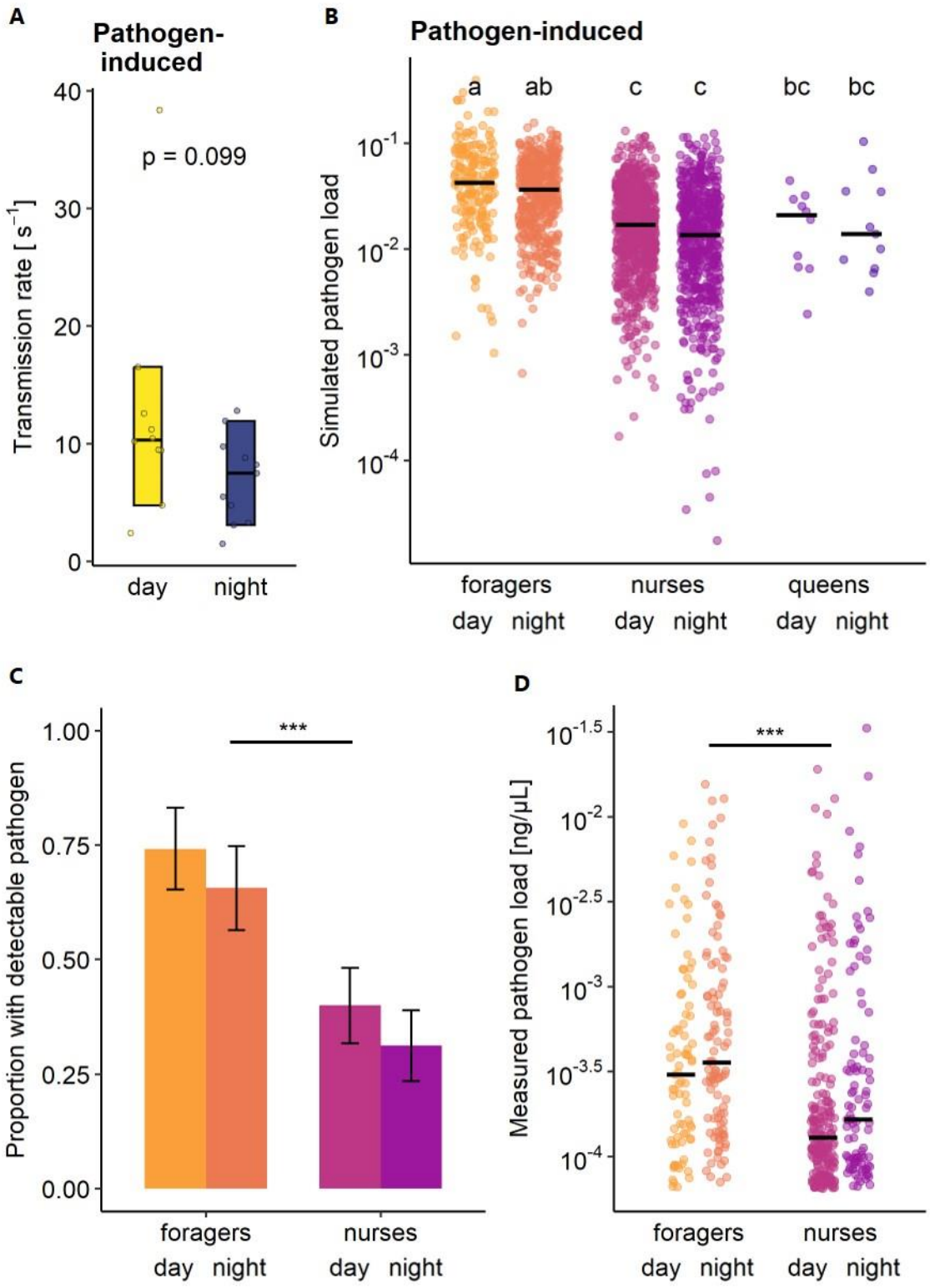

Fig. 11: Simulated and realised pathogen transmission. (A) Simulated transmission rate in pathogen-induced networks was similar during daytime and night-time (GLM; Table S12; $N = 21$ colonies). (B) Simulated pathogen loads for untreated foragers were comparable between day and night (GLMM; Table S13; $N = 649$ foragers, $N = 1325$ nurses. $N = 21$ queens). Nurses exhibited lower simulated loads than foragers, with no significant differences across day and night. Queens received intermediate simulated loads compared to foragers and nurses. In the realised pathogen transmission, (C) untreated foragers had a higher likelihood of contracting the pathogen than nurses (GLMM; Table S14; $N_{foragers.day} = 111$ workers, $N_{foragers.night} = 140$, $N_{nurses.day} = 550$, $N_{nurses.night} = 309$). (D) Among workers that acquired pathogen, foragers had higher pathogen loads than nurses (GLMM; Table S15; $N_{foragers.day} = 79$ workers, $N_{foragers.night} = 104$, $N_{nurses.day} = 220$, $N_{nurses.night} = 97$). Only two of the 13 analysed queens

(Fig.11 description continued) had detectable pathogen loads – one following daytime exposure ($1.1* 10^{-4}$ ng/µL) and one following night-time exposure ($0.9 * 10^{-4}$ ng/µL) – and were thus not included in the statistical analysis. Bars in (A) represent the median, with boxes indicating 95 % CIs. In (B) and (D), each point represents one individual, with bars showing the median. Error bars in (C) represent the standard error of the mean. Letters denote significant differences ($p < 0.05$) between groups following post-hoc tests, and *** indicates $p < 0.001$.

Sanitary care is preferentially performed by other foragers

To explore why untreated foragers were more likely to acquire pathogen than nurses, we analysed their overall contact and specifically their allogrooming interactions with pathogen-treated foragers.

Analysis of contact duration with treated foragers revealed a significant interaction between circadian phase and task group (GLMM, circadian phase × task group: $p = 0.028$; Table S16). Overall, untreated foragers had three times more contact with treated foragers than nurses (Fig. 12A). Post-hoc comparisons showed no differences in contact duration based on daytime or night-time exposure for either task group (Table S16). A similar pattern was observed for allogrooming rate, with untreated foragers performing allogrooming 3.7 times more frequently than nurses, regardless of time of day (Fig. 12B; GLMM, task group $p < 0.001$; circadian phase $p = 0.185$; Table S17). Overall, although predominantly performed by foragers, only 22 % of allogrooming occurred outside the nest, regardless of timing or type of exposure (GLM, $p = 0.895$; Table S18).

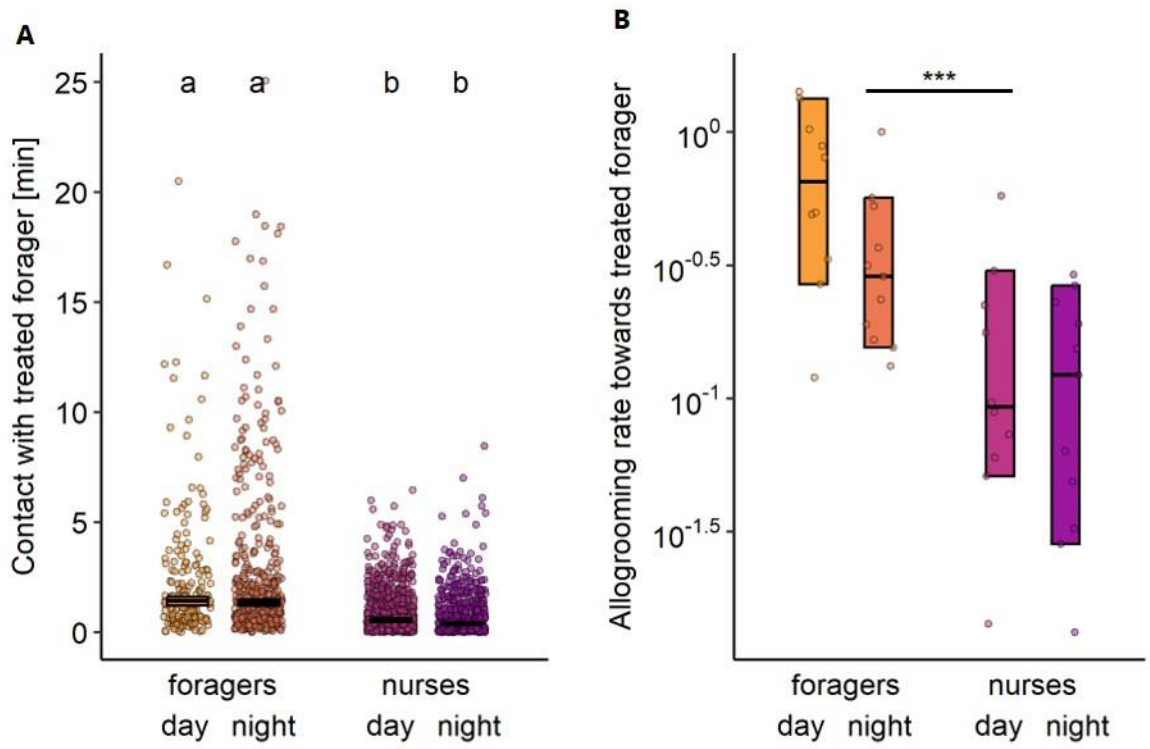

Fig. 12: Interactions with pathogen-treated foragers. (A) Untreated foragers were more likely to have contact with treated foragers compared to nurses (GLMM; Table S16). (B) Untreated foragers also allogroomed treated foragers more frequently than nurses did (aggregated per colony; GLMM; Table S17). Black bars represent the group medians, while boxes indicate the 95 % CIs. Letters denote significant differences ($p < 0.05$) between groups following post-hoc tests, and *** indicates $p < 0.001$. Sample sizes: $N = 649$ foragers, $N = 1322$ nurses, across 21 colonies.

4 Discussion

Our study revealed robust circadian patterns in colony network dynamics, which were largely resilient to our exposure treatments. Despite constitutive network properties favouring transmission within the forager community during the day, sanitary care behaviours and pathogen loads in pathogen-exposed colonies did not differ significantly between daytime and night-time exposure. Notably, the contamination risk for nurses and queens remained consistently low under all experimental conditions. This suggests that social immunity effectivity buffers against temporal variation in activity and pathogen exposure risks, continuously protecting the vulnerable colony centre from disease.

To investigate whether our colonies exhibit daily activity cycles, we analysed the activity of two distinct task groups: foragers and nurses. Foragers are workers responsible for leaving the nest to collect resources, while nurses remain inside to care for the brood. The queen's activity was not the focus of our analysis, as her primary role is egg-laying, and as a single individual per colony, she has minimal direct influence on colony network dynamics.

Similar to field observations of *Lasius niger*, our foragers exhibited a daily rhythm in activity, responding to changes in temperature and light (Depa, 2024; Yamauchi & Hayashida, 1970). These studies also highlighted, that foraging behaviour is influenced by weather and climate variations, with preferences that may vary widely – ranging from peak activity during the night or dawn in some cases to noon in others – or even disappear altogether, with no preference between day- and night-time foraging during warmer summer months. Depa (2024), investigating ant abundance in aphid colonies, speculated that the (counterintuitive) higher numbers during low temperatures coupled with high humidity could be due to ants remaining with the aphids during colder periods and then dispersing once temperatures rise. They also noted that increased rainfall, which was followed by a high humidity, might boost plant phloem sap production, thereby enhancing the quality or abundance of the aphids' honeydew (Douglas, 2006). Rival ant colonies and predators also influence ant movement, contributing to site-specific variations that can lead to contrasting observations of foraging preferences (Dolai et al., 2024; Orivel & Dejean, 2002). Since our experimental conditions were constant in their cycles over several days with food continuously provided *ad libitum*, our findings cannot generalise the circadian rhythm of *L. niger*. To assess their internal endogenous clock that oscillates over a 24-hour period, future studies would need to analyse behaviour in the absence of external cues that synchronise a daily rhythms, known as zeitgebers, such as light and temperature cycles (Dunlap et al., 2004).

The effect of zeitgebers varies in importance between foragers and nurses. While foragers' circadian patterns are more directly shaped by outside environmental factors, as described above, nurses remain inside the sheltered nests. Nonetheless, we observed that nurses also exhibited a diurnal activity pattern, albeit with a lower amplitude. Observing daily rhythms in nurses, even when the colony as a whole follows diurnal patterns, was unexpected (Charbonneau & Dornhaus, 2015). It is common in ants and bees for nurses to exhibit weaker or no daily rhythms compared to foragers. While nurses possess endogenous circadian clocks, these rhythms are often overridden by external zeitgebers, such as their social environment (Fuchikawa et al., 2016; Mildner & Roces, 2017). Social zeitgebers may include returning

foragers sharing resources (Fuchikawa et al., 2016; Lone & Sharma, 2011), or type of brood, with vulnerable eggs and larvae requiring constant care (Beer & Bloch, 2020; Fujioka et al., 2017). In our experiment, nurses cared for larvae and likely responded to feedback from the diurnal foragers.

We defined the two task groups, foragers and nurses, based on a binary classification, relying solely on time spent outside the nest (Stroeymeyt et al. 2018), instead of considering continuous "social maturity" scores that incorporate community structure, age, or spatial fidelity in the nest (Kay et al., 2024; Richardson et al., 2021; Richardson et al., 2022). While we explored such a community-based approach (Lin et al., 2008), we concluded it would not significantly enhance the interpretation of this study. In support of our binary classification, we observed clear differences in activity amplitude between task groups. Similarly, a recent study on the carpenter ant *Camponotus fellah* found social maturity positively correlated with age and time spent foraging, though social environment remained the dominant factor influencing behaviour and physiology (Kay et al., 2023).

Our approach also did not consider specific behaviours outside or inside the nest. For example, in *Diacamma sp*., performance of behaviours such as brood care, inactivity, walking and foraging do not exhibit a daily rhythm despite the species being predominantly diurnal (Fujioka, Okada, & Abe, 2021), underscoring the need of direct behavioural observations to understand rhythms in task allocation and division of labour. Although we did not analyse foraging behaviour directly, we observed faster walking speed at the same time of day as foragers spent more time outside the nest, consistent with findings that higher walking speeds correlate with active foraging in harvester ants (Davidson & Gordon, 2017). Ultimately, division of labour in many ant species fundamentally boils down to two groups: those caring for brood inside the nest, and those foraging outside (Kay et al., 2024; Richardson et al., 2021).

Crucially, we demonstrated that during the daytime, foragers spent more time in the foraging space and travelled greater distances. In natural settings, this would correspond to a higher risk of encountering and picking up pathogens, whether by moving across contaminated soil or contacting sporulating cadavers while collecting insect prey (Kurze et al., 2020; Pereira & Detrain, 2020). Although ants show some avoidance of fungal-contaminated soil and prey, this behaviour is highly variable between individuals (Pereira & Detrain, 2020; Tranter et al., 2015). Environmental spores, once picked up, have been shown to cause mortality (Rojas et al., 2018), with higher accumulating doses becoming increasingly lethal (Hughes et al., 2002; Okuno et al., 2012). This highlights how the elevated daytime activity by the foragers increases the colony's overall risk.

The increased daytime activity of both foragers and nurses was reflected in the colony's network properties, with more interaction partners (higher degree) and realised connections (higher density) during the day. This aligns with theoretical and empirical studies, showing that increased activity enhances interaction rates (Pie et al., 2004; Pinter-Wollman et al., 2011; Richardson et al., 2017), while greater foraging activity promotes the recruitment of potential foragers through brief interactions (Davidson & Gordon, 2017; Pinter-Wollman et al., 2013).

Consequently, this increased interaction rate led to highly connected cliques (higher clustering), where an individual's interaction partners were also likely to be connected (Danon

et al., 2012). Increased foraging also promotes interactions between subgroups via trophallaxis, the oral exchange of food (Charbonneau et al., 2013; Quevillon et al., 2015), which reduced community structure (lower modularity). These daytime characteristics, in combination with the rise in connections, slightly reduced the average pathway length between individuals (higher efficiency) and shortened the longest direct pathway in the colony (lower diameter) (Petter Holme & Saramäki, 2012).

Taken together, these network dynamics likely reflect the effective exchange of food and information during the colony's most active time of the day (Greenwald et al., 2015; Latora & Marchiori, 2001; Quevillon et al., 2015). However, studies on disease transmission dynamics suggest that our daytime networks would also show faster transmission of pathogens (Miller, 2009; Otterstatter & Thomson, 2007), which was confirmed by our transmission simulations (see also Box 1). This makes the colony more vulnerable during the daytime – when likelihood of contaminated foragers returning to the nest is already higher.

Indeed, our simulation across interaction of constitutive networks predicted a higher pathogen load for untreated foragers during the day, whereas the day network dynamics did not lead to a risk of higher loads for nurses and queens. This suggests that the protection of the valuable colony centre through organisational immunity is independent of when a pathogen is introduced. Similarly, Quevillon et al. (2015) found that interactions with returning foragers did not result in higher simulated transmission to the queen, providing strong evidence that constitutive organisational immunity in colonies is robust against daily activity rhythms.

That said, these predictions rely on the network properties of pathogen-free colonies and would only hold under the assumption that ants are unable to detect or react to the presence of a pathogen threat.

Ants are known to recognise fungal spores through their chemical cues (Stock et al., 2023) and respond by mechanically removing the spores from their contaminated nest mates' cuticle (Bos et al., 2012; Okuno et al., 2012; Qiu et al., 2014; Tranter et al., 2015; Walker & Hughes, 2009); a behaviour also observed in termites (Bulmer et al., 2023; Chen et al., 2023; Davis et al., 2018; Liu, Wang, et al., 2019; Rosengaus et al., 1998). In our study, this sanitary care response (i.e. allogrooming) was particularly evident upon the return of treated foragers. The overall increase in allogrooming was especially strong during the first thirty minutes. This aligns with the timeline of dynamic pathogen detection and removal described by Casillas-Pérez et al. (2023) in a closely related host-pathogen system, where *Lasius neglectus* ants were treated with *Metarhizium robertsii* spores. Their study demonstrates how ants, in groups of six, dynamically react to changing pathogen loads by sanitary care behaviour. Notably, allogrooming peaks just 10 minutes after exposure to the same spore dose used in our experiments (a 0.3 µL droplet of 10^9 spores/mL), before returning almost to baseline levels after 90 minutes (Casillas-Pérez et al., 2023). In our analysis of the post-exposure period, the initial increase in allogrooming did not differ significantly between treatment types (control or pathogen) but was more intense following daytime exposure, possibly because ants were already more active at that time. Yet, colonies treated at night quickly caught up, and no lasting day-night difference in allogrooming intensity was observed. This suggests that ants can reliably activate their social immunity response even during the less active night phase, ensuring a consistent and effective defence against disturbances regardless of the time of day.

Across the full sanitary care phase, covering both the peak and the return to baseline, allogrooming was more intense after pathogen exposure, though colonies also responded to the control treatment by increasing their allogrooming.

At first glance, the strong response in the control group may seem surprising. However, allogrooming is a common behaviour in ants, serving multiple functions beyond pathogen removal, such as maintaining a shared colony odour (Lenoir et al., 2001; Soroker et al., 1998). Ants also respond to pure surfactants, such as the oral secretions used by caterpillars to defend against predatory ants or detergents like Triton-X 100 used to suspend hydrophobic spores for experimental application (as in our study), by increasing grooming (Casillas-Pérez et al., 2023; Rostás & Blassmann, 2009). The surfactants commonly used in behavioural ecology experiments like Triton or Tween differ in chemical composition. For instance, Tween-80 resembles oleic acid, a known death signal in ants that attracts nest mates (Diez et al., 2013), while Tween-20 resembles lauric acid, a methyl-branched fatty acid found in gram-positive bacteria (Bernard et al., 1991). Compared to Tween, Triton likely contains fewer potentially bioactive compounds but still exhibits the surfactant effect (Brand et al., 1973), similar e.g. to the caterpillar oral secretions mentioned above.

Differences in application methods, and thus spore concentrations, as well as fungal strains further contribute to variation in the allogrooming literature. For instance, allowing ants to walk across contaminated surfaces elicited comparable levels of allogrooming in both control (water, Tween-20) and pathogen treatments (low and high doses of *Metarhizium*), as observed during scan-samplings at 10, 30 and 70 minutes post-exposure (Reber et al., 2011). Lastly, Stock et al. 2023 identified ergosterol as a pathogen-derived allogrooming trigger and demonstrated that ergosterol levels, which can vary between fungal strains, is directly linked to allogrooming levels.

We conclude that the strength of ants' allogrooming responses to pathogen versus control treatments across studies reflect two main factors: (i) the baseline allogrooming levels elicited by the surfactant control, and (ii) the response to the pathogen itself, which depends on concentration used and variations in the chemical profile.

Post-exposure, the colony networks generally maintained their circadian patterns, with the ants' reactions to the pathogen exposure remaining consistent between day and night. When comparing colonies exposed during daytime to their pre-exposure night phase and colonies exposed during night-time to their pre-exposure day phase, the circadian day-night differences became somewhat more pronounced following daytime exposure and less distinct after night-time exposure. With the exceptions of efficiency and diameter under night-time exposure, the overall network's circadian patterns remained intact across treatments and exposure time points, highlighting the remarkable robustness of these circadian differences in network properties.

During the first three hours post-exposure, an increase in network density and degree would suggest a transmission-enhancing effect, since both are typically linked to an enhanced transmission rate (Otterstatter & Thomson, 2007; Volz et al., 2011). Yet, such an apparent maladaptive effect of network changes following exposure could instead be attributed to the transient increase in sanitary care. Allogrooming relies on intense interaction between workers

and removes pathogenic spores from the colony as ants collect the spores in their infrabuccal pockets and then expel them in disinfected pellets (Casillas-Pérez et al., 2023; Tragust et al., 2013). This increase in intense interactions can affect network properties in ways typically associated with faster disease transmission, even though it effectively reduces spore numbers. Thus, without identifying the specific behaviours responsible for particular network changes, interpretations based only on proximity modelling may contradict their actual effects. The same network properties can result from behaviours that either promote or mitigate pathogen transmission. Importantly, this issue was only revealed through our additional analysis of allogrooming, made possible by the novel *Behavioural Inference Tool* developed by Wanderlingh (2024), which enabled the automated detection of allogrooming events directly from the marker-based tracking data. Relying exclusively on proximity represents a significant caveat when interpreting the effects of network properties and simulating disease transmission in network analysis. Interactions can have both positive and negative effects (Mersch, 2016; Quevillon et al., 2015), yet such biological underpinnings are not always accounted for in transmission simulations.

By analysing the nine hours immediately following exposure, our analysis combined two biologically distinct phases: the initial three-hour period of heightened sanitary care and the subsequent six-hour period, during which allogrooming returned nearly to baseline and residual spores on treated foragers could transmit through the colony. Over time, density, degree and efficiency decreased, while modularity increased, suggesting the colonies were in the process of reversing these transmission-enhancing effects to reach the transmission-inhibiting network properties demonstrated by Stroeymeyt at al. (2018). Their study focused exclusively on the 24-hour transmission phase, starting after the sanitary care period had subsided (hours 3 to 26 post-exposure). They showed that upon pathogen exposure, *L. niger* colonies further reduced transmission rates by increasing community structures. This was achieved through compartmentalisation into highly connected cliques of workers within the same task group (i.e., enhanced network modularity, clustering and task assortativity), while simultaneously reducing the average connection efficiency (lower network efficiency) (Stroeymeyt et al., 2018).

We explored this possibility by analysing the temporal changes in network properties over the three-hour post-exposure intervals. This analysis revealed that the positively correlated properties of density, degree, and clustering decreased after the sanitary care phase (i.e., from the second interval onward). Similarly, during the transmission phase, modularity increased while efficiency decreased, aligning with the changes reported by Stroeymeyt et al. (2018). It is plausible that with a longer post-exposure observation period, we might have observed a more pronounced increase in modularity and decrease in efficiency over time. However, extending the experiment was not feasible in this study, as our primary focus was to investigate the influence of circadian network patterns on pathogen transmission. This required concluding the experiment nine hours post-exposure to quantify individual pathogen loads.

In addition to the shorter post-treatment analysis window, our study also used a lower pathogen load at both the individual and the colony levels, which may have dampened the ants' responses to pathogen exposure. While Stroeymeyt et al. (2018) exposed 10 % of the colonies' workers to an application dose of 500,000 spores per individual, we exposed only 5 % of the colony to

300,000 spores each. This represents 50 % fewer workers treated, each with 60 % of the spore dose used by Stroeymeyt et al. (2018). Consequently, if the relationship of pathogen quantity and induced response were linear, we might expect one-third of the pathogen-induced changes observed in the earlier study. We chose this lower pathogen load because in Stroeymeyt et al. (2018) the pathogen had spread throughout the entire colony, with members differing only by their respective pathogen loads (either associated with disease or immunisation). In contrast, our objective was to capture the unsaturated phase of colony contamination. Indeed, by the end of our nine-hour post-exposure period, many workers in our experiment remained uncontaminated. Notably, only 2 of the 13 analysed queens and approximately one-third of the nurses picked up the pathogen, whereas three-quarters of the untreated foragers did. Moreover, among the workers with detectable loads, the pathogen load of a contaminated forager was on average double that of a contaminated nurse.

Importantly, we observed no differences in the pathogen load of foragers between day and night exposures. This finding suggests that even the relatively small post-exposure changes to network structure effectively mitigated the predicted higher contamination load of day-foragers compared to night-foragers in constitutive (i.e., pre-exposure) networks. Alternatively, this result may indicate that contact networks alone are imperfect predictors of transmission, particularly when differences in contamination loads are small.

The observed pathogen transmission aligned with simulated individual loads for the pathogen-exposed networks at the end of the nine-hour post-exposure period. Interestingly, the same pattern of individual loads was observed in control-exposed networks, despite these networks having a faster transmission rate (i.e., pathogen spread) during the day. In pathogen-exposed networks, the day-night difference in transmission rate that we also saw in constitutive networks was no longer present. This indicates that, although pathogen-induced changes in network properties were minimal, the post-exposure day and night networks no longer differed in the speed of pathogen transmission. The ants' responses to both pathogen and control treatments effectively mitigated the higher infection risk for day-foragers predicted in constitutive networks – a risk that could have persisted had the ants not detected (Tranter 2015; Stock 2023) and responded to (Stroeymeyt 2018) the contamination.

Importantly, in all our experimental conditions – pre-exposure, daytime exposure, and night-time exposure – nurses and queens consistently remained well-protected, as predicted by our models. This was further confirmed by our measured pathogen load data, where only one-third of nurses and one-sixth of queens exhibited any detectable pathogen load. Notably, queens were exceptionally well-protected, even surpassing predictions from simulations, which had estimated their loads to be intermediate to those of foragers and nurses.

This highlights the robustness of organisational immunity in safeguarding colony members based on their value to the colony. The highest protection was afforded to queens, who are crucial for colony reproduction and, in case of *L. niger*, irreplaceable. This was followed by younger nurses, who care for the queen and brood, and ultimately by older foragers, who received the least protection. This hierarchical protection was consistently maintained, even under varying external conditions, demonstrating the effectiveness and adaptability of the colony's collective defence strategies.

The higher contamination risk for untreated foragers compared to other colony members may stem from their higher interaction rates with treated foragers post-exposure. This aligns with the concept that individuals within a task group interact more frequently with each other, creating a community structure that is also reflected in their spatial segregation within the nest (Mersch et al., 2013; Richardson et al., 2021; Richardson et al., 2022). While our study did not look at spatial segregation, this likely limited the physical overlap between nurses and foragers, reducing nurses' involvement in sanitary care directed toward treated foragers. Consequently, this separation may shield nurses from both direct and indirect transmission routes (Richardson & Gorochowski, 2015), resulting in lower spore loads among nurses.

Moreover, the greater likelihood of foragers becoming contaminated and grooming other foragers may enhance their immune competence (Cini et al., 2020; Konrad et al., 2012; Liu, Wang, et al., 2019). In turn, ants with lower susceptibility to a pathogen have been shown to invest more time in allogrooming their nest mates (Konrad et al., 2018).

While this study provides valuable insights into the interaction between daily rhythms in activity, network properties, and pathogen transmission, some limitations should be acknowledged. The large, single-chambered nest design may not reflect the structural complexity of natural *L. niger* colonies (Khuong et al., 2016), which could influence transmission dynamics (Leckie et al., 2024; Pie et al., 2004). Additionally, while humidity was regulated in the tracking system, the relatively dry nests potentially affected ant movement into the foraging space.

Despite these limitations, this study captured both the immediate sanitary care phase and the onset of the transmission of spores that remained on the treated foragers' body surfaces after intense allogrooming (Casillas-Pérez et al., 2023). *Metarhizium* spores are initially loosely bound to the host cuticle through hydrophobic interactions but later firmly attach via germination and the formation of the appressorium, after approximately 12 to 48 hours (Hänel, 1982; Vestergaard et al., 1995). While Stroeymeyt et al. (2018) focused primarily on the later transmission phase, we included the early sanitary care phase and its effects on network properties, thereby emphasising the importance of distinguishing interactions types in disease transmission dynamics. Integrating allogrooming dynamics explicitly into the transmission simulation models (Fefferman et al., 2007) would be a valuable next step to disentangle interactions that may either inhibit or enhance pathogen spread.

The novel *Behavioural Inference Tool* developed by Wanderlingh (2024) enabled the automated detection of allogrooming events. Future research could benefit from extending this tool to detect trophallaxis behaviour, which requires close contact between individuals to share fluids (Meurville & LeBoeuf, 2021). Observations in *Metarhizium*-treated ants over several days show either no differences in trophallaxis rates of healthy and control ants (Konrad et al., 2012) or an increase by day three, when ants are infected but no longer infectious (Qiu et al., 2016). In contrast, tracking of a bee colony revealed that virus infections reduce trophallaxis events with infectious nest mates (Geffre et al., 2020). Trophallaxis may also serve as a mechanism to distribute protective immune effectors throughout the colony (Hamilton et al.,

2011). However, its role in transmission of pathogenic fungal spores from infectious but healthy nest mates to naïve nest mates remains unclear.

Our findings highlight how diurnal ant colonies maintain robust daily patterns in network properties while flexibly adapting to pathogen exposure. Regardless of the time of day, ants effectively upregulate sanitary care, ensuring the protection of their most valuable individuals – nurses and, particularly, queens – demonstrating the remarkable robustness of their social immune response. These results underscore the adaptive capacity of ant colonies to manage the trade-offs between daily activity rhythms and disease defence.

5 Supplementary Materials

5.1 Supplementary Figures

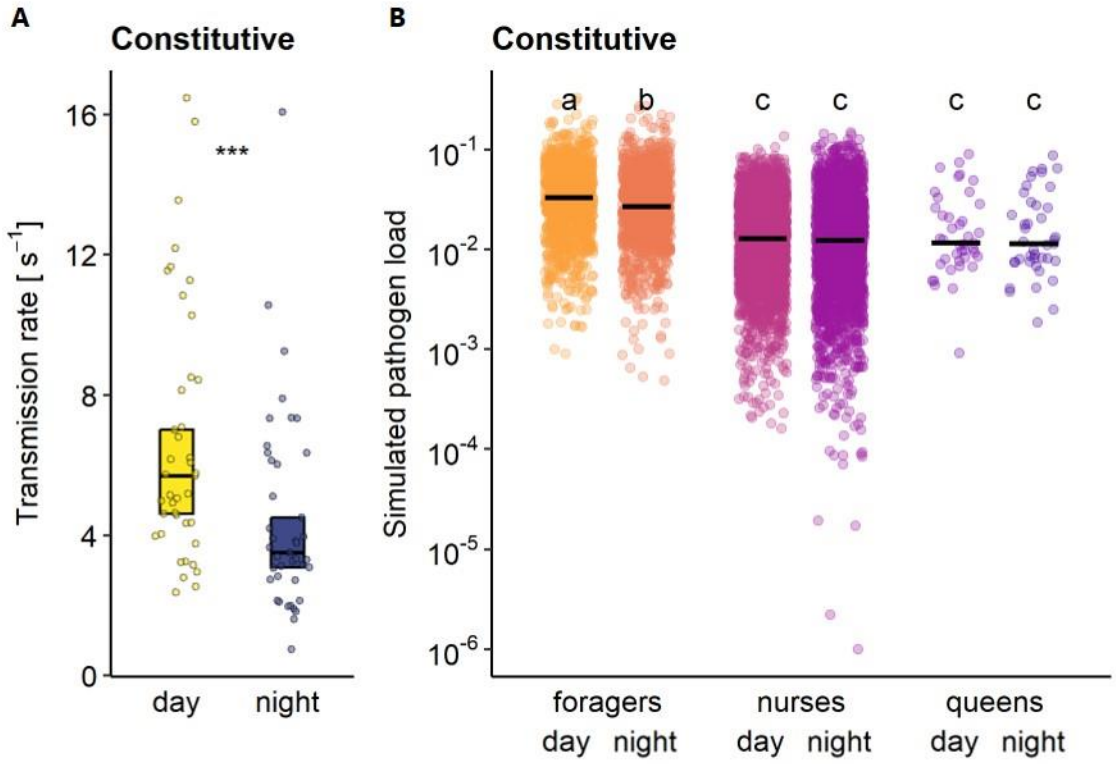

Fig. S1: Constitutive transmission simulations. (A) Simulated transmission rate in constitutive networks (i.e., pre-exposure) was significantly higher during the day compared to the night (GLMM; Table S4). (B) Simulated pathogen loads were highest for foragers during the day, and significantly higher compared to the night. Nurses and queens exhibited lower simulated loads than foragers, with no significant differences between nurses and queens or across day and night (GLMM; Table S5). Bars in (A) represent the median, and boxes indicate 95 % CIs (N = 41 colonies). In (B), each point represents one individual, with bars showing the median (N = 1360 foragers, N = 2706 nurses. N = 41 queens). Significant day-night differences in (A) are denoted by *** ($p < 0.001$). In (B) letters denote significant differences ($p < 0.05$) between groups following post-hoc tests.

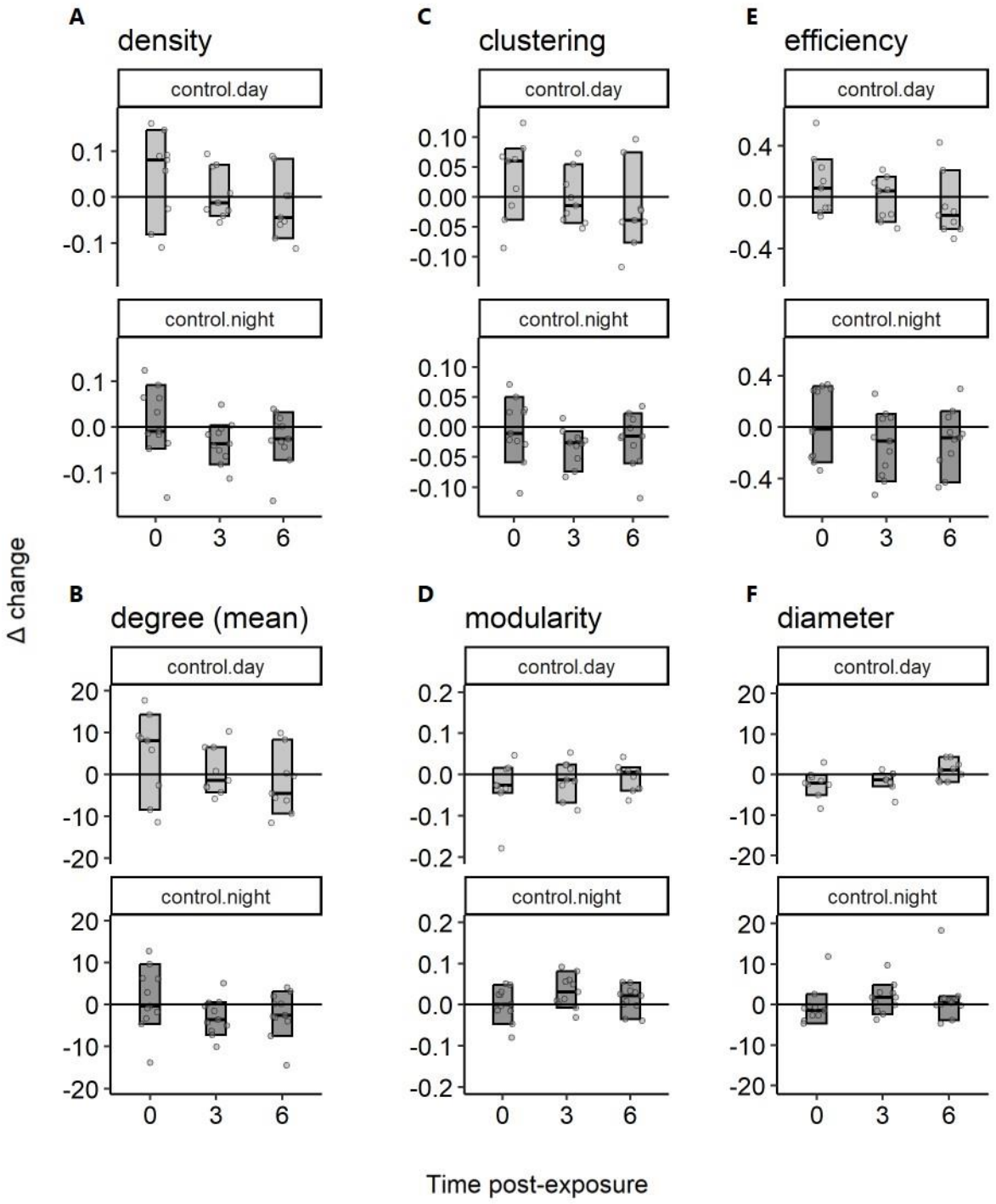

Fig. S2: Timeline of induced changes in network properties following control exposure. The plot shows control-induced changes during the first, second and third three-hour post-exposure intervals, separately for day- and night colonies, in (A) network density, (B) degree, (C) clustering, (D) modularity, (E) efficiency, and (F) diameter. Δ changes were calculated by subtracting pre1-values from post-values within each colony and interval, with the zero line indicating no induced changes. Bars represent the median, and boxes indicate 95 % CIs ($N_{control.day}$ = 9 colonies, $N_{control.night}$ = 11 colonies). For diameter, one extreme Δ-value (control.night, time post exposure 0, Δ = - 48) was removed from the plot after calculating the median and 95 % CIs to improve visibility.

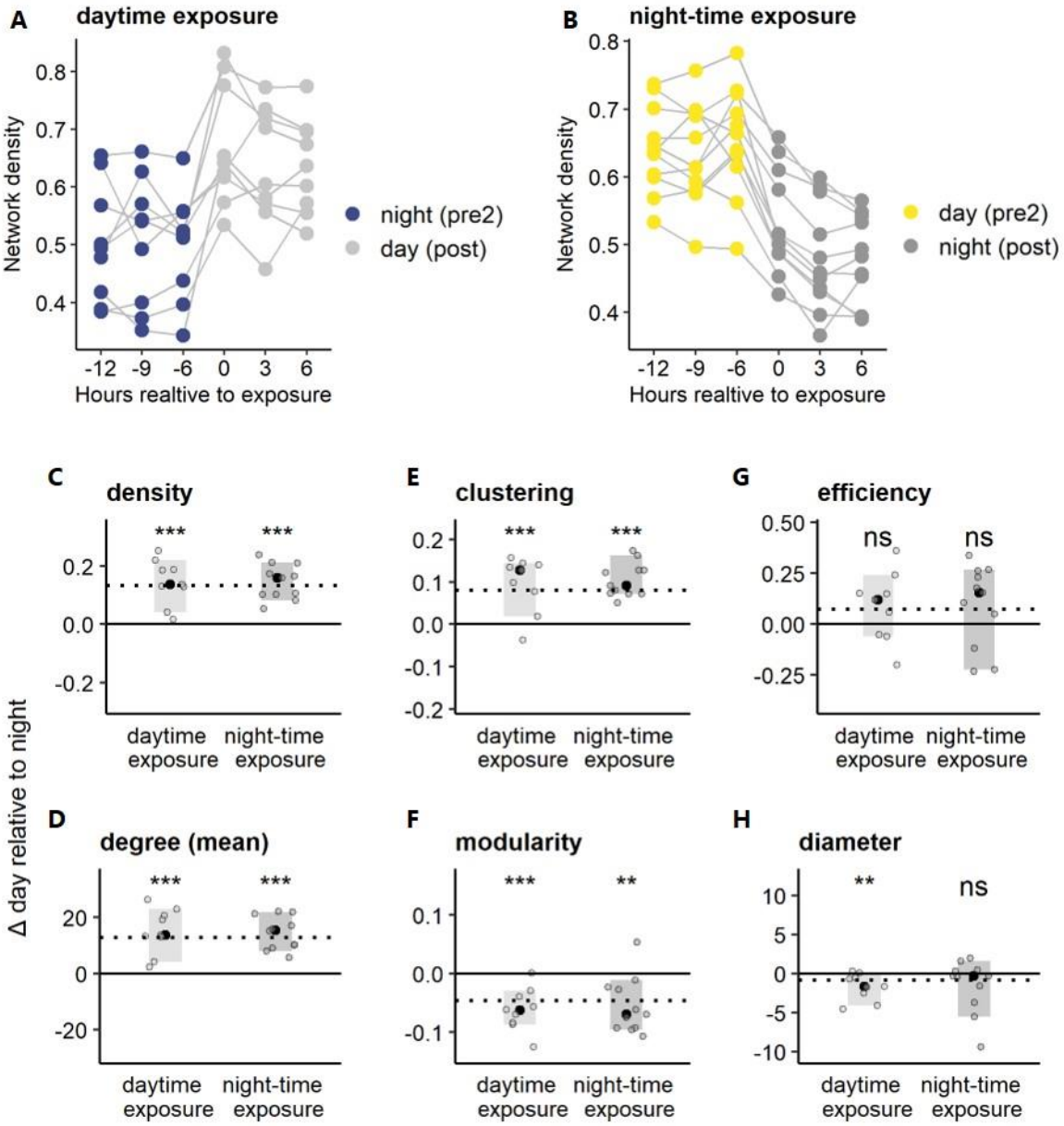

Fig. S3: Robust day-night differences after control exposure. (A) and (B) show colony network density during the circadian phases directly before (pre2) and after (post) control exposure. To visualise the robustness of day-night differences post-exposure, we calculated the "Δ day relative to night" (C - H): the night-values were subtracted from the day-values, such that the solid zero line indicates no day-night differences. This analysis was done separately for colonies experiencing daytime exposure and those experiencing night-time exposure, i.e., colonies treated at the start of the day, or the night, respectively. The daytime exposure Δ represents day(post) minus night(pre2), while the night-time delta represents day(pre2) minus night(post). The dashed line represents the median day-night differences observed in constitutive colonies (Δ day minus night; Fig. 6). In (C - H), black dots represent the median, and shaded boxes indicate 95 % CIs, based on $N_{daytime.exposure}$ = 9 colonies, and $N_{night\text{-}time.exposure}$ =11 colonies. Significant day-night differences are denoted by ** ($p < 0.01$) and *** ($p < 0.001$), while ns ($p > 0.05$) denotes non-significant differences.

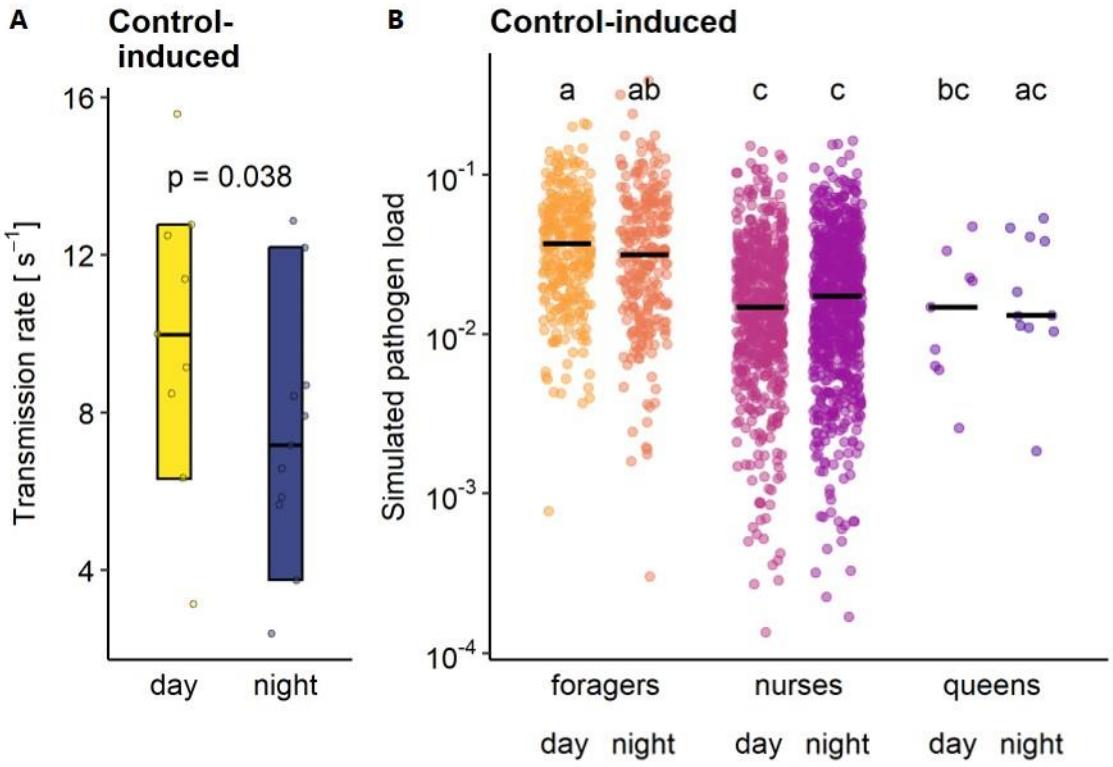

Fig. S4: Control-induced transmission simulations. (A) Simulated transmission rate in control-induced networks was significantly higher during the day compared to the night (GLM; Table S10). (B) Simulated pathogen loads were equal for untreated foragers during the day and night. Nurses exhibited lower simulated loads than foragers, with no significant differences across day and night. Queens received simulated loads intermediate between foragers and nurses, with no differences between day and night (GLMM; Table S11). Bars in (A) represent the median, and boxes indicate 95 % CIs (N = 20 colonies). In (B), each point represents one individual, with bars showing the median (N = 530 foragers, N = 1376 nurses. N = 20 queens). Significant day-night differences in (A) are denoted by p = 0.038. In (B) letters denote significant differences ($p < 0.05$) between groups following post-hoc tests.

5.2 Supplementary Tables

Table S1: Statistical results for the proportion of time spent outside the nest by foragers during daytime and night-time. We used a generalised linear mixed model (GLMM) with beta error distribution, including circadian phase (day/night) as main effect and controlling for colony size and colony ID. The proportion of time spent "outside" (i.e. in the foraging space) was aggregated for each colony to test differences between day and night ($N = 1360$ foragers; $N = 41$ colonies). Nurses were excluded from this analysis as they, by definition, don't spend more than 1 % of their time outside the nest. The table reports model details (response variable and main predictor in bold), test statistic (χ^2), degrees of freedom (df), p-value (exact unless < 0.001), and effect size (odds ratio day/night). All p-values are two-sided, bolded when significant (< 0.05).

Prop. of time foragers spend outside the nest				
GLMM	overall model			
prop. time outside ~ circadian phase + colony size + (1|colony)	χ^2	df	p-value	Effect size (odds ratio)
	15.228	1	**<0.001**	1.83

Table S2: Statistical results for the activity of foragers and nurses during daytime and night-time. GLMM results, including circadian phase (day/night) as main effect and controlling for colony size and colony ID. The behaviours (time active, speed while active, and distance travelled) were aggregated for each colony to test differences between day and night, separately for (a) foragers (N = 1360) and (b) nurses (N = 2706; N = 41 colonies). The tables report model details (response variable and main predictor in bold), test statistics (χ^2), degrees of freedom (df), p-values (exact unless < 0.001), and effect sizes (partial η^2). All p-values are two-sided, bolded when significant (< 0.05).

(a)

Forager behaviour during daytime vs night-time					
GLMM	behaviours	overall model			
behaviour ~ circadian phase + colony size + (1|colony)		χ^2	df	p-value	Effect size (partial η^2)
	time active	23.790	1	**<0.001**	0.44
	speed while active	48.229	1	**<0.001**	0.69
	distance travelled	39.048	1	**<0.001**	0.61

(b)

Nurse behaviour during daytime vs night-time					
GLMM	behaviours	overall model			
behaviour ~ circadian phase + colony size + (1|colony)		χ^2	df	p-value	Effect size (partial η^2)
	time active	18.993	1	**<0.001**	0.37
	speed while active	55.578	1	**<0.001**	0.74
	distance travelled	69.211	1	**<0.001**	0.82

Table S3: Statistical results for constitutive colony network properties during daytime and night-time. GLMM results, including circadian phase (day/night) as main effect. In addition to colony size and colony ID, we controlled for starting phase (day-/night-colonies), i.e. whether the colonies started the experimental tracking during daytime (N= 19) or night-time (N = 22). The network properties were aggregated for each colony. The table reports model details (response variable and main predictor in bold), test statistics (χ^2), degrees of freedom (df), p-values (exact unless < 0.001), and effect sizes (partial η^2). All p-values are two-sided and bolded when significant (< 0.05).

Network properties during daytime vs night-time					
GLMM	network properties	overall model			
network property ~ circadian phase + starting phase + colony size + (1|colony)		χ^2	df	p-value	Effect size (partial η^2)
	clustering	64.353	1	**<0.001**	0.79
	mean degree	62.205	1	**<0.001**	0.78
	density	62.509	1	**<0.001**	0.78
	diameter	6.150	1	**0.009**	0.16
	efficiency	6.690	1	**0.010**	0.15
	modularity	37.450	1	**<0.001**	0.60
	task assortativity	0.060	1	0.806	-

Table S4: Simulated transmission rate in constitutive colony networks during daytime and night-time. GLMM results, including circadian phase (day/night) as main effect and controlling for starting phase (day-/night-colonies), colony size and colony ID. The simulation was run on the constitutive networks for both the nine hours of daytime and nine hours of night-time (N = 41 colonies), originating from the same workers, that were later exposed. The table reports model details (response variable and main predictor in bold), test statistic (χ^2), degrees of freedom (df), p-value (exact unless < 0.001), and effect size (partial η^2). All p-values are two-sided and bolded when significant (< 0.05).

Simulated transmission rate in constitutive networks (seeds: treated foragers)				
GLMM	overall model			
transmission rate ~ circadian phase + starting phase + colony size + (1|colony)	χ^2	df	p-value	Effect size (partial η^2)
	20.194	1	**<0.001**	0.39

Table S5: Simulated pathogen load in constitutive networks. GLMM results, including task group (forager/nurse) and circadian phase (day/night) as main effects, including their interaction. We controlled for colony size and colony ID. Based on $N = 1360$ foragers, $N = 2706$ nurses. $N = 41$ queens across 41 colonies. The table reports model details (response variable and main predictor in bold), test statistics (χ^2), degrees of freedom (df), p-values (exact unless < 0.001), and effect size (partial η^2). All p-values are two-sided and bolded when significant (< 0.05).

Simulated pathogen load in constitutive networks (seeds: treated foragers)										
GLMM	overall model			interaction				pair-wise comparisons		
sim. load ~ task group * circadian phase + colony size + (1|colony)	χ^2	df	p-values	χ^2	df	p-values	Effect size (partial η^2)		z-values	p-values (Tukey contrasts)
	1181.847	5	**<0.001**	8.129	2	**0.017**	0.001	forager.night – forager.day	-4.647	**<0.001**
								nurse.day – forager.day	-28.682	**<0.001**
								nurse.night – forager.day	-30.049	**<0.001**
								queen.day – forager.day	-5.755	**<0.001**
								queen.night – forager.day	-5.816	**<0.001**
								nurse.day – forager. night	-23.636	**<0.001**
								nurse.night - forager.night	-25.003	**<0.001**
								queen.day - forager.night	-4.552	**<0.001**
								queen.night - forager.night	-4.614	**<0.001**
								nurse.night - nurse.day	-1.906	0.343

								queen.day - nurse.day	1.091	0.859
								queen.night - nurse.day	1.029	0.886
								queen.day - nurse.night	1.421	0.666
								queen.night - nurse.night	1.359	0.707
								queen.night - queen.day	-0.044	1.000

(Table S5 continued)

Table S6: Exposure-induced changes in allogrooming received by treated foragers. We used a negative binomial GLMM with a logit link function to test for changes in allogrooming events. The main effects were exposure (control/pathogen), circadian phase (day/night) and experimental period (pre1/post), including all their interactions. The experimental periods covered (a) the first 30 minutes of the tracking (pre1) compared to the first 30 minutes after exposure (post), or (b) the first three hours of the tracking (pre1) compared to the first three hours after exposure (post). We controlled for time of day (beginning of the 15-minute intervals) and colony ID for tests with multiple values per colony. Based on 187 treated foragers across 41 colonies. The tables report model details (response variable and main predictor in bold), test statistics (χ^2), degrees of freedom (df), p-values (exact unless < 0.001), and effect sizes (odds ratio). All p-values are two-sided, bolded when significant (< 0.05), and corrected for multiple testing using BH method for the tests reported in (a) and (b). Whenever the interactions were non-significant, the effects of the main predictors were estimated from the reduced model.

(a)

Change in allogrooming events received by treated foragers before and after exposure (first 30 minutes)												
GLMM	overall model			interactions				main effects				Effect size (odds ratio)
allogrooming ~ exposure * circadian phase * experimental period + (1|time of day)	χ^2	df	p-values		χ^2	df	p-values		χ^2	df	p-values	
	118.504	7	**< 0.001**	exposure x circadian phase x experimental period	0.194	1	0.659	exposure	1.813	1	0.178	-
				exposure x circadian phase	1.178	1	0.278	circadian phase	-	-	-	-
				exposure x experimental period	0.129	1	0.720	experimental period	-	-	**-**	-
				circadian phase x experimental period	5.142	1	**0.023**					0.421

(b)

Change in allogrooming events received by treated foragers before and after exposure (first three hours)												
GLMM	overall model			interactions				main effects				Effect size (odds ratio)
allogrooming ~ exposure * circadian phase * experimental period + (1|time of day) + (1|colony)	χ^2	df	p-values		χ^2	df	p-values		χ^2	df	p-values	
	320.370	7	**< 0.001**	exposure x circadian phase x experimental period	0.450	1	0.502	exposure	-	-	-	-
				exposure x circadian phase	0.707	1	0.400	circadian phase	0.324	1	0.569	-
				exposure x experimental period	5.587	1	**0.018**	experimental period	-	-	**-**	1.45
				circadian phase x experimental period	< 0.001	1	0.984					

(Table S6 continued)

Table S7: Exposure-induced changes in network properties during the first and third three-hour windows. GLMM results, including exposure (control/pathogen), experimental period (pre1/post) and circadian phase (day/night) as main effects, including all their interactions. The experimental periods covered (a) the first three-hour window of the tracking (pre1) and the first three-hour window post exposure (post), or (b) the third three-hour window of the tracking (pre1) and the third three-hour window of the tracking (post). We controlled for colony size and colony ID. Based on 10 "pathogen day"-colonies, 11 "pathogen night"-colonies, 9 "control day"-colonies, and 11 "control night"-colonies. The tables report model details (response variable and main predictor in bold), test statistics (χ^2), degrees of freedom (df), p-values (exact unless < 0.001), and effect sizes (partial η^2). All p-values are two-sided, bolded when significant (< 0.05), and corrected for multiple testing, i.e., testing the first and third three-hour window, using BH method for each network property. Because the interactions were non-significant, the effects of the main predictors were estimated based on the reduced model.

(a)

Change in network properties during the first three-hour window post-exposure													
GLMM	network properties	overall model			interactions				main effects				Effect size (partial η^2)
network property ~ exposure * experimental period * circadian phase + colony size + (1|colony)		χ^2	df	p-values		χ^2	df	p-values		χ^2	df	p-values	
	clustering	16.289	7	**0.023**	exposure x experimental period x circadian phase	1.062	1	0.303	exposure	0.292	1	0.569	-
					exposure x experimental period	0.264	1	0.608	experimental period	3.209	1	0.073	-
					exposure x circadian phase	0.795	1	0.373	circadian phase	10.880	1	**< 0.001**	0.21
					experimental period x circadian phase	0.961	1	0.327					-
	mean degree	25.702	7	**< 0.001**	exposure x experimental period x circadian phase	1.436	1	0.231	exposure	0.001	1	0.982	-
					exposure x experimental period	0.616	1	0.432	experimental period	9.061	1	**0.003**	0.18

					exposure x circadian phase	0.105	1	0.746	circadian phase	18.529	1	**< 0.001**	0.31
					experimental period x circadian phase	0.032	1	0.859					-
	density	23.405	7	**0.001**	exposure x experimental period x circadian phase	1.436	1	0.231	exposure	0.001	1	0.972	-
					exposure x experimental period	0.825	1	0.364	experimental period	8.984	1	**0.003**	0.18
					exposure x circadian phase	0.128	1	0.720	circadian phase	14.804	1	**< 0.001**	0.27
					experimental period x circadian phase	0.037	1	0.847					-
	diameter	10.382	7	0.168	exposure x experimental period x circadian phase	-	-	-	exposure	-	-	-	-
					exposure x experimental period	-	-	-	experimental period	-	-	-	-
					exposure x circadian phase	-	-	-	circadian phase	-	-	-	-
					experimental period x circadian phase	-	-	-					-
	efficiency	5.433	7	0.607	exposure x experimental period x circadian phase	-	-	-	exposure	-	-	-	-
					exposure x experimental period	-	-	-	experimental period	-	-	-	-
					exposure x circadian phase	-	-	-	circadian phase	-	-	-	-
					experimental period x circadian phase	-	-	-					-

	modularity	9.332	7	0.230	exposure x experimental period x circadian phase	-	-	-	exposure	-	-	-	-
					exposure x experimental period	-	-	-	experimental period	-	-	-	-
					exposure x circadian phase	-	-	-	circadian phase	-	-	-	-
					experimental period x circadian phase	-	-	-					-

(Table S7a continued)

(b)

Change in network properties during the third three-hour window post-exposure													
GLMM	network properties	overall model			interactions				main effects				Effect size (partial η^2)
network property ~ exposure * experimental period * circadian phase + colony size + (1|colony)		χ^2	df	p-values		χ^2	df	p-values		χ^2	df	p-values	
	clustering	28.197	7	**< 0.001**	exposure x experimental period x circadian phase	0.023	1	0.879	exposure	0.075	1	0.785	-
					exposure x experimental period	0.032	1	0.859	experimental period	9.566	1	**0.002**	0.19
					exposure x circadian phase	1.307	1	0.253	circadian phase	22.609	1	**< 0.001**	0.36
					experimental period x circadian phase	0.003	1	0.957					-

	mean degree	28.586	7	**< 0.001**	exposure x experimental period x circadian phase	0.026	1	0.871	exposure	0.041	1	0.839	-
					exposure x experimental period	0.221	1	0.639	experimental period	4.079	1	**0.043**	0.09
					exposure x circadian phase	0.373	1	0.542	circadian phase	32.721	1	**< 0,001**	0.44
					experimental period x circadian phase	0.006	1	0.938					-
	density	26.329	7	**< 0.001**	exposure x experimental period x circadian phase	0.069	1	0.794	exposure	0.069	1	0.792	-
					exposure x experimental period	0.178	1	0.673	experimental period	4.409	1	**0.036**	0.10
					exposure x circadian phase	0.425	1	0.514	circadian phase	28.203	1	**< 0.001**	0.41
					experimental period x circadian phase	0.001	1	0.974					-
	efficiency	7.444	7	0.607	exposure x experimental period x circadian phase	-	-	-	exposure	-	-	-	-
					exposure x experimental period	-	-	-	experimental period	-	-	-	-
					exposure x circadian phase	-	-	-	circadian phase	-	-	-	-
					experimental period x circadian phase	-	-	-					-
	modularity	12.487	7	0.171	exposure x experimental period x circadian phase	-	-	-	exposure	-	-	-	-

					exposure x experimental period	-	-	-	experimental period	-	-	-	-
					exposure x circadian phase	-	-	-	circadian phase	-	-	-	-
					experimental period x circadian phase	-	-	-					-

(Table S7b continued)

Table S8: Slope analysis of the exposure-induced changes in network properties across all three three-hour windows. GLMM results, including exposure (control/pathogen), circadian phase (day/night), and time hours post (0/3/6; start time of the three-hour window post exposure) as main effects, including all their interactions. The experimental periods covered the first nine hours of the tracking (pre1) and the last nine hours (post). We controlled for colony size and colony ID. The analysis was done on the delta values (post minus pre1) of each colony per time window in post. Based on 10 "pathogen day"-colonies, 11 "pathogen night"-colonies, 9 "control day"-colonies, and 11 "control night"-colonies. The table reports model details (response variable and main predictor in bold), test statistics (χ^2), degrees of freedom (df), p-values (exact unless < 0.001), and effect sizes (partial η^2). All p-values are two-sided and bolded when significant (< 0.05). Because the interactions were non-significant, the effects of the main predictors were estimated based on the reduced model.

Change in network properties during the first three-hour window post-exposure												
GLMM	network properties	overall model			interactions				main effects				Effect size (partial η^2)
network property ~ exposure * circadian phase * time hours post + colony size + (1|colony)		χ^2	df	p-values		χ^2	df	p-values		χ^2	df	p-values	
	clustering	27.003	7	**< 0.001**	exposure x circadian phase x time hours post	1.071	1	0.313	exposure	0.664	1	0.415	-
					exposure x circadian phase	1.145	1	0.284	circadian phase	0.056	1	0.813	-
					exposure x time hours post	0.574	1	0.449	time hours post	25.524	1	**< 0.001**	0.24
					circadian phase x time hours post	1.353	1	0.245					

	mean degree	25.975	7	**< 0.001**	exposure x circadian phase x time hours post	1.348	1	0.246	exposure	1.756	1	0.185	-
					exposure x circadian phase	1.666	1	0.197	circadian phase	0.297	1	0.586	-
					exposure x time hours post	0.235	1	0.628	time hours post	23.659	1	**< 0.001**	0.22
					circadian phase x time hours post	0.064	1	0.800					-
	density	27.189	7	**< 0.001**	exposure x circadian phase x time hours post	1.355	1	0.244	exposure	1.995	1	0.158	-
					exposure x circadian phase	1.995	1	0.158	circadian phase	0.216	1	0.642	-
					exposure x time hours post	0.424	1	0.515	time hours post	24.371	1	**< 0.001**	0.23
					circadian phase x time hours post	0.056	1	0.814					-
	diameter	13.626	7	0.058	exposure x circadian phase x time hours post	-	-	-	exposure	-	-	-	-
					exposure x circadian phase	-	-	-	circadian phase	-	-	-	-
					exposure x time hours post	-	-	-	time hours post	-	-	-	-
					circadian phase x time hours post	-	-	-					-
	efficiency	17.622	7	0.014	exposure x circadian phase x time hours post	2.282	1	0.131	exposure	0.610	1	0.435	-
					exposure x circadian phase	0.335	1	0.563	circadian phase	0.097	1	0.756	-

					exposure x time hours post	0.488	1	0.485	time hours post	10.745	1	**0.001**	0.12
					circadian phase x time hours post	3.799	1	0.051					-
	modularity	21.679	7	**0.003**	exposure x circadian phase x time hours post	0.382	1	0.536	exposure	0.007	1	0.935	-
					exposure x circadian phase	1.205	1	0.272	circadian phase	0.839	1	0.360	-
					exposure x time hours post	3.671	1	0.055	time hours post	17.249	1	**< 0.001**	0.17
					circadian phase x time hours post	0.004	1	0.953					-

(Table S8 continued)

Table S9: Day-night differences within colonies transitioning from the pre-exposure period into the post-exposure period. GLMM results, including circadian phase (day/night) as main effect, and controlling for colony size and colony ID. The experimental periods covered the second nine-hour interval of the tracking (pre2) and the last nine hours (post). The analysis was done separately for the four treatment groups, (a) 10 "pathogen day"-colonies transitioning from pre(night) to post(day), (b) 11 "pathogen night"-colonies transitioning from pre(day) to post(night), (c) 9 "control day"-colonies transitioning from pre(night) to post(day), and (d) 11 "control night"-colonies transitioning from pre(day) to post(night). The tables report model details (response variable and main predictor in bold), test statistics (χ^2), degrees of freedom (df), p-values (exact unless < 0.001), and effect sizes (partial η^2). All p-values are two-sided and bolded when significant (< 0.05).

(a)

Day-night differences in network properties: pre(night) to pathogen(day)					
GLMM	network properties	overall model			
network property ~ circadian phase + colony size + (1|colony)		χ^2	df	p-value	Effect size (partial η^2)
	clustering	18.024	1	**<0.001**	0.84
	mean degree	18.914	1	**<0.001**	0.85
	density	18.914	1	**<0.001**	0.85
	diameter	8.787	1	**0.003**	0.58
	efficiency	6.461	1	**0.011**	0.48
	modularity	19.721	1	**<0.001**	0.86

(b)

Day-night differences in network properties: pre(day) to pathogen(night)					
GLMM	network properties	overall model			
network property ~ circadian phase + colony size + (1|colony)		χ^2	df	p-value	Effect size (partial η^2)
	clustering	14.413	1	**<0.001**	0.73
	mean degree	13.053	1	**<0.001**	0.69
	density	13.280	1	**<0.001**	0.70
	diameter	3.774	1	0.052	-
	efficiency	0.259	1	0.611	-
	modularity	12.943	1	**<0.001**	0.69

(c)

Day-night differences in network properties: pre(night) to control(day)					
GLMM	network properties	overall model			
network property ~ circadian phase + colony size + (1|colony)		χ^2	df	p-value	Effect size (partial η^2)
	clustering	10.979	1	**<0.001**	0.70
	mean degree	14.219	1	**<0.001**	0.79
	density	13.037	1	**<0.001**	0.76
	diameter	6.734	1	**0.009**	0.53
	efficiency	2.275	1	0.131	-
	modularity	12.843	1	**<0.001**	0.76

(d)

Day-night differences in network properties: pre(day) to control(night)					
GLMM	network properties	overall model			
network property ~ circadian phase + colony size + (1|colony)		χ^2	df	p-value	Effect size (partial η^2)
	clustering	25.012	1	**<0.001**	0.88
	mean degree	23.070	1	**<0.001**	0.86
	density	22.975	1	**<0.001**	0.87
	diameter	2.353	1	0.125	-
	efficiency	2.293	1	0.130	-
	modularity	9.932	1	**0.002**	0.59

(Table S9 continued)

Table S10: Simulated transmission rate in control-induced colony networks during daytime and night-time. GLM results, including circadian phase (day/night) as main effect and controlling for colony size. The simulation was run on the control-induced networks for both the nine hours of daytime ($N = 9$), and nine hours of night-time ($N = 11$), originating from the treated foragers. The table reports model details (response variable and main predictor in bold), test statistic (χ^2), degrees of freedom (df), exact p-value, and effect size (partial η^2). All p-values are two-sided and bolded when significant (< 0.05).

Simulated transmission rate in control-induced networks (seeds: treated foragers)				
GLM	overall model			
transmission rate ~ circadian phase + colony size	Sum of Squares	df	p-value	Effect size (partial η^2)
	0.991	1	**0.038**	0.11

Table S11: Simulated pathogen load in control-induced networks. GLMM results, including task group (forager/nurse) and circadian phase (day/night) as main effects, including their interaction. We controlled for colony size and colony ID. Based only on the control-treated colonies (daytime exposure $N = 9$, and night-time exposure $N = 11$). The table reports model details (response variable and main predictor in bold), test statistics (χ^2), degrees of freedom (df), p-values (exact unless < 0.001), and effect size (partial η^2). All p-values are two-sided and bolded when significant (< 0.05).

Simulated pathogen load in control-induced networks (seeds: treated foragers)										
GLMM	overall model			interaction				pair-wise comparisons		
sim. load ~ task group * circadian phase + colony size + (1|colony)	χ^2	df	p-values	χ^2	df	p-values	Effect size (partial η^2)		z-values	p-values (Tukey contrasts)
	263.815	5	**<0.001**	6.760	2	**0.034**	0.004	forager.night – forager.day	-0.595	0.988
								nurse.day – forager.day	-13.163	**<0.001**
								nurse.night – forager.day	-4.320	**<0.001**
								queen.day – forager.day	-3.404	**0.006**
								queen.night – forager.day	-2.287	0.153
								nurse.day – forager. night	-4.382	**<0.001**
								nurse.night - forager.night	-10.387	**<0.001**
								queen.day - forager.night	-2.585	0.074
								queen.night - forager.night	-2.308	0.146
								nurse.night - nurse.day	0.736	0.968

								queen.day - nurse.day	-0.193	1.000
								queen.night - nurse.day	0.673	0.979
								queen.day - nurse.night	-0.563	0.990
								queen.night - nurse.night	0.299	1.000
								queen.night - queen.day	0.632	0.984

(Table S11 continued)

Table S12: Simulated transmission rate in pathogen-induced colony networks during daytime and night-time. GLM results, including circadian phase (day/night) as main effect and controlling for colony size. The simulation was run on the pathogen-induced networks for both the nine hours of daytime ($N = 10$), and nine hours of night-time ($N = 11$), originating from treated foragers. The table reports model details (response variable and main predictor in bold), test statistic (χ^2), degrees of freedom (df) and exact, two-sided p-value.

Simulated transmission rate in pathogen-induced networks (seeds: treated foragers)			
GLM	overall model		
transmission rate ~ circadian phase + colony size	Sum of Squares	df	p-value
	1.350	1	0.099

Table S13: Simulated pathogen load in pathogen-induced networks. GLMM results, with task group (forager/nurse) and circadian phase (day/night) as main effects, including their interaction. We controlled for colony size and colony ID. Based only on the pathogen-treated colonies (daytime exposure $N = 10$, and night-time exposure $N = 11$). The table reports model details (response variable and main predictor in bold), test statistics (χ^2), degrees of freedom (df), p-values (exact unless < 0.001), and effect size (partial η^2). All p-values are two-sided and bolded when significant (< 0.05).

Simulated pathogen load in pathogen-induced networks (seeds: treated foragers)										
GLMM	overall model			interaction				pair-wise comparisons		
sim. load ~ task group * circadian phase + colony size + (1|colony)	χ^2	df	p-values	χ^2	df	p-values	Effect size (partial η^2)		z-values	p-values (Tukey contrasts)
	320.505	5	**<0.001**	12.122	2	**0.002**	0.006	forager.night – forager.day	-2.725	0.052
								nurse.day – forager.day	-14.621	**<0.001**
								nurse.night – forager.day	-7.581	**<0.001**
								queen.day – forager.day	-4.015	**<0.001**
								queen.night – forager.day	-3.276	**0.001**
								nurse.day – forager. night	-4.503	**<0.001**
								nurse.night - forager.night	11.582	**<0.001**
								queen.day - forager.night	-2.222	0.181
								queen.night - forager.night	2.092	0.237
								nurse.night - nurse.day	-0.646	0.982

								queen.day - nurse.day	-0.040	1.000
								queen.night - nurse.day	0.421	0.998
								queen.day - nurse.night	0.276	1.000
								queen.night - nurse.night	0.841	0.946
								queen.night – queen.day	0.338	0.999

(Table S13 continued)

Table S14: Proportion of workers with detectable pathogen loads. Results for GLMM with binomial error distribution, including circadian phase (day/night) and task group (forager/nurse) as main effects, as well as their interaction. We controlled for colony ID. Based only on a subset of the pathogen-treated colonies (daytime exposure $N = 660$ workers across 7 colonies, and night-time exposure $N = 449$ across 6 colonies). The table reports model details (response variable and main predictor in bold), test statistics (χ^2), degrees of freedom (df), p-values (exact unless < 0.001), and effect size (odds ratio). All p-values are two-sided and bolded when significant (< 0.05). Because the interaction was non-significant, the effects of the main predictors were estimated from the reduced model.

Proportion of ants that carry pathogen after 9 h											
GLMM	overall model			interaction			main effects				
contaminated ~ circadian phase * task group + (1|colony)	χ^2	df	p-values	χ^2	df	p-values		χ^2	df	p-values	Effect size (odds ratio)
	89.470	3	**<0.001**	0.001	1	0.978	circadian phase	0.567	1	0.452	---
							task group	81.885	1	**<0.001**	4.88

Table S15: Measured qPCR pathogen loads. GLMM results, with circadian phase (day/night) and task group (forager/nurse) as main effects, including their interaction. We controlled for colony ID. Based only on those workers that had detectable pathogen loads (daytime exposure $N = 299$ workers across 7 colonies, and night-time exposure $N = 201$ workers across 6 colonies). The table reports model details (response variable and main predictor in bold), test statistics (χ^2), degrees of freedom (df), p-values (exact unless < 0.001), and effect size (partial η^2). All p-values are two-sided and bolded when significant (< 0.05). Because the interaction was non-significant, the effects of the main predictors were estimated from the reduced model.

Measured pathogen loads after 9 h											
GLMM	overall model			interaction			main effects				
pathogen load ~ circadian phase * task group + (1|colony)	χ^2	df	p-values	χ^2	df	p-values		χ^2	df	p-values	Effect size (partial η^2)
	42.062	3	**<0.001**	0.002	1	0.963	circadian phase	1.011	1	0.315	---
							task group	41.351	1	**<0.001**	0.08

Table S16: Duration of contact with treated foragers. GLMM results, with task group (forager/nurse) and circadian phase (day/night) as main effects, including their interaction. We controlled for colony ID. Based only on the pathogen-treated colonies (daytime exposure $N = 10$, and night-time exposure $N = 11$). The table reports model details (response variable and main predictor in bold), test statistics (χ^2), degrees of freedom (df), p-values (exact unless < 0.001), and effect size (partial η^2). All p-values are two-sided and bolded when significant (< 0.05).

Duration of contact with treated foragers									
GLMM	overall model			interaction				pair-wise comparisons	
contact duration~ task group * circadian phase + (1|colony)	χ^2	df	p-values	χ^2	df	p-values	Effect size (partial η^2)		z-values	p-values (Tukey contrasts)
	262.283	3	**<0.001**	4.827	1	**0.028**	0.003	forager.night – forager.day	-1.036	0.685
								nurse.day – forager.day	-12.625	**<0.001**
								nurse.night – forager.day	-3.971	**<0.001**
								nurse.day – forager. night	-2.850	**0.016**
								nurse.night - forager.night	-11.005	**<0.001**
								nurse.night - nurse.day	-0.156	0.998

Table S17: Allogrooming rate direct toward treated foragers. GLMM results, with circadian phase (day/night) and task group (forager/nurse) as main effects, including their interaction. We controlled for colony ID. Based only on the pathogen-treated colonies (daytime exposure $N = 10$, and night-time exposure $N = 11$). The table reports model details (response variable and main predictor in bold), test statistics (χ^2), degrees of freedom (df), p-values (exact unless < 0.001), and effect size (partial η^2). All p-values are two-sided and bolded when significant (< 0.05). Because the interaction was non-significant, the effects of the main predictors were estimated from the reduced model.

Allogrooming rate received by treated foragers											
GLMM	overall model			interaction			main effects				
contaminated ~ circadian phase * task group + (1|colony)	χ^2	df	p-values	χ^2	df	p-values		χ^2	df	p-values	Effect size (partial η^2)
	30.185	3	**<0.001**	1.461	1	0.227	circadian phase	1.759	1	0.185	---
							task group	54.268	1	**<0.001**	0.72

Table S18: Proportion of allogrooming received by treated foragers outside the nest. Results for GLM with beta error distribution, including circadian phase (day/night) and exposure (control/pathogen) as main effects, as well as their interaction. Based only on the pathogen-treated colonies (daytime exposure $N = 10$, and night-time exposure $N = 11$). The table reports model details (response variable and main predictor in bold), test statistics (χ^2), degrees of freedom (df), and exact, two-sided p-value.

Prop. of allogrooming taking place in the foraging space			
GLM	overall model		
prop. grooming outside ~ circadian phase * exposure	χ^2	df	p-value
	0.607	3	0.895

Table S19: List of consumables.

Item	**Distributor**	**REF**
Fluon®AD309E	deMonchy	I0113
Triton™ X-100	Sigma-Aldrich	T8787
2.8 mm ceramic beads	Qiagen	13114-325
1 mm zirconia beads	Lactan	N0381
Glass beads, acid-washed, 425-600µm	Sigma-Aldrich	G8772-1KG
DNeasy 96 Blood & Tissue Kit	Qiagen	69582
Ethanol puriss p.a. 99.8% (Honeywell)	Bartelt	32221-1L
primer	Sigma-Aldrich	-
Water suitable for PCR	Sigma-Aldrich	WA502
KAPA SYBR® FAST for LightCycler® 480	Sigma-Aldrich	KK461
50 µL pipette tips	Beckman Coulter	B85888
SafeSeal tube, 2 ml, PP	Sarstedt	72.695.500
DNA-LoBind Tubes 1.5 ml	Eppendorf	0030108051
Eppendorf Tubes® 5.0 mL	Eppendorf	0030119487
PCR microplates	Axygen	PCR-384-LC480-W

References

Arnan, X., Cerdá, X., & Retana, J. (2017). Relationships among taxonomic, functional, and phylogenetic ant diversity across the biogeographic regions of Europe. *Ecography*, *40*(3), 448–457. https://doi.org/10.1111/ecog.01938

Aron, S., Steinhauer, N., & Fournier, D. (2009). Influence of queen phenotype, investment and maternity apportionment on the outcome of fights in cooperative foundations of the ant *Lasius niger*. *Animal Behaviour*, *77*(5), 1067–1074. https://doi.org/10.1016/j.anbehav.2009.01.009

Aschoff, J. (1960). Exogenous and endogenous components in circadian rhythms. *Cold Spring Harbor Symposia on Quantitative Biology*, *25*, 11–28. https://doi.org/10.1101/sqb.1960.025.01.004

Barthélemy, M., Barrat, A., Pastor-Satorras, R., & Vespignani, A. (2005). Dynamical patterns of epidemic outbreaks in complex heterogeneous networks. *Journal of Theoretical Biology*, *235*(2), 275–288. https://doi.org/10.1016/j.jtbi.2005.01.011

Bates, D., Mächler, M., Bolker, B., & Walker, S. (2015). Fitting Linear Mixed-Effects Models Using lme4. *Journal of Statistical Software*, *67*(1). https://doi.org/10.18637/jss.v067.i01

Beer, K., & Bloch, G. (2020). Circadian plasticity in honey bees. *The Biochemist*, *42*(2), 22–26. https://doi.org/10.1042/BIO04202002

Benjamini, Y., & Hochberg, Y. (1995). Controlling the False Discovery Rate: A Practical and Powerful Approach to Multiple Testing. *Journal of the Royal Statistical Society Series B: Statistical Methodology*, *57*(1), 289–300. https://doi.org/10.1111/j.2517-6161.1995.tb02031.x

Ben-Shachar, M., Lüdecke, D., & Makowski, D. (2020). effectsize: Estimation of Effect Size Indices and Standardized Parameters. *Journal of Open Source Software*, *5*(56), 2815. https://doi.org/10.21105/joss.02815

Bernard, K. A., Bellefeuille, M., & Ewan, E. P. (1991). Cellular fatty acid composition as an adjunct to the identification of asporogenous, aerobic gram-positive rods. *Journal of Clinical Microbiology*, *29*(1), 83–89. https://doi.org/10.1128/jcm.29.1.83-89.1991

Bischoff, J. F., Rehner, S. A., & Humber, R. A. (2009). A multilocus phylogeny of the *Metarhizium anisopliae* lineage. *Mycologia*, *101*(4), 512–530. https://doi.org/10.3852/07-202

Bizzell, F., & Pull, C. D. (2024). Ant queens cannibalise infected brood to contain disease spread and recycle nutrients. *Current Biology*, *34*(18), R848-R849. https://doi.org/10.1016/j.cub.2024.07.062

Bloch, G., Herzog, E. D., Levine, J. D., & Schwartz, W. J. (2013). Socially synchronized circadian oscillators. *Proceedings. Biological Sciences*, *280*(1765), 20130035. https://doi.org/10.1098/rspb.2013.0035

Blondel, V. D., Guillaume, J.-L., Lambiotte, R., & Lefebvre, E. (2008). Fast unfolding of communities in large networks. *Journal of Statistical Mechanics: Theory and Experiment*, *2008*(10), P10008. https://doi.org/10.1088/1742-5468/2008/10/P10008

Blonder, B., & Dornhaus, A. (2011). Time-ordered networks reveal limitations to information flow in ant colonies. *PloS One*, *6*(5), e20298. https://doi.org/10.1371/journal.pone.0020298

Bolker, B. (2019). Getting started with the package glmmTMB.

Bolker, B. M., Brooks, M. E., Clark, C. J., Geange, S. W., Poulsen, J. R., Stevens, M. H. H., & White, J.-S. S. (2009). Generalized linear mixed models: A practical guide for ecology and evolution. *Trends in Ecology & Evolution*, *24*(3), 127–135. https://doi.org/10.1016/j.tree.2008.10.008

Boomsma, J. J., & van der Have, T. M. (1998). Queen mating and paternity variation in the ant *Lasius niger*. *Molecular Ecology*, *7*(12), 1709–1718. https://doi.org/10.1046/j.1365-294x.1998.00504.x

Bos, N., Lefèvre, T., Jensen, A. B., & d'Ettorre, P. (2012). Sick ants become unsociable. *Journal of Evolutionary Biology*, *25*(2), 342–351. https://doi.org/10.1111/j.1420-9101.2011.02425.x

Brand, J. M., Fales, H. M., Sokoloski, E. A., MacConnell, J. G., Blum, M. S., & Duffield, R. M. (1973). Identification of mellein in the mandibular gland secretions of carpenter ants. *Life Sciences*, *13*(3), 201–211. https://doi.org/10.1016/0024-3205(73)90019-2

Brütsch, T., Avril, A., & Chapuisat, M. (2017). No evidence for social immunity in co-founding queen associations. *Scientific Reports*, *7*(1), 16262. https://doi.org/10.1038/s41598-017-16368-4

Bulmer, M. S., Franco, B. A., Biswas, A., & Greenbaum, S. F. (2023). Overcoming immune deficiency with allogrooming. *Insects*, *14*(2). https://doi.org/10.3390/insects14020128

Casillas-Pérez, B., Boďová, K., Grasse, A. V., Tkačik, G., & Cremer, S. (2023). Dynamic pathogen detection and social feedback shape collective hygiene in ants. *Nature Communications*, *14*(1), 3232. https://doi.org/10.1038/s41467-023-38947-y

Casillas-Pérez, B., Pull, C. D., Naiser, F., Naderlinger, E., Matas, J., & Cremer, S. (2022). Early queen infection shapes developmental dynamics and induces long-term disease protection in incipient ant colonies. *Ecology Letters*, *25*(1), 89–100. https://doi.org/10.1111/ele.13907

Charbonneau, D., Blonder, B., & Dornhaus, A. (2013). Social Insects: A model system for network dynamics. In P. Holme & J. Saramäki (Eds.), *Temporal Networks* (pp. 217–244). Springer Berlin Heidelberg.

Charbonneau, D., & Dornhaus, A. (2015). Workers 'specialized' on inactivity: Behavioral consistency of inactive workers and their role in task allocation. *Behavioral Ecology and Sociobiology*, *69*(9), 1459–1472. https://doi.org/10.1007/s00265-015-1958-1

Chen, Y., Zhao, C., Zeng, W., Wu, W., Zhang, S., Zhang, D., & Li, Z. (2023). The effect of ergosterol on the allogrooming behavior of termites in response to the entomopathogenic fungus *Metarhizium anisopliae*. *Insect Science*, *30*(1), 185–196. https://doi.org/10.1111/1744-7917.13055

Cini, A., Bordoni, A., Cappa, F., Petrocelli, I., Pitzalis, M., Iovinella, I., Dani, F. R., Turillazzi, S., & Cervo, R. (2020). Increased immunocompetence and network centrality of allogroomer workers suggest a link between individual and social immunity in honeybees. *Scientific Reports*, *10*(1), 8928. https://doi.org/10.1038/s41598-020-65780-w

Cole, B. J. (1991). Short-Term Activity Cycles in Ants: Generation of periodicity by worker interaction. *The American Naturalist*, *137*(2), 244–259. https://doi.org/10.1086/285156

Cremer, S., Armitage, S. A. O., & Schmid-Hempel, P. (2007). Social immunity. *Current Biology*, *17*(16), R693-702. https://doi.org/10.1016/j.cub.2007.06.008

Cremer, S., Pull, C. D., & Fürst, M. A. (2018). Social immunity: Emergence and evolution of colony-level disease protection. *Annual Review of Entomology*, *63*, 105–123. https://doi.org/10.1146/annurev-ento-020117-043110

Cremer, S., & Sixt, M. (2009). Analogies in the evolution of individual and social immunity. *Philosophical Transactions of the Royal Society of London. Series B, Biological Sciences*, *364*(1513), 129–142. https://doi.org/10.1098/rstb.2008.0166

Cros, S., Cerdá, X., & Retana, J. (1997). Spatial and temporal variations in the activity patterns of Mediterranean ant communities. *Écoscience*, *4*(3), 269–278. https://doi.org/10.1080/11956860.1997.11682405

Czechowski, W. (1984). Tournaments and raids in *Lasius niger* (L.) (Hymenoptera, Formicidae). *Annales Zoologici*, *38*(2), 81–91.

Danon, L., House, T. A., Read, J. M., & Keeling, M. J. (2012). Social encounter networks: Collective properties and disease transmission. *Journal of the Royal Society, Interface*, *9*(76), 2826–2833. https://doi.org/10.1098/rsif.2012.0357

Das, B., & Bekker, C. de (2022). Time-course RNASeq of *Camponotus floridanus* forager and nurse ant brains indicate links between plasticity in the biological clock and behavioral division of labor. *BMC Genomics*, *23*(1), 57. https://doi.org/10.1186/s12864-021-08282-x

Davidson, J. D., & Gordon, D. M. (2017). Spatial organization and interactions of harvester ants during foraging activity. *Journal of the Royal Society, Interface*, *14*(135). https://doi.org/10.1098/rsif.2017.0413

Davis, H. E., Meconcelli, S., Radek, R., & McMahon, D. P. (2018). Termites shape their collective behavioural response based on stage of infection. *Scientific Reports*, *8*(1), 14433. https://doi.org/10.1038/s41598-018-32721-7

Depa, Ł. (2024). Circadian pattern in attendance of aphid colonies by ants. *Acta Oecologica*, *124*, 104009. https://doi.org/10.1016/j.actao.2024.104009

Diez, L., Moquet, L., & Detrain, C. (2013). Post-mortem changes in chemical profile and their influence on corpse removal in ants. *Journal of Chemical Ecology*, *39*(11-12), 1424–1432. https://doi.org/10.1007/s10886-013-0365-1

Dolai, A., Soltani, S., Smarr, B., & Das, A. (2024). Divergent circadian foraging strategies in response to diurnal predation versus persistent rain in Asian weaver ant, *Oecophylla smaragdina*, suggest possible energetic trade-offs. *Journal of Biological Rhythms*, *39*(3), 295–307. https://doi.org/10.1177/07487304241233778.

Douglas, A. E. (2006). Phloem-sap feeding by animals: Problems and solutions. *Journal of Experimental Botany*, *57*(4), 747–754. https://doi.org/10.1093/jxb/erj067

Dunlap, J. C., Loros, J. J., & DeCoursey, P. J. (2004). *Chronobiology: Biological timekeeping*. Sinauer Associates.

Evans, J. D., & Spivak, M. (2010). Socialized medicine: Individual and communal disease barriers in honey bees. *Journal of Invertebrate Pathology*, *103 Supplement 1*, S62-72. https://doi.org/10.1016/j.jip.2009.06.019

Fefferman, N. H., Traniello, J. F. A., Rosengaus, R. B., & Calleri, D. V. (2007). Disease prevention and resistance in social insects: modeling the survival consequences of immunity, hygienic behavior, and colony organization. *Behavioral Ecology and Sociobiology*, *61*(4), 565–577. https://doi.org/10.1007/s00265-006-0285-y

Fox, J., & Weisberg, S. (2019). *An R Companion to Applied Regression* (Version Third Edition) [Computer software]. Sage. https://socialsciences.mcmaster.ca/jfox/Books/Companion/

Fuchikawa, T., Eban-Rothschild, A., Nagari, M., Shemesh, Y., & Bloch, G. (2016). Potent social synchronization can override photic entrainment of circadian rhythms. *Nature Communications*, *7*(1). https://doi.org/10.1038/ncomms11662

Fujioka, H., Abe, M. S., Fuchikawa, T., Tsuji, K., Shimada, M., & Okada, Y. (2017). Ant circadian activity associated with brood care type. *Biology Letters*, *13*(2). https://doi.org/10.1098/rsbl.2016.0743

Fujioka, H., Abe, M. S., & Okada, Y. (2019). Ant activity-rest rhythms vary with age and interaction frequencies of workers. *Behavioral Ecology and Sociobiology*, *73*(3). https://doi.org/10.1007/s00265-019-2641-8

Fujioka, H., Abe, M. S., & Okada, Y. (2021). Individual ants do not show activity-rest rhythms in nest conditions. *Journal of Biological Rhythms*, *36*(3), 297–310. https://doi.org/10.1177/07487304211002934

Fujioka, H., Okada, Y., & Abe, M. S. (2021). Bipartite network analysis of ant-task associations reveals task groups and absence of colonial daily activity. *Royal Society Open Science*, *8*(1), 201637. https://doi.org/10.1098/rsos.201637

Geffre, A. C., Gernat, T., Harwood, G. P., Jones, B. M., Morselli Gysi, D., Hamilton, A. R., Bonning, B. C., Toth, A. L., Robinson, G. E., & Dolezal, A. G. (2020). Honey bee virus causes context-dependent changes in host social behavior. *Proceedings of the National Academy of Sciences of the United States of America*, *117*(19), 10406–10413. https://doi.org/10.1073/pnas.2002268117

Giehr, J., Grasse, A. V., Cremer, S., Heinze, J., & Schrempf, A. (2017). Ant queens increase their reproductive efforts after pathogen infection. *Royal Society Open Science*, *4*(7), 170547. https://doi.org/10.1098/rsos.170547

Greenwald, E., Segre, E., & Feinerman, O. (2015). Ant trophallactic networks: Simultaneous measurement of interaction patterns and food dissemination. *Scientific Reports*, *5*, 12496. https://doi.org/10.1038/srep12496

Grizanova, E. V., Coates, C. J., Dubovskiy, I. M., & Butt, T. M. (2019). *Metarhizium brunneum* infection dynamics differ at the cuticle interface of susceptible and tolerant morphs of *Galleria mellonella*. *Virulence*, *10*(1), 999–1012. https://doi.org/10.1080/21505594.2019.1693230

Hamilton, C., Lejeune, B. T., & Rosengaus, R. B. (2011). Trophallaxis and prophylaxis: Social immunity in the carpenter ant *Camponotus pennsylvanicus*. *Biology Letters*, *7*(1), 89–92. https://doi.org/10.1098/rsbl.2010.0466

Hänel, H. (1982). The life cycle of the insect pathogenic fungus *Metarhizium anisopliae* in the termite *Nasutitermes exitiosus*. *Mycopathologia*, *80*(3), 137–145. https://doi.org/10.1007/BF00437576

Holme, P., & Saramäki, J. (2012). Temporal networks. *Physics Reports*, *519*(3), 97–125. https://doi.org/10.1016/j.physrep.2012.03.001

Hothorn, T., Bretz, F., & Westfall, P. (2008). Simultaneous inference in general parametric models. *Biometrical Journal*, *50*(3), 346–363.

Hughes, W. O. H., Eilenberg, J., & Boomsma, J. J. (2002). Trade-offs in group living: Transmission and disease resistance in leaf-cutting ants. *Proceedings. Biological Sciences*, *269*(1502), 1811–1819. https://doi.org/10.1098/rspb.2002.2113

Ingram, K. K., Krummey, S., & LeRoux, M. (2009). Expression patterns of a circadian clock gene are associated with age-related polyethism in harvester ants, *Pogonomyrmex occidentalis*. *BMC Ecology*, *9*, 7. https://doi.org/10.1186/1472-6785-9-7

Ingram, K. K., Kutowoi, A., Wurm, Y., Shoemaker, D., Meier, R., & Bloch, G. (2012). The molecular clockwork of the fire ant *Solenopsis invicta*. *PloS One*, *7*(11), e45715. https://doi.org/10.1371/journal.pone.0045715

Jaeger, B. (2017). *r2glmm: Computes R Squared for Mixed (Multilevel) Models* [Computer software]. https://CRAN.R-project.org/package=r2glmm

Janet, C. (1907). Anatomie du corselet et histolyse des muscles vibrateurs, après le vol nuptial: chez la reine de la fourmi (*Lasius niger*). *Impr.-Librairie Ducourtieux Et Gout*, *1*.

Julian, G. E., & Gronenberg, W. (2002). Reduction of brain volume correlates with behavioral changes in queen ants. *Brain, Behavior and Evolution*, *60*(3), 152–164. https://doi.org/10.1159/000065936

Kay, T., Liberti, J., Richardson, T. O., McKenzie, S. K., Weitekamp, C. A., La Mendola, C., Rüegg, M., Kesner, L., Szombathy, N., McGregor, S., Romiguier, J., Engel, P., & Keller, L. (2023). Social network position is a major predictor of ant behavior, microbiota composition, and brain gene expression. *PLoS Biology*, *21*(7), e3002203. https://doi.org/10.1371/journal.pbio.3002203

Kay, T., Motes-Rodrigo, A., Royston, A., Richardson, T. O., Stroeymeyt, N., & Keller, L. (2024). Ant social network structure is highly conserved across species. *Proceedings. Biological Sciences*, *291*(2027), 20240898. https://doi.org/10.1098/rspb.2024.0898

Keller, S., Kessler, P., & Schweiz, C. (2003). Distribution of insect pathogenic soil fungi in Switzerland with special reference to *Beauveria brongniartii* and *Metharhizium anisopliae*. *BioControl*, *48*(3), 307–319. https://doi.org/10.1023/A:1023646207455

Khuong, A., Gautrais, J., Perna, A., Sbaï, C., Combe, M., Kuntz, P., Jost, C., & Theraulaz, G. (2016). Stigmergic construction and topochemical information shape ant nest architecture. *Proceedings of the National Academy of Sciences of the United States of America*, *113*(5), 1303–1308. https://doi.org/10.1073/pnas.1509829113

Konrad, M., Pull, C. D., Metzler, S., Seif, K., Naderlinger, E., Grasse, A. V., & Cremer, S. (2018). Ants avoid superinfections by performing risk-adjusted sanitary care. *Proceedings of the National Academy of Sciences of the United States of America*, *115*(11), 2782–2787. https://doi.org/10.1073/pnas.1713501115

Konrad, M., Vyleta, M. L., Theis, F. J., Stock, M., Tragust, S., Klatt, M., Drescher, V., Marr, C., Ugelvig, L. V., & Cremer, S. (2012). Social transfer of pathogenic fungus promotes active immunisation in ant colonies. *PLoS Biology*, *10*(4), e1001300. https://doi.org/10.1371/journal.pbio.1001300

Kramer, B. H., Schaible, R., & Scheuerlein, A. (2016). Worker lifespan is an adaptive trait during colony establishment in the long-lived ant *Lasius niger*. *Experimental Gerontology*, *85*, 18–23. https://doi.org/10.1016/j.exger.2016.09.008

Kurze, C., Jenkins, N. E., & Hughes, D. P. (2020). Evaluation of direct and indirect transmission of fungal spores in ants. *Journal of Invertebrate Pathology*, *172*, 107351. https://doi.org/10.1016/j.jip.2020.107351

Latora, V., & Marchiori, M. (2001). Efficient behavior of small-world networks. *Physical Review Letters*, *87*(19), 198701. https://doi.org/10.1103/PhysRevLett.87.198701

Leckie, L., Andon, M. S., Bruce, K., & Stroeymeyt, N. (2024). Architectural Immunity: ants alter their nest networks to fight epidemics. *BioRxiv*. Advance online publication. https://doi.org/10.1101/2024.08.30.610481

Lehue, M., & Detrain, C. (2019). What's going on at the entrance? A characterisation of the social interface in ant nests. *Behavioural Processes*, *160*, 42–50. https://doi.org/10.1016/j.beproc.2018.12.006

Lei, Y., Zhou, Y., Lü, L., & He, Y. (2019). Rhythms in foraging behavior and expression patterns of the foraging gene in *Solenopsis invicta* (Hymenoptera: Formicidae) in relation to photoperiod. *Journal of Economic Entomology*, *112*(6), 2923–2930. https://doi.org/10.1093/jee/toz175

Lenoir, A., Hefetz, A., Simon, T., & Soroker, V. (2001). Comparative dynamics of gestalt odour formation in two ant species *Camponotus fellah* and *Aphaenogaster senilis*

(Hymenoptera: Formicidae). *Physiological Entomology*, *26*(3), 275–283. https://doi.org/10.1046/j.0307-6962.2001.00244.x

Lenth, R. V. (2023). *emmeans: Estimated Marginal Means, aka Least-Squares Means* [Computer software]. https://CRAN.R-project.org/package=emmeans

Lin, Y.-R., Chi, Y., Zhu, S., Sundaram, H., & Tseng, B. L. (2008). Facetnet. In J. Huai, R. Chen, H.-W. Hon, Y. Liu, W.-Y. Ma, A. Tomkins, & X. Zhang (Eds.), *Proceedings of the 17th international conference on World Wide Web* (pp. 685–694). ACM. https://doi.org/10.1145/1367497.1367590

Liu, L., Wang, W., Liu, Y., Sun, P., Lei, C., & Huang, Q. (2019). The Influence of allogrooming behavior on individual innate immunity in the subterranean termite *Reticulitermes chinensis* (Isoptera: Rhinotermitidae). *Journal of Insect Science (Online)*, *19*(1). https://doi.org/10.1093/jisesa/iey119

Liu, L., Zhao, X.-Y., Tang, Q.-B., Lei, C.-L., & Huang, Q.-Y. (2019). The mechanisms of social immunity against fungal infections in eusocial insects. *Toxins*, *11*(5). https://doi.org/10.3390/toxins11050244

Lloyd-Smith, J. O., Schreiber, S. J., Kopp, P. E., & Getz, W. M. (2005). Superspreading and the effect of individual variation on disease emergence. *Nature*, *438*(7066), 355–359. https://doi.org/10.1038/nature04153

Lone, S. R., & Sharma, V. K. (2011). Timekeeping through social contacts: Social synchronization of circadian locomotor activity rhythm in the carpenter ant *Camponotus paria*. *Chronobiology International*, *28*(10), 862–872. https://doi.org/10.3109/07420528.2011.622676

Masson, F., Brown, R. L., Vizueta, J., Irvine, T., Xiong, Z., Romiguier, J., & Stroeymeyt, N. (2024). Pathogen-specific social immunity is associated with erosion of individual immune function in an ant. *Nature Communications*, *15*(1), 9260. https://doi.org/10.1038/s41467-024-53527-4

Mersch, D. P. (2016). The social mirror for division of labor: what network topology and dynamics can teach us about organization of work in insect societies. *Behavioral Ecology and Sociobiology*, *70*(7), 1087–1099. https://doi.org/10.1007/s00265-016-2104-4

Mersch, D. P., Crespi, A., & Keller, L. (2013). Tracking individuals shows spatial fidelity is a key regulator of ant social organization. *Science (New York, N.Y.)*, *340*(6136), 1090–1093. https://doi.org/10.1126/science.1234316

Meurville, M.-P., & LeBoeuf, A. C. (2021). Trophallaxis: the functions and evolution of social fluid exchange in ant colonies (Hymenoptera: Formicidae). *Myrmecological News*, *31*, 1–30. https://doi.org/10.25849/myrmecol.news_031:001

Mildner, S., & Roces, F. (2017). Plasticity of daily behavioral rhythms in foragers and nurses of the ant *Camponotus rufipes*: Influence of social context and feeding times. *PloS One*, *12*(1), e0169244. https://doi.org/10.1371/journal.pone.0169244

Miller, J. C. (2009). Spread of infectious disease through clustered populations. *Journal of the Royal Society, Interface*, *6*(41), 1121–1134. https://doi.org/10.1098/rsif.2008.0524

Naug, D. (2009). Structure and resilience of the social network in an insect colony as a function of colony size. *Behavioral Ecology and Sociobiology*, *63*(7), 1023–1028. https://doi.org/10.1007/s00265-009-0721-x

Naug, D., & Camazine, S. (2002). The role of colony organization on pathogen transmission in social insects. *Journal of Theoretical Biology*, *215*(4), 427–439. https://doi.org/10.1006/jtbi.2001.2524

Naug, D., & Smith, B. (2007). Experimentally induced change in infectious period affects transmission dynamics in a social group. *Proceedings. Biological Sciences*, *274*(1606), 61–65. https://doi.org/10.1098/rspb.2006.3695

Newman, M. E. J. (2002). Assortative mixing in networks. *Physical Review Letters*, *89*(20), 208701. https://doi.org/10.1103/PhysRevLett.89.208701

Newman, M. E. J. (2003). Mixing patterns in networks. *Physical Review. E, Statistical, Nonlinear, and Soft Matter Physics*, *67*(2 Pt 2), 26126. https://doi.org/10.1103/PhysRevE.67.026126

Nieuwenhuis, R., te Grotenhuis, M., & Pelzer, B. (2012). influence.ME: Tools for detecting influential data in mixed effects models. *R Journal*, *4*(2), 38–47.

Okuno, M., Tsuji, K., Sato, H., & Fujisaki, K. (2012). Plasticity of grooming behavior against entomopathogenic fungus *Metarhizium anisopliae* in the ant *Lasius japonicus*. *Journal of Ethology*, *30*(1), 23–27. https://doi.org/10.1007/s10164-011-0285-x

Olson, E. (2011). AprilTag: A robust and flexible visual fiducial system. In *2011 IEEE International Conference on Robotics and Automation* (pp. 3400–3407). IEEE. https://doi.org/10.1109/ICRA.2011.5979561

Orivel, J., & Dejean, A. (2002). Ant activity rhythms in a pioneer vegetal formation of French Guiana (Hymenoptera: Formicidae). *Sociobiology*, *39*(1), 65–76.

Otterstatter, M. C., & Thomson, J. D. (2007). Contact networks and transmission of an intestinal pathogen in bumble bee (*Bombus impatiens*) colonies. *Oecologia*, *154*(2), 411–421. https://doi.org/10.1007/s00442-007-0834-8

Pedras, M. S. C., Irina Zaharia, L., & Ward, D. E. (2002). The destruxins: Synthesis, biosynthesis, biotransformation, and biological activity. *Phytochemistry*, *59*(6), 579–596. https://doi.org/10.1016/S0031-9422(02)00016-X

Pereira, H., & Detrain, C. (2020). Pathogen avoidance and prey discrimination in ants. *Royal Society Open Science*, *7*(2), 191705. https://doi.org/10.1098/rsos.191705

Pie, M. R., Rosengaus, R. B., & Traniello, J. F. (2004). Nest architecture, activity pattern, worker density and the dynamics of disease transmission in social insects. *Journal of Theoretical Biology*, *226*(1), 45–51. https://doi.org/10.1016/j.jtbi.2003.08.002

Pinter-Wollman, N., Bala, A., Merrell, A., Queirolo, J., Stumpe, M. C., Holmes, S., & Gordon, D. M. (2013). Harvester ants use interactions to regulate forager activation and availability. *Animal Behaviour*, *86*(1), 197–207. https://doi.org/10.1016/j.anbehav.2013.05.012

Pinter-Wollman, N., Wollman, R., Guetz, A., Holmes, S., & Gordon, D. M. (2011). The effect of individual variation on the structure and function of interaction networks in harvester ants. *Journal of the Royal Society, Interface*, *8*(64), 1562–1573. https://doi.org/10.1098/rsif.2011.0059

Pull, C. D., & Cremer, S. (2017). Co-founding ant queens prevent disease by performing prophylactic undertaking behaviour. *BMC Evolutionary Biology*, *17*(1), 219. https://doi.org/10.1186/s12862-017-1062-4

Pull, C. D., Hughes, W. O. H., & Brown, M. J. F. (2013). Tolerating an infection: An indirect benefit of co-founding queen associations in the ant *Lasius niger*. *Die Naturwissenschaften*, *100*(12), 1125–1136. https://doi.org/10.1007/s00114-013-1115-5

Pull, C. D., Metzler, S., Naderlinger, E., & Cremer, S. (2018). Protection against the lethal side effects of social immunity in ants. *Current Biology*, *28*(19), R1139-R1140. https://doi.org/10.1016/j.cub.2018.08.063

Pull, C. D., Ugelvig, L. V., Wiesenhofer, F., Grasse, A. V., Tragust, S., Schmitt, T., Brown, M. J. F., & Cremer, S. (2018). Destructive disinfection of infected brood prevents systemic

disease spread in ant colonies. *ELife*, *7*(e32073). https://doi.org/10.7554/eLife.32073.001

Qiu, H., Lu, L., Shi, Q., & He, Y. (2014). Fungus exposed *Solenopsis invicta* ants benefit from grooming. *Journal of Insect Behavior*, *27*(5), 678–691. https://doi.org/10.1007/s10905-014-9459-z

Qiu, H., Lu, L., Zalucki, M. P., & He, Y. (2016). *Metarhizium anisopliae* infection alters feeding and trophallactic behavior in the ant *Solenopsis invicta*. *Journal of Invertebrate Pathology*, *138*, 24–29. https://doi.org/10.1016/j.jip.2016.05.005

Quevillon, L. E., Hanks, E. M., Bansal, S., & Hughes, D. P. (2015). Social, spatial, and temporal organization in a complex insect society. *Scientific Reports*, *5*, 13393. https://doi.org/10.1038/srep13393

R Core Team. (2023). *R: A language and environment for statistical computing* [Computer software]. R Foundation for Statistical Computing. https://www.R-project.org/

Reber, A., Purcell, J., Buechel, S. D., Buri, P., & Chapuisat, M. (2011). The expression and impact of antifungal grooming in ants. *Journal of Evolutionary Biology*, *24*(5), 954–964. https://doi.org/10.1111/j.1420-9101.2011.02230.x

Richardson, T. O., & Gorochowski, T. E. (2015). Beyond contact-based transmission networks: The role of spatial coincidence. *Journal of the Royal Society, Interface*, *12*(111), 20150705. https://doi.org/10.1098/rsif.2015.0705

Richardson, T. O., Kay, T., Braunschweig, R., Journeau, O. A., Rüegg, M., McGregor, S., Los Rios, P. de, & Keller, L. (2021). Ant behavioral maturation is mediated by a stochastic transition between two fundamental states. *Current Biology*, *31*(10), 2253-2260.e3. https://doi.org/10.1016/j.cub.2020.05.038

Richardson, T. O., Liechti, J. I., Stroeymeyt, N., Bonhoeffer, S., & Keller, L. (2017). Short-term activity cycles impede information transmission in ant colonies. *PLoS Computational Biology*, *13*(5), e1005527. https://doi.org/10.1371/journal.pcbi.1005527

Richardson, T. O., Stroeymeyt, N., Crespi, A., & Keller, L. (2022). Two simple movement mechanisms for spatial division of labour in social insects. *Nature Communications*, *13*(1), 6985. https://doi.org/10.1038/s41467-022-34706-7

Roberts, D. W., & St Leger, R. J. (2004). *Metarhizium spp*., cosmopolitan insect-pathogenic fungi: Mycological aspects. *Advances in Applied Microbiology*, *54*, 1–70. https://doi.org/10.1016/S0065-2164(04)54001-7

Rojas, M. G., Elliott, R. B., & Morales-Ramos, J. A. (2018). Mortality of *Solenopsis invicta* workers (Hymenoptera: Formicidae) after indirect exposure to spores of three entomopathogenic fungi. *Journal of Insect Science (Online)*, *18*(3). https://doi.org/10.1093/jisesa/iey050

Rosengaus, R. B., Maxmen, A. B., Coates, L. E., & Traniello, J. F. A. (1998). Disease resistance: a benefit of sociality in the dampwood termite *Zootermopsis angusticollis* (Isoptera: Termopsidae). *Behavioral Ecology and Sociobiology*, *44*(2), 125–134. https://doi.org/10.1007/s002650050523

Rostás, M., & Blassmann, K. (2009). Insects had it first: Surfactants as a defence against predators. *Proceedings of the Royal Society of London. Series B: Biological Sciences*, *276*(1657), 633–638. https://doi.org/10.1098/rspb.2008.1281

Sah, P., Leu, S. T., Cross, P. C., Hudson, P. J., & Bansal, S. (2017). Unraveling the disease consequences and mechanisms of modular structure in animal social networks. *Proceedings of the National Academy of Sciences of the United States of America*, *114*(16), 4165–4170. https://doi.org/10.1073/pnas.1613616114

Schlichting, M., & Helfrich-Förster, C. (2015). Photic entrainment in *Drosophila* assessed by locomotor activity recordings. *Methods in Enzymology*, *552*, 105–123. https://doi.org/10.1016/bs.mie.2014.10.017

Schmid-Hempel, P. (2017). Parasites and their social hosts. *Trends in Parasitology*, *33*(6), 453–462. https://doi.org/10.1016/j.pt.2017.01.003

Sharma, V. K., Lone, S. R., Goel, A., & Chandrashekaran, M. K. (2004). Circadian consequences of social organization in the ant species *Camponotus compressus*. *Die Naturwissenschaften*, *91*(8), 386–390. https://doi.org/10.1007/s00114-004-0544-6

Shykoff, J. A., & Schmid-Hempel, P. (1991). Parasites and the advantage of genetic variability within social insect colonies. *Proceedings of the Royal Society of London. Series B: Biological Sciences*, *243*(1306), 55–58. https://doi.org/10.1098/rspb.1991.0009

Siehler, O., Wang, S., & Bloch, G. (2021). Social synchronization of circadian rhythms with a focus on honeybees. *Philosophical Transactions of the Royal Society B: Biological Sciences*, *376*(1835), Article 20200342. https://doi.org/10.1098/rstb.2020.0342

Signorelli, A. (2024). *DescTools: Tools for Descriptive Statistics* [Computer software]. https://CRAN.R-project.org/package=DescTools

Simone-Finstrom, M. (2017). Social immunity and the superorganism: Behavioral defenses protecting honey bee colonies from pathogens and parasites. *Bee World*, *94*(1), 21–29. https://doi.org/10.1080/0005772X.2017.1307800

Sommer, K., & Hölldobler, B. (1995). Colony founding by queen association and determinants of reduction in queen number in the ant *Lasius niger*. *Animal Behaviour*, *50*(2), 287–294. https://doi.org/10.1006/anbe.1995.0244

Soroker, V., Fresneau, D., & Hefetz, A. (1998). Formation of colony odor in ponerine ant. *Journal of Chemical Ecology*, *24*(6), 1077–1090. https://doi.org/10.1023/A:1022306620282

Stock, M., Milutinović, B., Hoenigsberger, M., Grasse, A. V., Wiesenhofer, F., Kampleitner, N., Narasimhan, M., Schmitt, T., & Cremer, S. (2023). Pathogen evasion of social immunity. *Nature Ecology & Evolution*, *7*(3), 450–460. https://doi.org/10.1038/s41559-023-01981-6

Stroeymeyt, N., Casillas-Pérez, B., & Cremer, S. (2014). Organisational immunity in social insects. *Current Opinion in Insect Science*, *5*, 1–15. https://doi.org/10.1016/j.cois.2014.09.001

Stroeymeyt, N., Grasse, A. V., Crespi, A., Mersch, D. P., Cremer, S., & Keller, L. (2018). Social network plasticity decreases disease transmission in a eusocial insect. *Science (New York, N.Y.)*, *362*(6417), 941–945. https://doi.org/10.1126/science.aat4793

Theis, F. J., Ugelvig, L. V., Marr, C., & Cremer, S. (2015). Opposing effects of allogrooming on disease transmission in ant societies. *Philosophical Transactions of the Royal Society of London. Series B, Biological Sciences*, *370*(1669). https://doi.org/10.1098/rstb.2014.0108

Tomioka, K., & Matsumoto, A. (2015). Circadian molecular clockworks in non-model insects. *Current Opinion in Insect Science*, *7*, 58–64. https://doi.org/10.1016/j.cois.2014.12.006

Tragust, S., Mitteregger, B., Barone, V., Konrad, M., Ugelvig, L. V., & Cremer, S. (2013). Ants disinfect fungus-exposed brood by oral uptake and spread of their poison. *Current Biology*, *23*(1), 76–82. https://doi.org/10.1016/j.cub.2012.11.034

Tranter, C., LeFevre, L., Evison, S. E., & Hughes, W. O. (2015). Threat detection: contextual recognition and response to parasites by ants. *Behavioral Ecology*, *26*(2), 396–405. https://doi.org/10.1093/beheco/aru203

Ugelvig, L. V., & Cremer, S. (2007). Social prophylaxis: Group interaction promotes collective immunity in ant colonies. *Current Biology*, *17*(22), 1967–1971. https://doi.org/10.1016/j.cub.2007.10.029

Vestergaard, S., Gillespie, A. T., Butt, T. M., Schreiter, G., & Eilenberg, J. (1995). Pathogenicity of the hyphomycete fungi *Verticillium lecanii* and *Metarhizium anisopliae* to the western flower thrips, *Frankliniella occidentalis*. *Biocontrol Science and Technology*, *5*(2), 185–192. https://doi.org/10.1080/09583159550039909

Villalta, I., Oms, C. S., Angulo, E., Molinas-González, C. R., Devers, S., Cerdá, X., & Boulay, R. (2020). Does social thermal regulation constrain individual thermal tolerance in an ant species? *The Journal of Animal Ecology*, *89*(9), 2063–2076. https://doi.org/10.1111/1365-2656.13268

Volz, E. M., Miller, J. C., Galvani, A., & Ancel Meyers, L. (2011). Effects of heterogeneous and clustered contact patterns on infectious disease dynamics. *PLoS Computational Biology*, *7*(6), e1002042. https://doi.org/10.1371/journal.pcbi.1002042

Walker, T. N., & Hughes, W. O. H. (2009). Adaptive social immunity in leaf-cutting ants. *Biology Letters*, *5*(4), 446–448. https://doi.org/10.1098/rsbl.2009.0107

Wanderlingh, A. A. (2024). *Effects of Group Size on Disease Transmission Risk and Immune Strategies in Ants* [Doctoral dissertation]. University of Bristol, Bristol, England.

Wang, J., & Olson, E. (2016). AprilTag 2: Efficient and robust fiducial detection. In *2016 IEEE/RSJ International Conference on Intelligent Robots and Systems (IROS)* (pp. 4193–4198). IEEE. https://doi.org/10.1109/IROS.2016.7759617

Wickham, H. (2016). *ggplot2: Elegant Graphics for Data Analysis*. https://ggplot2.tidyverse.org

Wickham, H., François, R., Henry, L., Müller, K., & Vaughan, D. (2023). *dplyr: A Grammar of Data Manipulation* [Computer software]. https://CRAN.R-project.org/package=dplyr

Wilke, C. O. (2020). *cowplot: Streamlined Plot Theme and Plot Annotations for 'ggplot2'* [Computer software]. https://CRAN.R-project.org/package=cowplot

Yamauchi, K., & Hayashida, K. (1970). Taxonomic studies on the genus *Lasius* in Hokkaido, with ethological and ecological notes (Formicidae, Hymenoptera). : II. The Subgenus *Lasius*. *Journal of the Faculty of Science, Hokkaido University*, *17*(3), 501–519.